

A FRAMEWORK FOR DESIGNING AND OPTIMIZING GREEN INFRASTRUCTURE
NETWORK UNDER UNCERTAINTY

BY

BARDIA HEIDARI HARATMEH

DISSERTATION

Submitted in partial fulfillment of the requirements
for the degree of Doctor of Philosophy in Civil Engineering
in the Graduate College of the
University of Illinois at Urbana-Champaign, 2019

Urbana, Illinois

Doctoral Committee:

Professor Barbara Minsker, Chair
Research Assistant Professor Arthur Schmidt, Chair
Professor Robert Brunner
Professor Halit Uster, Southern Methodist University

Abstract

Green infrastructure (GI) is becoming a common solution to mitigate stormwater-related problems. Despite wide acknowledgement of GI benefits, there is a lack of decision support tools that allow practitioners to interactively identify and evaluate the performance of small GI practices using hydrologic models under uncertainty. Also, the benefits and costs of GI practices are not fully understood when the analysis scale changes from a household to a subwatershed to an entire watershed. Moreover, recognition of optimal locations in a watershed, given the uncertainty in modelling parameters, is also another challenge for GI planning and design. To address these needs, an online Cloud-based interactive tool — called Interactive DEsign and Assessment System for Green Infrastructure (IDEAS_GI)— has been developed. This study demonstrates the application of the tool, using hydrologic and empirical models, to estimate life cycle cost, stormwater volume reduction and treatment, and air pollutant deposition. The tool was applied in two small watersheds in the Baltimore metropolitan area. The results show that GI properties do not significantly affect performance of individual GI practices during design storm events due to the intensity of the storms exceeding the capacity of GI practices to treat and capture stormwater. Using the tool to identify potential locations for GI placement, the study then provides a quantitative and comparative analysis of environmental benefits and economic costs of GI using two metrics [Benefit-Cost Ratios (BCRs) and nutrient removal costs] at household, subwatershed, and watershed scales. The results for a case study in Baltimore show that the unit cost of nutrient removal in some of the subwatersheds is lower than the unit costs at either the watershed or household scales, calling for optimization frameworks to determine the features that dictate optimality at the subwatershed level. Moreover, rain gardens provide far more efficient stormwater treatment at the household scale in comparison to watershed scale, for which large-scale dry or wet basins are more efficient. The results show that for BCR, smaller subwatersheds are more cost effective for GI implementation, while for nutrient removal cost, upstream subwatersheds are more suitable. Furthermore, self-installation of rain gardens greatly reduces nutrient removal costs. Finally, to identify preferable locations for GI implementation, the numerical hydrologic model used in IDEAS_GI, SWMM,

has been merged with a probabilistic noisy genetic algorithm (GA). The GA uses a probabilistic selection method that requires numerous sampling realizations to estimate the uncertainties associated with the fitness (objective function) values, which are cumulative stormwater volume reduction and GI life cycle cost. To overcome the computational challenge and to identify significant features for preferable locations, the GA is merged with artificial neural networks, which act as surrogates for the numerical models. The surrogate models use GA-generated archives as training datasets to predict the mean and standard deviation of cumulative stormwater volume reduction. The results show that the addition of meta-models decreases average computational time required to reach Pareto frontiers similar to the ones generated by the noisy GA by more than 95%.

Acknowledgments

I would like to express my great appreciation to my advisor, Professor Barbara Minsker, for her guidance in finishing my doctorate degree. I greatly appreciate all the support she provided throughout the years, both at the University of Illinois and at Southern Methodist University. Thank you for your trust in accepting me as part of your group, and for continuing to support me even after you moved from Illinois to Texas.

I would also like to greatly thank my co-advisor, Professor Arthur Schmidt, for your guidance and your insightful help throughout the years. I thank my other thesis committee members, Professor Robert Brunner and Professor Halit Uster, for providing me with helpful guidance and suggestions during the PhD study.

I would like to credit Dr. Lorne Leonard, Professor Larry Band, Dr. Brian Miles, Dr. Jong Lee, and other members of NCSA who greatly helped me with setting up IDEAS_GI, specifically by designing GI Designer. I also want to thank Richard England and Dr. Robert Kalescky for helping me to run the models on the SMU ManeFrame II system.

I am indebted to my group members in Professor Barbara Minsker's group and Professor Arthur Schmidt's group. I will never forget the joy of working beside you.

I gratefully acknowledge financial support from the National Science Foundation (NSF) (award numbers 1331807 and 1261582). I also acknowledge the funding and support provided by the National Socio-Environmental Synthesis Center (SESYNC) (award number DBI-1639145), which allowed national working and advisory groups from five cities to meet and provide input to this work. I would also like to thank all of the participants in the IDEAS_GI workshop held in April 2017 for their helpful input on the software design and implementation.

Finally, I would like to express my deepest thanks and love to my parents and my sister for their encouragement and love.

Table of Contents

CHAPTER 1: INTRODUCTION	1
CHAPTER 2: CASE STUDIES.....	6
CHAPTER 3: IDEAS_GI: INTERACTIVE DESIGN AND ASSESSMENT SYSTEM FOR GREEN INFRASTRUCTURE	9
CHAPTER 4: SPATIAL SCALE EFFECTS ON UNCERTAINTY AND SENSITIVITY IN GREEN INFRASTRUCTURE COST/BENEFIT ASSESSMENT	46
CHAPTER 5: OPTIMIZATION OF GREEN INFRASTRUCTURE NETWORKS TO MAXIMIZE STORMWATER-RELATED BENEFITS AND MINIMIZE LIFE CYCLE COST USING GENETIC ALGORITHMS AND SURROGATE MODELS	86
CHAPTER 6: CONCLUSIONS AND FUTURE RESEARCH	116
REFERENCES	122
APPENDIX A: LISTS OF SESYNC VENTURE MEETING PARTICIPANTS/CONTRIBUTORS	136
APPENDIX B: INSTRUCTION MANUAL TO PREPARE IDEAS_GI JUPYTER NOTEBOOK	139
APPENDIX C: INSTRUCTION MANUAL TO EXECUTE IDEAS_GI_DEADRUN	143
APPENDIX D: INPUT PARAMETERS FOR THE REQUIRED SUPPORTING FILES TO SUCCESSFULLY EXECUTE IDEAS_GI FOR ANY GIVEN WATERSHED	146
APPENDIX E: UNCERTAIN CONTINUOUS PARAMETERS	147
APPENDIX F: UNCERTAIN CATEGORICAL PARAMETERS	150
APPENDIX G: SUPPLEMENTARY RESULTS ON CO-BENEFITS/ COSTS ASSOCIATED WITH DESIGN SCENARIOS AT THE TWO CASE STUDY WATERSHEDS	151
APPENDIX H: GEOGRAPHIC SPECIFICATION OF CASE STUDY I IN SECTION 3.5.2.....	154
APPENDIX I: COMPUTATION OF STORMWATER REDUCTION AS A FUNCTION OF GI COVERAGE AREA	156

Chapter 1: Introduction

1.1. Green infrastructure

Currently, Green Infrastructure (GI) is becoming one of the most commonly used practices in sustainable city development projects, as it presents a feasible solution to address stormwater management problems (Sandström 2002). Waste and pollution transported by stormwater are recurring issues that have led city planners and engineers to develop different strategies to control and mitigate surface runoff (Barbosa et al. 2012). According to the Environmental Protection Agency (EPA 2014), GI refers to a patchwork of natural areas that promote healthier habitats, stronger flood protection, and cleaner water and air at city and regional scales. However, at the parcel scale, GI refers to stormwater management systems that mimic nature by absorbing and storing water. Currently in the US, rain gardens, bioswales, green roofs, urban forests, rain barrels, permeable pavements, planter boxes, trees, and constructed wetlands are commonly used as GI to manage stormwater (EPA 2014). Their structural design and operational management are primarily geared towards their primary function: stormwater runoff control and treatment (Mell 2008; Berndtsson 2010a; Kabir et al. 2014). However, there are other GI benefits and trade-offs to incorporating semi-natural lands into highly urbanized areas that can potentially promote GI design and implementation (Tzoulas et al. 2007).

In addition to stormwater volume capture, GI has many other benefits that can improve health and the environment. GI design elements can remove nutrients, namely nitrogen and phosphorous, from surface water, leading to healthier ecosystem function (Berndtsson 2010a). GI has also been demonstrated to reduce heavy metal and ion load from surface water runoff (Kabir et al. 2014). Additionally, GI has been shown to reduce air pollutant concentrations in urban areas (Nowak 2000; Yang et al. 2004; Nowak et al. 2006). GI may also help mitigate urban heat island effect by reducing outdoor temperatures (Shin and Lee 2005). Furthermore, GI has demonstrated positive effects on human health by different means, including

more active lifestyle choices, exposure to green spaces, etc. (Van den Berg et al. 2003; Hartig et al. 2014; Jiang et al. 2015;).

1.2. Existing decision-making frameworks for GI placement and analysis

GI has been increasingly implemented throughout the US as an environmental amenity in recent years. GI has mostly been implemented by the private sector (i.e., property owners). The entities responsible for urban planning generally either treat GI as ad hoc green initiatives or investment opportunities (Brown 2005; Chini et al. 2017). GI implementation can be significantly improved if planning, design, monitoring, and performance assessment of GI at larger scales are conducted using rigorous quantitative analysis with engineering models to assess trade-offs between different solutions (Nylen and Kiparsky 2015). The lack of monitoring programs and standardized widely accepted benefit evaluation processes are the two main problems resulting in knowledge gaps in the GI implementation decision-making process.

A myriad of tools has been developed to address GI design and performance assessment, each having their own specific features and limitations. However, these tools are generally used to either simulate performance of GI or aid in the design of individual GI practices. These tools take advantage of different modeling approaches, including experimentally driven (empirical) formulations, analytical calculations, numerical simulations, or data-driven approaches. Experimentally-driven formulations are the first options to be used for stormwater capture, quality improvement, urban heat island mitigation, air pollutant deposition, etc. (Felson and Pickett 2005; Janhäll 2015). Numerical simulation methods have also been extensively developed for stormwater simulation and GI design (see Elliott and Trowsdale 2007, and Jayasooriya and Ng 2014 for reviews). Data-driven approaches are generated based on input and output data collected from the real-world performance of a phenomenon and lack physics-based justifications (Khan et al. 2013). All these models provide valuable insight on how GI practice performs in the real world. However, they do not provide guidelines on suitable spatial scale and locations for GI to serve different

objectives. To locate suitable potential locations, a comprehensive framework is needed to evaluate benefits and costs of alternative scenarios and determine tradeoffs among different GI implementation objectives.

Current tools, called Decision Support Systems (DSS), focus on stormwater quality and quantity, rather than other environmental benefits, as the main objectives for GI design (Matlock and Morgan 2010). Well-known DSS for GI include System for Urban Stormwater Treatment and Analysis Integration, or SUSTAIN (Lee et al. 2012) and Model for Urban Stormwater Improvement Conceptualization, or MUSIC (Wong et al. 2002a). SUSTAIN uses the numerical hydrologic/hydraulics model SWMM (Rossman and Huber 2015) and the water quality estimation model HSPF (Rossman and Huber 2016) along with a life cycle cost database for different GI types to determine the optimal design scenario given certain design criteria. MUSIC helps determine the best arrangement of GI network to meet design criteria using total life cycle cost and performance assessment with the SimHyd model (Chiew and Siriwardena 2005). Despite the numerous benefits of these two decision support systems, they do not assess co-benefits, the environmental, social, and economic benefits of GI beyond stormwater functionality. Also, since they use deterministic simulation models, they do not assess how uncertainties inherent in the modeling approaches may affect their results. Ideally, a decision support analysis/system needs to provide insight on how uncertainties affect tradeoffs among optimal designs in the real world.

Moreover, these frameworks do not assess uncertainties associated with the effects of spatial scale. In reality, the effects of GI projects involve different stakeholders. For instance, residential energy savings from green roofs are beneficial for homeowners, while peak flow reductions are tangible at the watershed/subwatershed scale and are useful for municipalities and eventually the whole contributing community. Therefore, benefits can be analyzed at multiple scales (e.g., household, neighborhood, watershed, etc.).

Also, such models do not assess whether GI investment is financially justifiable. To do so, GI design scenarios require cost-benefit analysis that can inform practitioners of the potential outcomes of their investments. Therefore, tools are still needed that facilitate cost/benefit assessment and support decisions

on financial aspects of GI projects. This thesis develops such a decision-making framework that can address several spatial scales (including household, subwatershed, and watershed), provide insights on the uncertainties inherent in GI modeling, and determine optimal locations for GI practices given tradeoffs among different objectives.

1.3. Dissertation outline and research questions

This dissertation creates a decision-making framework, along with implementation guidelines, to help practitioners and decision makers recognize preferred locations for small GI practices in urban/ semi-urbanized watersheds to address water quality and quantity functionalities of GI at multiple scales. This dissertation specifically focuses on rain gardens as small-scale practices that can be used throughout a watershed, although the framework can be applied to other types of GI. Numerical simulation models, uncertainty quantification methods, meta-heuristic optimization methods, and data-driven machine learning methods are used to determine where GI practices should be placed. This provides a generalizable approach and guidelines for siting different types and potential locations of small GI practice under uncertainty.

The second chapter of this dissertation specifies details of the case studies used in this study. The details include features and characteristics of the case studies, as well as descriptions, assumptions, and methods used for each numerical simulation model.

The third chapter highlights the capabilities of a software platform developed to allow practitioners to interactively identify and evaluate the performance of small GI practices using scientific models. The online Cloud-based interactive tool — called IDEAS_GI, or Interactive DEsign and ASsessment of GI — assesses GI performance using hydrologic and empirical models to estimate cost, stormwater volume reduction and treatment, and air pollutant deposition. The tool is designed to be used as an initial screening platform to identify potential locations for GI implementation across case study watersheds and to provide an overview of GI performance across spatial scales. In other words, the chapter addresses the following research question: “How can the potential locations for GI implementation, as well as their performance, be assessed more interactively via an open source Cloud-based online software platform?”

The fourth chapter of this study examines how the scale of implementation (i.e., household, sub-watershed, or watershed), affects the cost and benefits of GI, focusing on rain gardens. This chapter assesses the extent of GI implementation and its effects on overall cost/benefit assessments of GI. However, one of the main challenges in addressing such questions is parameter uncertainty, which eventually contributes to uncertainty in the overall modeling results. Therefore, the following research question is addressed in this chapter: “How does spatial scale affect uncertainty and sensitivity in green infrastructure cost/benefit assessment?”

The fifth chapter provides a framework for identifying preferable locations to place GI. This chapter, using water quality results from previous chapters, shows locations where subwatersheds are more suitable for GI placement from the standpoints of water quantity and life cycle cost. The chapter uses noisy meta-heuristic optimization algorithms to find preferable arrangement and location of GI practices in a semi-urbanized watershed. To search for preferable designs in an efficient manner and to overcome the computational burden of the search process, the genetic algorithms are merged with surrogate machine learning models. The surrogate models are trained to replace the computationally-intensive numerical models using datasets generated during the search process. By running the surrogate models, the optimization algorithms can run numerous times to address uncertainty and alternative scenarios, and subsequently drive more insight on preferred conditions for GI implementation locations. Therefore, the chapter addresses the following research questions:

1. “What will be the preferable locations and arrangements of small-scale GI practices in urbanized/semi-urbanized watersheds to mitigate stormwater quantity problems as well as life cycle cost?”
2. “What surrogate modelling approach can determine the preferable locations and arrangements of GI practices, considering the uncertainties in the objective values, in a more efficient manner than noisy heuristic optimization algorithms?”

The final chapter summarizes the conclusions and results drawn from this study, as well as future steps needed to further advance this study for practical and research purposes.

Chapter 2: Case studies

2.1. General description

Two watersheds, Dead Run and Stoney Run, serve as case studies for this research. Dead Run is located in Gwynns Falls Watershed, Baltimore County, Maryland, while Stoney Run is in the Jones Falls Watershed in Baltimore City, Maryland (Fig. 2.1). Data and models (e.g. streamflow and hydrograph data, rainfall data, and SWMM models) were based on the Baltimore Ecological Study (BES), which has collected long term stream discharge and nutrient loads in watersheds over a land use gradient in Baltimore and Baltimore County. One goal of the BES study has been to analyze and determine efficient methods to reduce water pollutant and nutrient load into Chesapeake Bay (Pickett & Cadenasso 2006; Miles 2014; Duncan et al. 2017a; Duncan et al. 2017b).

2.1.1. Dead Run (Case Study I)

Dead Run has a USGS streamflow gauge (USGS 2013) at the outlet of the watershed that has been monitoring and recording flows and water levels for a continuous period since August 1998. The watershed within Dead Run that is the subject of this study is referred to as Dead Run 5 (DR5), with an area of 1.5 km² and is geographically located in the Baltimore County. The watershed has been the subject of numerous hydrologic research studies (Miles & Band, 2015; Heidari et al. 2016; Minsker et al. 2017; Leonard et al. 2019). Fig. 2.1.a shows the boundaries of the DR5 watershed and the subwatersheds modeled in SWMM 5.0. SWMM provides a graphical user interface by which the entire watershed can be represented as connected subwatersheds with user-specified contributing areas (Rossman and Huber 2016).

The SWMM model for the Dead Run case study was calibrated by engineers at Tetra Tech Inc. using streamflow gage data records from 2007 and 2010 with a one-minute routing time step. The calibrated model consists of 138 subwatersheds that vary in size from 0.0007 to 0.2 km², and in slope from 0.01 to 7.35 percent slope. Out of 138 subwatersheds, 67 subwatersheds have potential candidate areas for rain garden implementation. Approximately 20% of the watershed consists of impervious surfaces. The area

and extent of the subwatersheds are based on topography and pipeline and sewer shed maps. The conveyance network consists of pipes, mostly circular, ranging in diameter size from 1 to 5 feet.

Infiltration follows Green-Ampt equations for clay loam soil with a suction head of 8.22 inches (20.9 cm) and hydraulic conductivity of 0.08 in/hr (2.0 mm/hr) assigned to all subwatersheds. The model did not include any GI practices. The kinematic flow routing method is used to carry stormwater across the open-channels connecting one subwatershed outlet to the next. Also, the baseline model does not include any existing GI practices.

2.1.2. Stoney Run (Case Study II)

The Stoney Run Watershed is ~8.5 km² and had an operating USGS streamflow gauge until 2015 (USGS 2015). The watershed used in this study is an urbanized portion of Stoney Run with an area of 0.12 km², with an imperviousness ratio of 50%, and is referred to as “SR5” in this study. This watershed is located in the city of Baltimore and contains an aging sewer system. Therefore, geographic maps that represent the existing network, its tributary area, and its capacity are lacking specific details. The author was provided with the calibrated SWMM 5.0 models for the area, which were designed to mimic the hydrograph at the USGS gages for the continuous period of 2007- 2011. Fig. 2.1.b shows the SR5 watershed boundaries and the subwatersheds that were modeled in SWMM 5.0. Similar to DR5, kinematic routing methods were used for routing from subwatershed outlet to subwatershed outlet. The conveyance network consists of pipes, mostly circular, ranging in diameter from 1 to 3 feet. The soil characteristics and infiltration methods for SR5 were similar to those of DR5.



Fig. 2.1. Boundaries of the modeled (a) DR5 and (b) SR5 watersheds in the state of Maryland, and their subwatersheds modeled in SWMM 5.0, along with their relative locations

Chapter 3: IDEAS_GI: Interactive DEsign and Assessment System for Green Infrastructure

3.1. Introduction

This chapter presents a new online tool called IDEAS_GI, which was created to address some of the previously mentioned needs for assessment of green infrastructure practices. A myriad of tools exist to address GI design and performance assessment, each having its own specific features and limitations. Among the array of tools designed for GI planning, few tools can both simulate chemical/biological/physical behavior of stormwater after GI implementation and provide economic analysis of GI projects. A few well-known decision support systems are Urban Stormwater Treatment and Analysis INtegration, SUSTAIN, (Lee et al. 2012) and Model for Urban Stormwater Improvement Conceptualization, or MUSIC (Wong et al. 2002). SUSTAIN uses the numerical hydrologic/hydraulics model SWMM 5.0 (Rossman and Huber 2015) and the water quality estimation model HSPF (Bicknell et al. 1996), along with a life cycle cost database for different GI types, to recommend optimum design scenarios given certain design criteria. MUSIC is a decision support system that helps determine the best arrangement of a GI network to meet design criteria using total life cycle cost and performance assessment through the SimHyd model (Chiew and Siriwardena 2005).

Jayasooriya & Ng (2014) reviewed the mentioned tools developed to address economic evaluation of GI practices and found that development of participatory Web-based simulation methods that account for modelling uncertainties, provide GIS capabilities, and support decision making are lacking and should be the future path in GI modelling and software development. Lerer et al. (2015) have also reviewed different GI design and planning tools, categorizing the tools based on the type of planning questions they are designed to address. The authors found that the key question of locations in which GI practices are most suited to be placed has not been fully addressed by existing frameworks, nor has the extent of their performance in providing benefits been fully quantified (Lerer et al. 2015). Bach et al. (2014), through review of literature in the integrated urban water system modelling domain, have identified model

complexity, user friendliness, administrative fragmentation, and communication as the main barriers against adoption of integrated GI modelling in engineering practices. Haris et al. (2016) reviewed and categorized existing stormwater management models based on stormwater management and economic analysis aspects. These reviews highlight the importance of providing integrated interactive decision support systems in the next generation of GI planning tools.

Therefore, GI modelling and decision-making tools need improvement in three primary aspects: interactivity, uncertainty in modelling performance, and inter-connected modelling of different benefits/costs associated with their design. These shortcomings may be some of the reasons that decision support systems are not widely used for GI decision-making (Nylen and Kiparsky 2015). To address this need, this work develops a new decision support framework, called IDEAS_GI (Interactive DEsign and Assessment System for Green Infrastructure), that can interactively provide insights on the uncertainties inherent in modelling practices and assist in assessing other categories of environmental benefits associated with small GI practices at different spatial scales.

3.1.1. SESYNC venture

The requirements for the IDEAS_GI system emerged from a 3-year engagement with practitioners and stormwater engineers from five partner cities around the country as a collaborative “Venture” project sponsored by the National Science Foundation-funded National Socio-Environmental Synthesis Center (SESYNC). The Venture, which was in the form of a series of six hands-on workshops entitled “Research on the Perception, Role, and Function of Urban Green Infrastructure,” included a working group of 23 stormwater engineers, hydrologists, ecologists, computer scientists, social scientists, and landscape architects and an advisory group of nine representatives from the cities and non-governmental organizations involved in GI implementation (see list of contributors in Appendix A).

During the meetings, the advisory group emphasized that GI implementation and performance are poorly integrated and valued by users. The group mentioned that decision makers need to address the uncertainty

in benefits and costs associated with GI performance. Lack of quantification of the magnitudes of uncertainties in the benefits make it difficult for GI practitioners to communicate the value of GI to users. The uncertainty, or the miscommunication resulting from lack of uncertainty quantification, can result in challenges and issues with GI project prioritization, e.g. public opposition to new GI installations due to misconceptions about its value. Furthermore, GI practitioners identified a lack of dedicated user interfaces to improve GI model implementation at the preliminary design and planning levels. The advisory group proposed developing specific online Cloud-based GI decision support tools to improve collaborative decision making given that the GI decision-making process and governance are complex and require multi-stakeholder support.

One pathway to address these needs is to use technology and online Cloud computing tools that can integrate different models, provide on-line computational resources without local software installation, and are flexible enough to account for different modelling needs (e.g. GI co-benefit modelling, tuning modelling parameters, and accounting for uncertainties in modelling results). Such platforms can vary from online scientific workflow sharing to high performance computing environments and virtual machines hosting computations at remote servers. Ideally, the objectives, scope, and capabilities of such software should address GI modelling needs at several spatial scales, from parcel to watershed impacts, at short-term and long-term time-scales, and at different social scales, from residents to community and governmental levels (see Fig. 3.1).

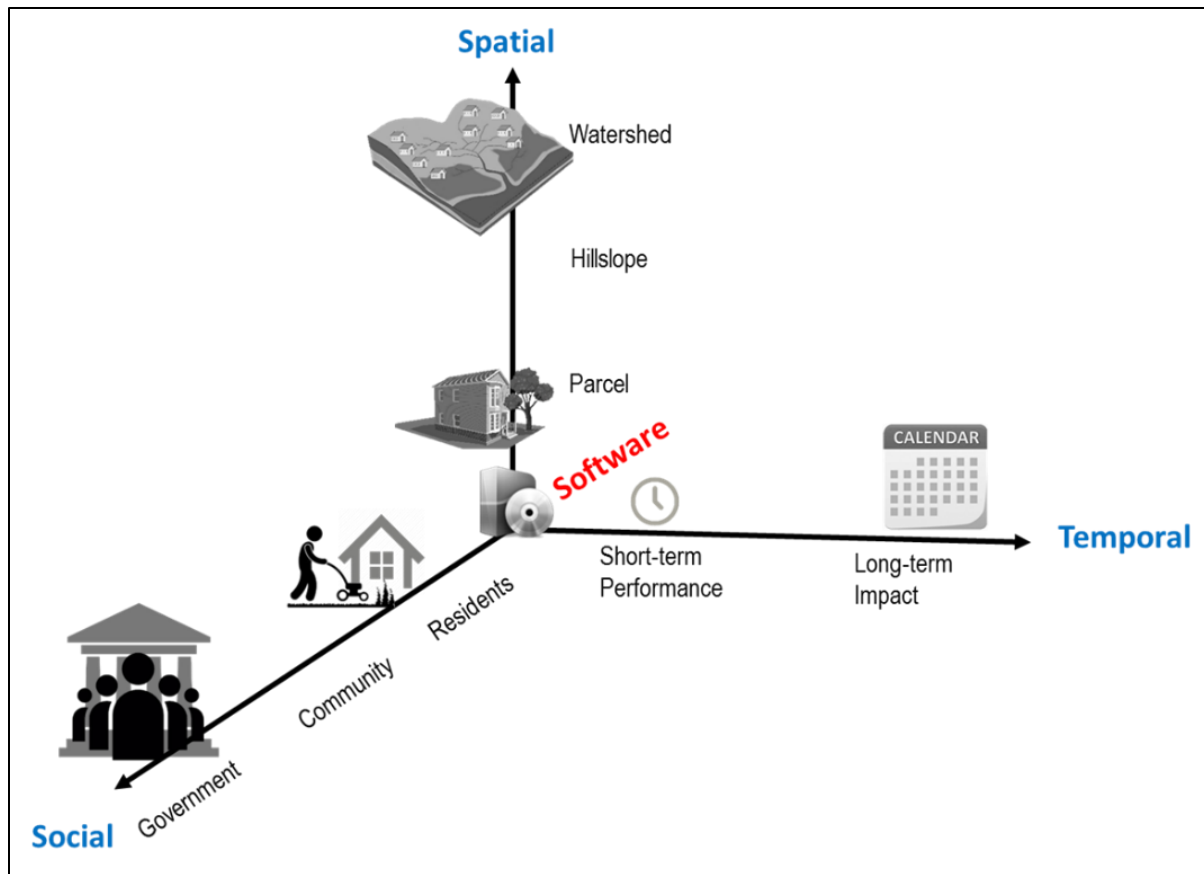


Fig. 3.1. Scope of the objectives that ideal GI design decision support software should address.

According to Fig. 3.1., the ideal GI decision support software should address performance of proposed designs at different spatial scales, varying from parcel to watershed, as well as temporal scales, varying from instantaneous to long-term performance and impacts. On the other hand, GI practices and designs are implemented and will be affecting different social dimensions. Residents, as the primary individuals responsible for GI practices; communities, who benefit from networks of GI practices; and governments, who either regulate or incentivize GI network implementation, have different priorities that need to be accounted for via an ideal decision support tool. Despite the challenges, SESYNC venture meeting attendees came to the conclusion that the IDEAS_GI platform should address such scope of GI-related objectives.

IDEAS_GI was developed in response to decision support needs highlighted by the SESYNC working and advisory groups, providing an online platform to assist in the conceptual design phase of identifying locations and types of small GI practices, prior to detailed site-scale design. Leonard et al. (2019) provide details on the software architecture and GI visualization using the RHESSys distributed eco-hydrological model (Tague and Band 2004) to determine the hydrological performance of GI practices at high spatial resolution scales— i.e., patch scales— with interactive Jupyter notebooks. This chapter demonstrates the full set of IDEAS_GI capabilities, including hosting services, execution protocol, GI type selection criteria, GI performance metrics, and modelling approaches.

The focus of this work is also on the application of IDEAS_GI with the SWMM 5.0 model and a set of empirical models. The SWMM 5.0 models determine performance of small GI practices in a watershed with respect to stormwater capture and treatment, while the empirical models estimate life cycle cost of GI practices, as well as air pollutant deposition over their leaf surface area throughout their life cycle. Both RHESSys and SWMM 5.0 can simulate the behavior of a watershed with respect to resulting hydrographs after rainfall events. However, SWMM 5.0 can also simulate the stormwater treatment functionality of GI practices in contrast to the version of RHESSys implemented in the previous version of IDEAS_GI (Leonard et al. 2019).

More importantly, SWMM 5.0 works at a lower resolution than RHESSys, with each spatial unit corresponding to a subwatershed. This results in lower simulation times needed for SWMM 5.0 to predict the GI system performance, allowing rapid assessment of uncertainties. This chapter includes applications of the software to the two case studies presented in the previous chapter, the future path for software development, feedback received from stormwater practitioners during a hands-on software workshop, and discussion of the existing scope, capabilities, and limitations that impact the future of GI design using interactive platforms coupled with hydrologic models.

3.2. Software design

This section describes the elements of the software architecture by explaining the Cloud hosting services, primary elements of the architecture, and IDEAS_GI execution protocol. Fig. 3.2 shows an overview of the main elements of the software design and the links between them.

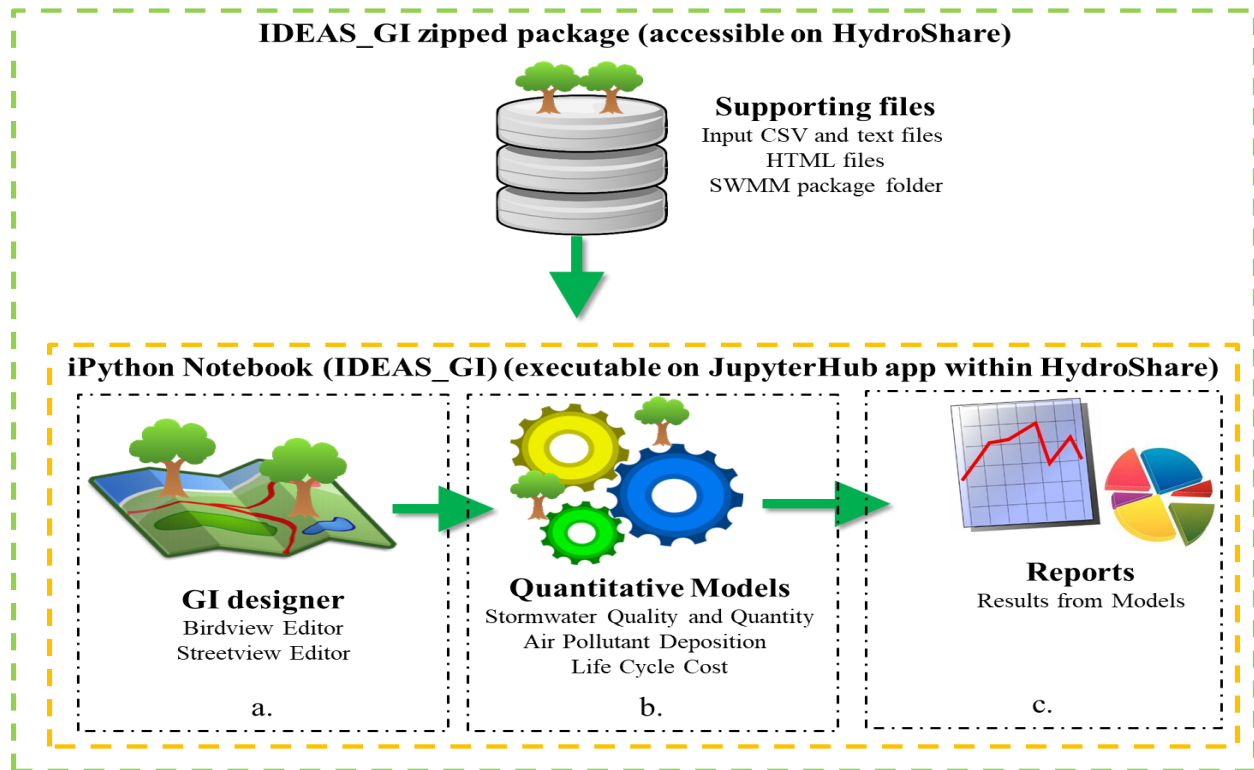


Fig. 3.2. Software architectural elements and hosting services. The zipped folder, which is accessible on HydroShare, contains several supporting files and a Jupyter Notebook (IDEAS_GI). IDEAS_GI contains several cells that facilitate: (a) GI Designer for placing and visualization of GI practices via bird view editor and street view editor, (b) execution of quantitative models, and (c) reporting the results.

3.2.1. Hosting services and architectural elements

The IDEAS_GI software package is available from HydroShare (Tarboton et al. 2014; Horsburgh et al. 2016), an online platform developed for open sharing of hydrologic data and models (CUAHSI 2019; Leonard et al. 2019). HydroShare allows users to access remote servers and conduct their analysis in the Cloud. The IDEAS_GI package is developed and published as a Resource Data+ Model publicly accessible to any registered HydroShare users (Heidari et al. 2017). Another version of IDEAS_GI that uses RHESys is also publicly accessible on HydroShare (Leonard & Band, 2017). HydroShare allows users to access

remote servers and conduct their analysis in the Cloud. The IDEAS_GI package is published as a zipped folder that contains several files and folders (listed in Table 3.1).

Table 3.1. Files included in zipped IDEAS_GI package

Type of files	Contents of the files
Jupyter notebook files (IDEAS)	<ul style="list-style-type: none"> • Jupyter (iPython) notebook to communicate with users, to get inputs from users, to send command to Python kernels for numerical simulation of stormwater behavior throughout the watershed, and to publish outputs
Input CSV and text files (Database), specific to case study area. (All the files in this category are designed and applied to the DR5 case study specified in Section 4.1)	<ul style="list-style-type: none"> • Input text files for stormwater hydrologic model, i.e. SWMM, for design scenarios • Database of air pollutant ambient concentrations within analysis time-periods (US EPA 2018) • Coordinates of watershed boundaries using Universal Transverse Mercator (UTM) projection system • Multiple time series for hydrographs generated at the watershed outlet during design storms under a baseline scenario without GI implementation • Probabilistic distribution of the stormwater pollutants/nutrients at subwatershed and watershed outlets for baseline scenario generated by running Monte Carlo simulations
HTML scripts (Database)	<ul style="list-style-type: none"> • Supporting files to facilitate visualization of performance report of each GI design scenario
SWMM Folders (Database)	<ul style="list-style-type: none"> • SWMM 5.0 python library for numerical simulation of stormwater flows and water quality adjusted to Linux system setup (Pathirana 2018)

IDEAS_GI, like other similar Jupyter notebook resources in HydroShare, requires a kernel to execute every command that users specify (Leonard et al. 2019). These commands are executed on a remote server using a JupyterHub. JupyterHub is a multi-user server that manages multiple instances of the single-user Jupyter notebook. To access the JupyterHub, users need to log-in to HydroShare, navigate to the resource page, and follow instructions through their Web browser. Fig. 3.3 shows the architecture of JupyterHub and IDEAS_GI and how users interact with the interface.

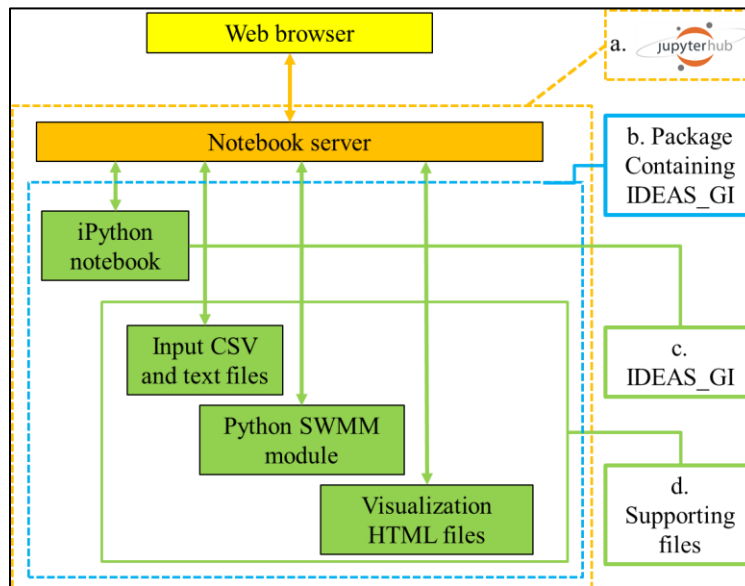


Fig. 3.3. Architecture of JupyterHub and its connection to IDEAS. Each user can access IDEAS_GI package using a Web browser and via the HydroShare website. The tool is executed using a JupyterHub environment (a). The IDEAS_GI package (b) contains several files, including the IDEAS_GI iPython notebook (c) and supporting files that are required for any case study (d).

3.2.2. IDEAS_GI execution protocol

IDEAS_GI is designed to allow decision makers to insert semi-representative schematics of rain gardens and trees (see Figs 3.4 and 3.5) into a real-world landscape and to estimate associated benefits and costs with their design. The Jupyter notebook includes several cells, i.e. multi-line text input fields, that are designed to execute Python scripts, provide an interface for GI design through Google™ Street -view and Google™ Satellite-view, provide a report of GI performance, or provide instructions to users. Each of the cells can be executed independently (by pressing the “enter + shift” keys), making the Jupyter notebook

modular. Once the initial cell is executed, required packages are loaded into the notebook environment. Then a page with a URL link to a remote server located at Pennsylvania State University is called, which enables users to geo-locate trees and rain gardens and a set of hydrologic and hydraulic settings assigned to each GI. This section of IDEAS_GI is called *GI Designer*. Fig. 3.4 shows the interface of GI Designer, including instructions for placing GI on the Google™ map-view. Leonard et al. (2019) provide more details on the architectural elements of the IDEAS_GI Web application, GI visualization mechanisms, and JupyterHub interactive environment, as well as their relationship to each other.

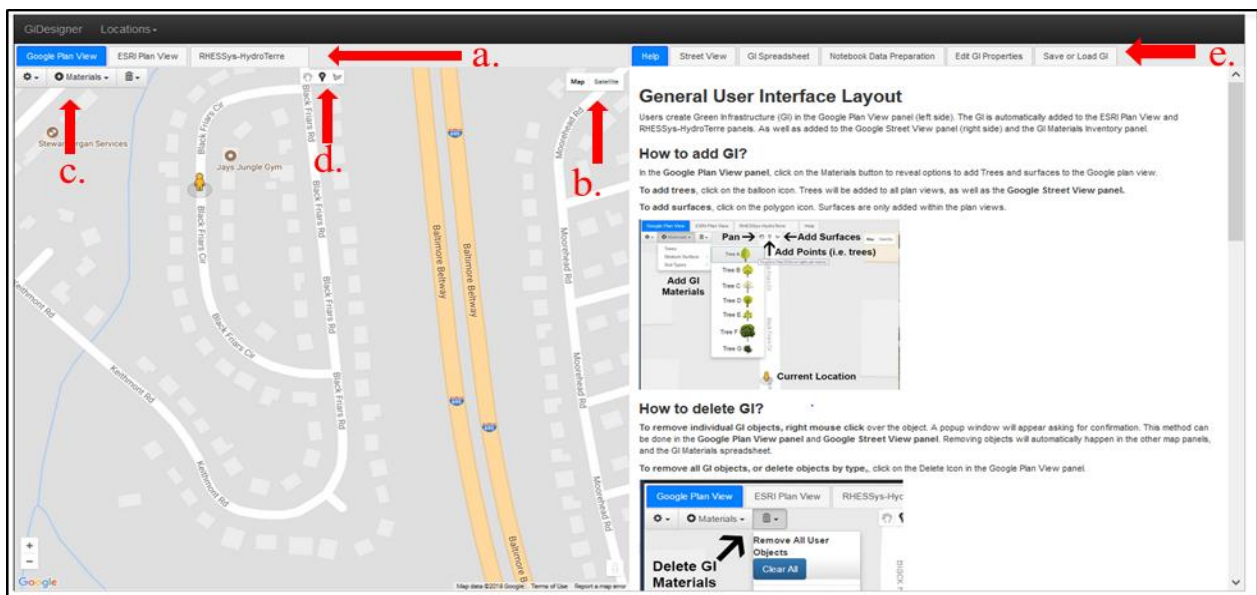


Fig. 3.4. GI Designer interface in IDEAS. The left-hand window provides an areal view of the region of interest to design and insert GI practices across the region.

Users can select three different maps using the map view toolbox: Google™ plan view, ESRI™ plan view, and RHESSys HydroTerre Maps (if already created for the watershed) (Leonard and Duffy 2013, 2014, 2016) (a). Users can also access either map view or Google™ satellite view of the region using the map/satellite view toolbox (b). To design GI features, users can specify the GI materials, edit and delete existing design features, and specify the size-related features of the trees using the toolbox on the left-hand side (c). Each design (tree or rain garden) can be inserted into the areal map or satellite view using the top center toolbox in the left-hand window (d). The right-hand window contains several tabs (e) that further assist

users in their design. Users can also review the instructions for designing GI features, view the Google™ street view corresponding to their map/satellite view, prepare the features associated with GI practices, and save or load GI into their Jupyter notebook for further analysis. The Web application interface (Fig. 3.4) allows users to define a tree or rain garden type and geo-locate it in the region of interest.

The GI representation of the area of interest can become more realistic using IDEAS_GI with the Google™ satellite and street view APIs. Once the GI is placed and its design is finalized, users can save GI-related designs to HydroShare. Upon saving GI designs to HydroShare, JavaScript Object Notation (JSON) data structures containing physical and geographical properties associated with a GI design scenario are stored in the user’s Jupyter notebook, which can also be downloaded to the user’s computer for use in simulation model executions (see Table 3.2 for details). All of the information in Table 3.2 can be modified in the GI Designer Web application using the “Edit GI properties” module (Fig. 3.5).

Fig. 3.5 shows more realistic views of the region of interest for GI design. The left-hand side shows the satellite view of the region, while the right-hand side shows the street view of the same region from the Google Pegman™ point of view. The figure contains areal and street-level schematics of the trees and rain gardens associated with a hypothetical design.

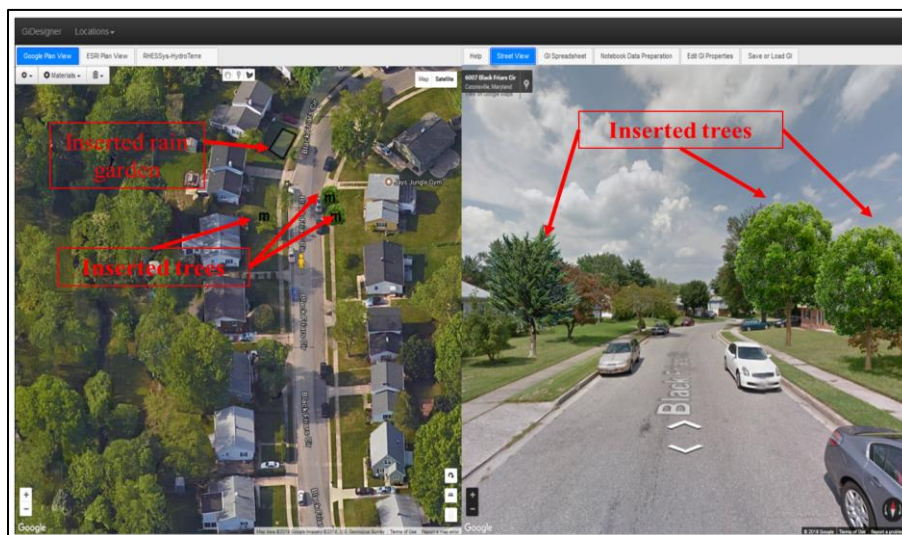


Fig. 3.5. GI Designer with Google™ satellite and Google™ street view interfaces.

Table 3.2. Information stored in JSON files and used for further simulation analysis

Tree feature (units, if applicable)	Rain garden features (units, if applicable)
Patch type (Horse Chestnut, Allegheny Serviceberry, American Hornbeam, Common Hackberry, American Yellowwood, Honey Locust, and SweetGum)	Total land area (m ²)
Stratum type (evergreen, eucalyptus, and deciduous)	Latitude and longitude for perimeter border points
Soil type (clay, silty clay, silt- clay- loam, sandy clay, sandy- clay- loam, clay loam, silt, silt loam, sand, loamy sand, sandy loam, and rock)	Soil type (clay, silty clay, silt- clay- loam, sandy clay, sandy- clay- loam, clay loam, silt, silt loam, sand, loamy sand, sandy loam, and rock)
Soil depth (m)	Soil depth (m)
Saturated conductivity (m s ⁻¹)	Saturated conductivity (m s ⁻¹)
Soil porosity (unitless)	Soil porosity (unitless)
Field capacity (unitless)	Field capacity (unitless)
Soil available water content (unitless)	Soil available water capacity (unitless)
Tree size (m ²)	
Latitude and longitude of the tree installation location	

By executing the next cell in the IDEAS_GI Jupyter notebook, the JSON files are imported to the Python kernel/ console and input parameters for the hydrologic, air pollutant deposition estimation, and life cycle cost models are adjusted according to the design specifications. More details on how the notebook can be executed step by step are presented in Appendices B and C. The modelling parameters are discussed in more detail in Chapter 4.

By running the following cells, the models (i.e. hydrologic, air pollutant deposition estimation, and life cycle cost) will be executed and their results will be stored into the Jupyter notebook environment. More details on the model types, their assumptions, and outputs are presented in the “Modelling Approaches” section.

After executing the model, results are visualized to provide a summary overview of the performance of the design at the watershed scale. Fig. 3.6 shows a sample of a report page for a hypothetical design. In addition to the report page, CSV files are generated upon successful execution of the notebook, which contain hydrograph data points at the outlets of subwatershed in which GI designs are implemented.

Fig. 3.6 contains several sections pertaining to design features, life cycle cost, SWMM 5.0 simulation, and air pollutant deposition estimation results as a GI report. The first box (Fig. 3.6a), GI Design Summary, contains information on the entire area of the watershed, the number of GI features in the design scenario, the total area of GI practices in the design scenario used, and the impervious drainage area that is being treated in the design scenario. The second box (Fig. 3.6b) contains information on the costs of GI practices, including capital cost, present value of total life cycle cost, annual cost, and present and annual values of total life cycle cost per treated area. The third box (Fig. 3.6c) presents results of a SWMM 5.0 hydrologic simulation captured at the watershed outlet after two design storms, including the average flow reduction throughout the simulation period, peak flow reductions, cumulative stormwater volume reduction, and average and standard deviation of the cumulative total nitrogen mass reduction. It also contains normalized hydrologic performance (i.e., divided by the total area that is supposed to be treated via GI) after the two design storms. Although the design storms for this case study are pre-defined based on design guidelines (Maryland Department of Environment 2009), they can be adjusted according to the modeler’s needs via the original uploaded SWMM 5.0 files as well as the report generating HTML files .

The next box (Fig. 3.6d), Co-Benefits, contains information on the mean annual ambient air pollutant deposition as the example co-benefit category used in this study. In Chapter 4, the justification for selecting this co-benefit for IDEAS_GI and the methods for quantification of this category of benefits are presented.

The last box (Fig. 3.6e) contains a spider chart that compares the results of the latest design scenario to the average of previous scenarios that have been executed since the start of the Jupyter session. The chart provides a comparative assessment of the design in relation to several analysis metrics (e.g. peak flow, cumulative flow volume, nitrogen load for the two design storms, and life cycle cost). HTML files, stored within the IDEAS_GI zip folder, are the template files that facilitate the visualization of the GI report.

The IDEAS_GI Jupyter notebook reads from zipped supporting files, listed in Table 1, that are uploaded to a HydroShare account and its associated JupyterHub remote server. To access such files, users need to open the Jupyter page and navigate to the work>notebooks folder. Upon execution of the analysis cell within the Jupyter notebook, new files are generated and stored in the same folder workspace. The files contain simulation results at the subwatershed level for the subwatersheds in which inserted GI designs are located. The files, which are stored as CSV, are also accessible for download.

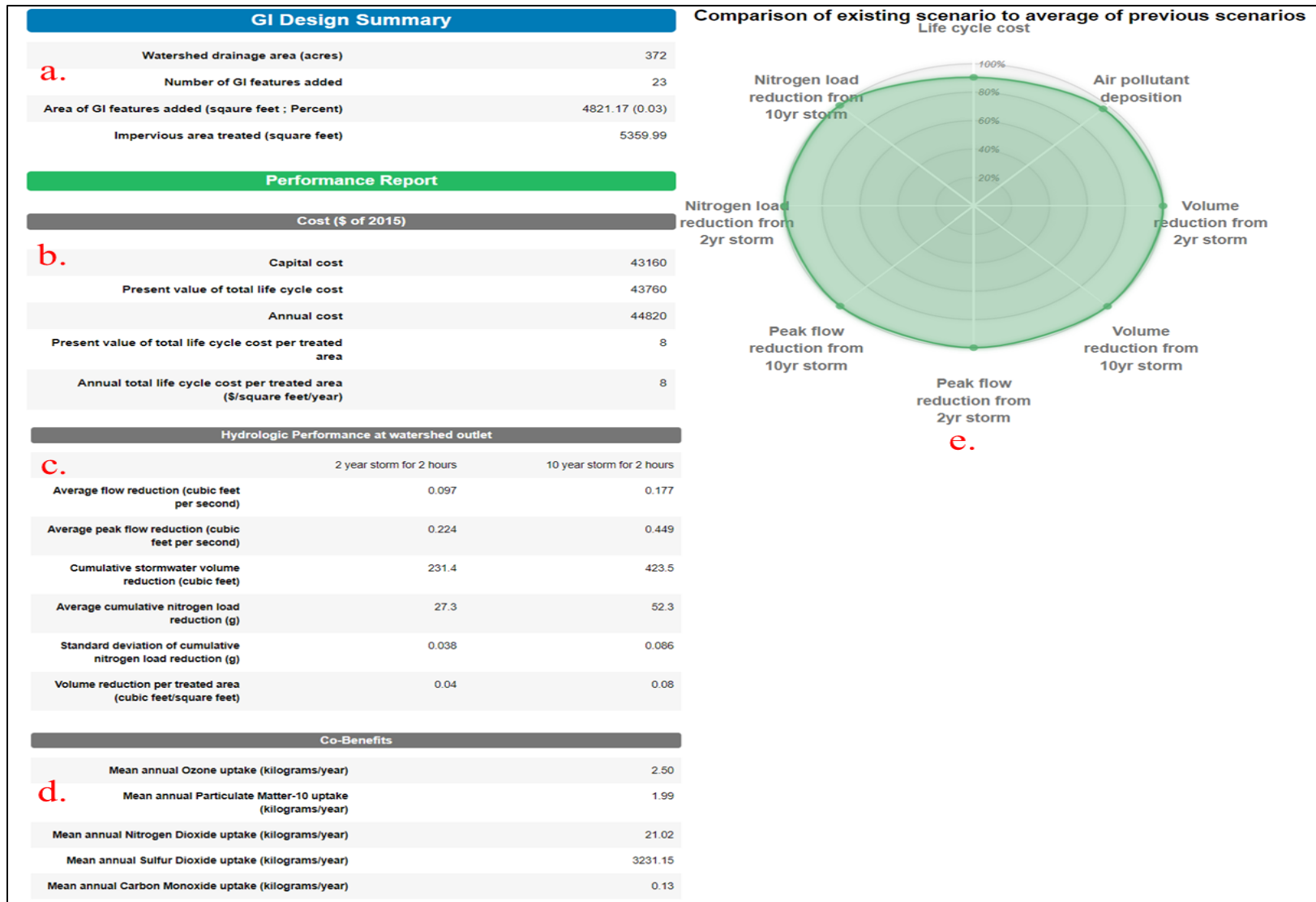


Fig. 3.6. Sample of GI report. The report consists of sections that contain (a) design summary features, (b) life cycle cost estimation outcomes, (c) hydrologic modelling performance outcomes, (d) air-pollutant deposition outcomes, and (e) comparative summary of the performance of the design to the average of prior designs.

3.3. Modelling approaches

This section elaborates on the types of GI practices, the categories of benefits, and the modelling practices included in the IDEAS_GI software framework.

3.3.1. Selection of GI practices

IDEAS_GI is designed mainly for small GI practices (e.g., rain gardens and trees) that can be installed at the household level, although their environmental impacts, e.g. stormwater quantity and quality management, air pollutant deposition, etc., can extend to the watershed scale and beyond. For the initial implementation of this tool, only rain gardens and trees are selected due to their widespread use and general applicability to different environments. Trees are presented with 2.5-D schematic representations, while rain gardens are only represented with 2-D aerial views (Leonard et al. 2019). The GI schematics (see Fig. 3.5) are only intended for initial conceptual designs, allowing stormwater practitioners and stakeholders to quickly understand the potential impact of GI designs. Users requiring detailed landscape designs and views would use Computer Aided Design (CAD) software as discussed in future directions.

3.3.2. Selection of benefit categories

As mentioned previously in the “Introduction” section, there is a suite of benefits and costs associated with GI implementation. Some of the benefits and costs are not easily quantified, including community cohesion, stress and anxiety reduction, and educational benefits. (Hartig et al. 2014; Jiang et al. 2014; Holtan, et al. 2015; Li and Sullivan 2016). Among the quantifiable categories of benefits and costs, some are highly uncertain. For instance, the impact of GI on property values has no consensus in the literature (McConnell and Walls 2005; Adelaja et al. 2008). There has been extensive research to quantify the impacts of green space on urban heat island mitigation (Gill et al. 2007; Santamouris 2014; Norton et al. 2015; Zhang et al. 2017). However due to data needs, complexity of urban heat island modeling, and lack of confidence in the impacts of rain gardens on urban heat island (Cameron et al. 2012), this co-benefit is not included in IDEAS_GI initially. Therefore, the IDEAS_GI tool is designed to assess GI performance in

terms of stormwater peak flow reduction, stormwater volume reduction, stormwater quality improvement, life cycle cost, and air pollutant deposition through the life cycle of GI practices (Fig. 3.6b). Due to the modular nature of the IDEAS_GI software, tools to evaluate other benefits (e.g. urban heat island, flash flooding potential reduction, etc.) can easily be added in the future if desired.

3.3.3. Cost/benefit assessment models

As mentioned in Section 3.2 and 3.3.2, the quantitative models within IDEAS_GI estimate and quantify the benefits/ costs associated with each design. Fig. 3.7. shows the types of models in IDEAS_GI and their links to the other IDEAS_GI components.

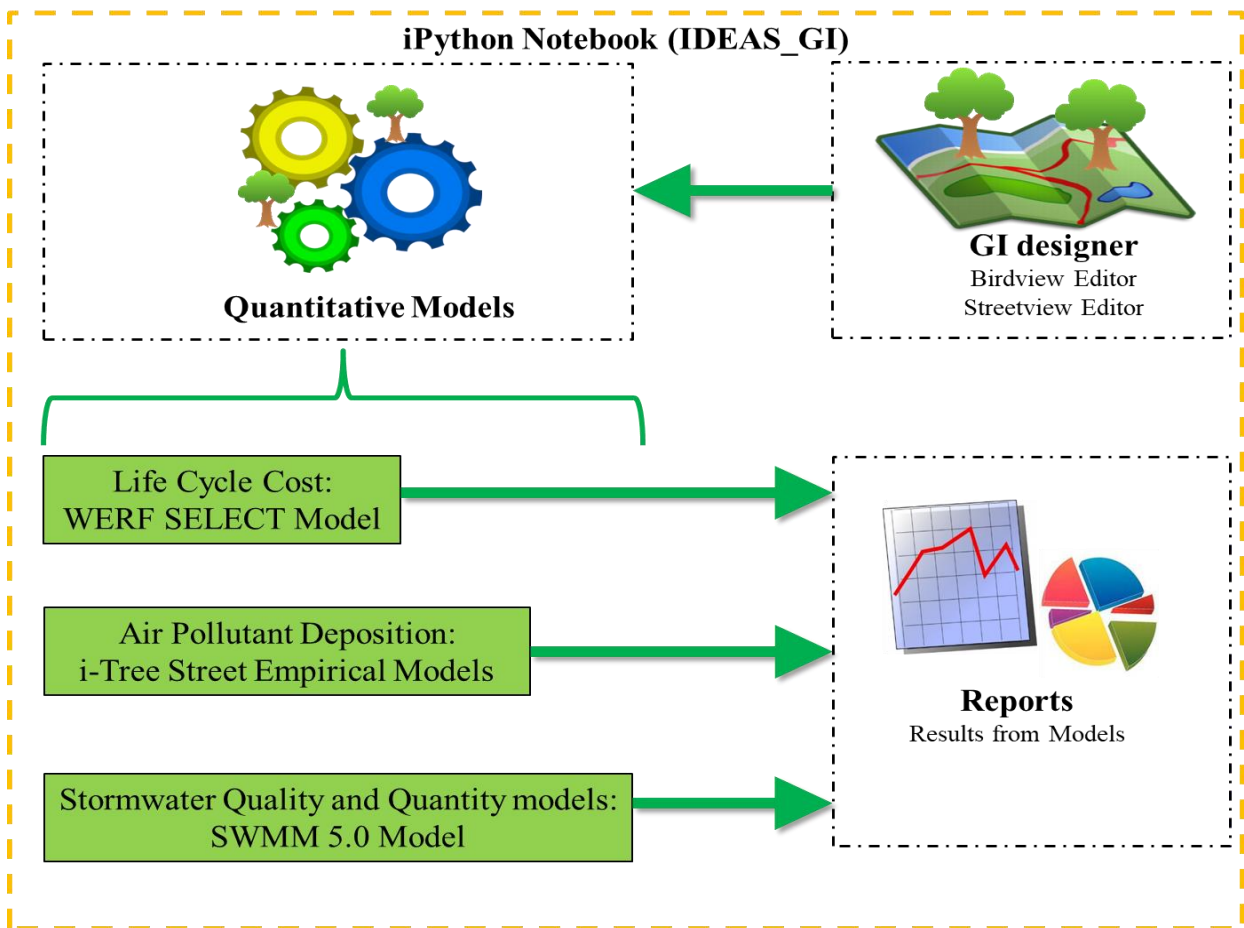


Fig. 3.7. Types of quantitative models and their links to other IDEAS_GI components

For each design scenario, as GI is inserted into the model, stormwater volume for the simulation period is generated using the selected hydrologic model. By executing the generated model with numerous Monte Carlo simulations specified by the users, uncertainty bounds and probabilistic distributions of the simulation results are computed to assess the GI design scenario performance.

One key assumption of the SWMM 5.0 model relates to the area contributing stormwater to each GI practice. SWMM 5.0 is a lumped model that assumes a portion of each subwatershed, including impervious and pervious land, is being treated via the GI practices. The portion treated is usually based on the stormwater practitioner’s judgment or detailed engineering technical reports. In the current version of IDEAS_GI, the portion of the subwatershed, referred to as the contributing area, is assigned as an uncertain parameter. The lower uncertainty bound for the small GI contributing area is equal to the small GI area. The upper bound is computed as follows:

$$\begin{aligned}
 &Max_{Contributing\ area} \\
 &= GI\ area + \frac{GI\ area}{subwatershed\ pervious\ area} \\
 &\quad * subwatershed\ impervious\ area
 \end{aligned}
 \tag{Eq. 3.1}$$

Eq. 3.1 assumes that small GI at their maximum capacity treat a contributing area smaller than their area plus a proportion of the subwatershed impervious area. In other words, the assumption is that the rest of the pervious area within the subwatershed should treat the rest of the impervious area. In the next chapter, it will be shown that pollutant removal cost does not significantly change, after accounting for uncertainty in modelling parameters, once contributing impervious area changes from a proportional portion of the subwatershed to the entire available impervious area of the subwatershed. Therefore, proportional contributing impervious area can be used as the upper bound in the uncertainties in stormwater quality performance assessment.

Moreover, initial saturation (i.e. antecedent moisture content) is treated as another uncertain parameter in IDEAS_GI, since the effects of initial soil saturation on GI functionality in SWMM has been shown to be significant for design storms (Merz and Plate 1997; Davis 2008). It is assumed that soil moisture does not fall below the wilting point because GI practices are typically watered in semi-urbanized environments. For small GI design purposes, it is assumed that the moisture content does not exceed field capacity, indicating that there is enough time lag between storm events to allow the excess moisture to drain from the GI practices. In the next chapter, the complete ranges for all the uncertain parameters required for the SWMM and cost/benefit models used in this study are demonstrated.

To model rain garden practices, the pre-defined rain garden practices are used in SWMM 5.0. Once users specify rain garden parameters via the GI Designer Web application, IDEAS_GI uses the relevant parameters, based on the inputs given by the users (highlighted in Table 3.2), and generates new SWMM 5.0 input files. The location feature is used to overlay the rain garden and tree area over the area specified by the SWMM 5.0 subwatersheds. In the instruction manuals for the supporting files (see Appendix D), the approach used for defining the relative coordinates for the SWMM model subwatershed boundaries is described. If the geo-locations of the subwatershed boundaries are defined accurately in SWMM 5.0, each rain garden and tree within the area of the watershed will be inserted into at least one subwatershed. If the area of the rain garden overlays multiple subwatersheds, the subwatershed that includes most of the area (>90%) is assumed to contain the entire rain garden area. Otherwise, the rain garden area is allocated proportionally among all of the subwatersheds that it overlays. The other soil-related parameters are imported directly into the rain garden module in the SWMM 5.0 model. To model stormwater capture of trees in SWMM, rain barrels with a geo-location equal to the location of the inserted tree are used. The storage volume of rain barrels is assumed to be equal to the Leaf Area Index multiplied by a storage factor, which is a function of stratum type (Tague and Band 2004b). Since there is little evidence on the significance of stormwater nutrient treatment using trees (Denman et al. 2006; Read et al. 2008), stormwater treatment is excluded from the tree benefits estimation.

Once the SWMM 5.0 models are executed, masses of pollutants are compared to a baseline scenario, in which there is no GI present, and the flows are calibrated with data specific to the watershed area. In the next chapter, the modelling parameters and approaches used in SWMM 5.0 to quantify the uncertainties of pollutant masses at watershed and subwatershed outlets across the case study watersheds are specified. The baseline time series are located within CSV supporting files, to which results of SWMM 5.0 simulations are compared. The comparison includes total cumulative flow reduction, total pollutant load reduction, peak flow reduction and average flow reduction at the watershed outlet throughout the entire simulation period.

To determine the life cycle cost of GI practices, the WERF SELECT model is used (WERF 2015). The model provides a flexible framework in which maintenance and life cycle costs of GI practices can be computed by entering user-specified parameters (e.g., installation type, maintenance frequency, and unit construction cost). The WERF model follows engineering economics concepts to determine return on investment of GI practices. To implement the model, it is extracted from spreadsheets and embedded it as a function in the IDEAS_GI Python script.

To determine the extent of air pollutant deposition, empirical deposition equations were deployed from the i-Tree Streets Model (Soares et al. 2011). This model estimates the mass of air pollutants that potentially deposit over the leaf area of GI practices throughout their life cycle. As with the cost estimation model, the empirical deposition equations were extracted and implemented them in the IDEAS_GI Python script with uncertainty ranges for ozone (O_3), particulate matter ($PM_{2.5}$), sulfur dioxide (SO_2), nitrogen dioxide (NO_2), and carbon monoxide (CO) throughout the entire simulation period. The simulation period for air pollutant deposition is different from the simulation period used for design storms, which is a few hours after the termination of rainfall. The air pollutant simulation period relies on the time-period specified by the users in the supporting files and should be at least a year, since the air pollutant deposition values are reported on an annual basis. For each day within the simulation period, average daily concentrations of each pollutant should be included in the supporting CSV files. It is assumed that the concentrations are uniformly distributed throughout the day and then, using empirical models from the i-Tree Streets model (Nowak et

al. 2006), the amount of pollutant deposition over the leaf surface area of the rain gardens and trees is computed for each scenario. The bounds for all uncertain parameters is provided in appendices G and H, which allows IDEAS_GI to provide ranges of results using Monte Carlo simulation for all categories of benefits and costs.

3.4. Application of IDEAS_GI to case studies

The two watersheds presented in Chapter 2, Dead Run and Stoney Run, serve as case studies for demonstrating IDEAS' capabilities.

3.4.1. Required steps to execute the two case studies

The two case studies demonstrate two different ways that users can apply IDEAS. IDEAS_GI has been programmed and designed to handle Dead Run (DR5) as an embedded case study. Therefore, supporting files for Case Study I (See Fig. 3.3 and Table 3.1) are stored in the IDEAS_GI zip folder when users run IDEAS_GI for the first time. This means that users are already equipped with SWMM 5.0 models, results of the baseline simulation, and a database of annual ambient air pollutant concentrations. As a result, users only need to log in to HydroShare, navigate to the resource page, follow instructions to access IDEAS_GI Jupyter notebook, and then easily design GI scenarios using GI Designer and produce results in the output report (Fig. 3.8a).

However, IDEAS_GI is also capable of assessing performance of GI practices at other locations, as illustrated by Case Study II, Stoney Run Watershed. As mentioned previously, users can execute IDEAS_GI for their region and time frame of choice using the supporting documentation to guide them. Users can also modify the scripts to adjust parameters to their region of interest. The IDEAS_GI package, accessible on HydroShare, contains two Jupyter notebooks, i.e. "IDEAS_GI_DeadRun" and "IDEAS_GI", "IDEAS_GI" notebook is the generic implementation for any watershed. Fig. 3.8 shows the steps required for each of the case studies.

Accessing the second version (Fig. 3.8b) requires similar steps to the first notebook. However, the second notebook requires users to upload SWMM 5.0 data and a model for their case study area into the Jupyter environment. Users also need to upload a database of the supporting files (see Table 3.1) specific to the case study area to the Jupyter compute environment. Then users navigate to the Jupyter IDEAS_GI notebook and execute initial cells to run baseline scenarios, as well as specify parameters needed for their analysis (e.g. period of the analysis and number of iterations that SWMM 5.0 models should be executed to generate probabilistic distributions of GI performance). The remaining steps (Fig. 3.8b) are similar to those of Case Study I with a pre-implemented SWMM 5.0 model. Appendix D shows the instructions and required parameters to run the second case study. More details about this version of IDEAS is provided in Appendices C and D.

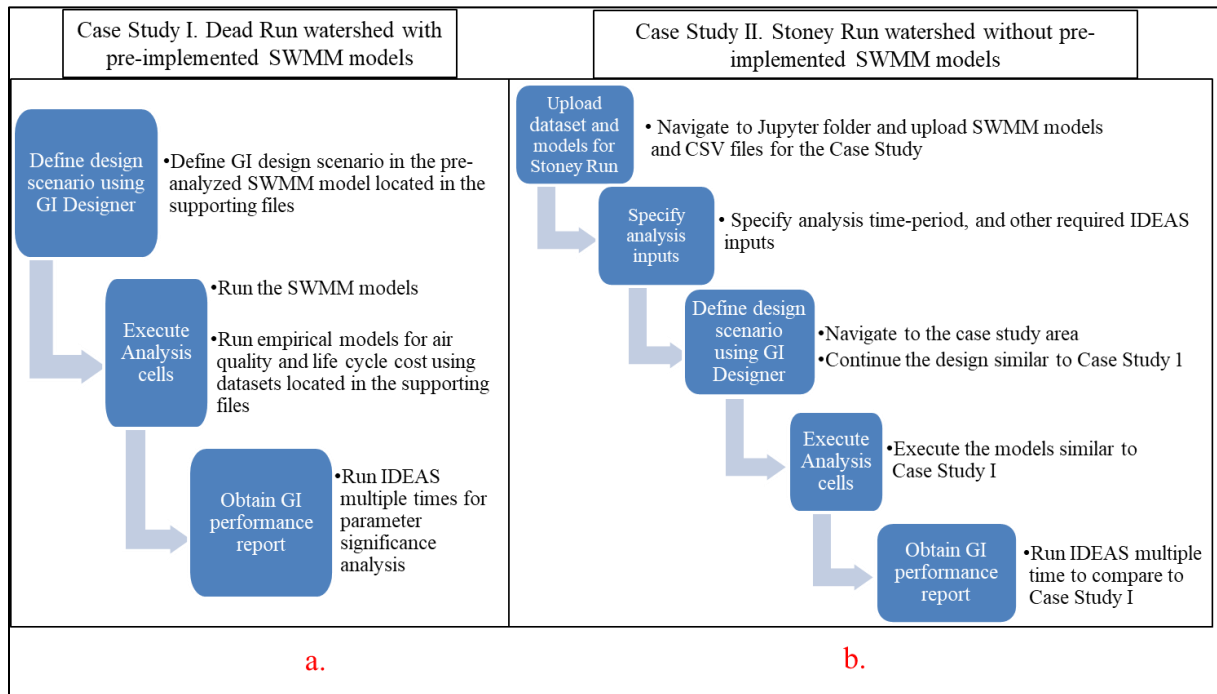


Fig. 3.8. Steps taken for the two case studies, demonstrating pre-implemented models (a. Case Study I) and generic models (b. Case Study II)

3.5. Results and discussion

In this section, the results of IDEAS_GI executions to address two different questions are discussed:

- How do IDEAS_GI simulation results differ between Case Study I and Case Study II (DR5 and SR5, respectively) for similar coverages of GI treatments?
- How do soil depth, soil type, stratum type, and stratum size affect stormwater capture and treatment results?

The first question addresses how implementation scale affects simulation results. Within the IDEAS_GI environment, in addition to location and geometric shape of GI features, users need to either specify or use pre-defined parameters to execute every GI scenario (Figs. 3.4d, and 3.4c). The parameters for rain gardens are soil depth and type, while trees require size, stratum type and species type. The second question focuses on how these parameters affect the results for the DR5 watershed, since the overall reduction of stormwater volume and peak flow were higher in DR5 compared to SR5. Moreover, SR5 had only a few potential locations to insert trees, and therefore it was not a representative case study to show the magnitude of tree impacts.

3.5.1. Comparison of Case Study I and II simulation results

To compare simulation results between the two watersheds, several design scenarios are defined in which a certain percentage of the total area available for GI implementation is allocated to GI, specifically rain garden practices. Then, benefits of the design scenarios are computed and compared for the two watersheds across 750 Monte Carlo simulations for all design scenarios. This minimum number of iterations was selected by simulating 100, 250, 500, 750, 1000, 1250, 1500, and 2000 Monte Carlo iterations for one individual subwatershed and observing the minimum value when the distribution of the total nitrogen load are stabilized. Table 3.3 shows the results of the simulations for each scenario with different percentages of impervious area treated by GI.

As shown in Table 3.3, with an increase in overall GI implementation in the two watersheds, absorbed storm water volume increases during the two design storms and peak flow decreases as expected. However, the rate of change in additional benefits provided through GI implementation does not increase linearly with more GI implementation.

It can be observed that, considering uncertainties in both nitrogen reduction and removal through treatment facilitated by GI, the amount of reduced nitrogen does not vary significantly across the GI coverage scenarios. This observation suggests that GI nitrogen treatment reaches its maximum capacity at a percentage equal to or lower than 16% for the two watersheds under the two design storms. It can be concluded that stormwater volume reduction and treatment, once normalized by the subwatershed area of GI, are generally larger for scenarios with a lower percentage of GI than those with higher coverages, with the modelling assumption used in this case study, (routing, lack of exchange between stormwater and underground water tables, etc.). This shows that covering the entire available area with GI does not yield higher efficiency in stormwater treatment and capture.

Furthermore, comparing the two watersheds together, we notice that the percentages of stormwater volume removal and peak flow reduction are significantly lower for SR5 compared to DR5. In fact, the percentages in volume reduction for the DR5 watershed were higher than those for SR5, $5.0\% \pm 0.3\%$ vs $0.6\% \pm 0.3\%$ and $4.4\% \pm 1.1\%$ vs $1.2\% \pm 0.1\%$ for the 2-year design storm and 10-year design storm, respectively, compared to the SR5 watershed. Also, the percentages in peak flow reduction for the DR5 watershed were higher than those for SR5, $4.5\% \pm 0.3\%$ vs $1.0\% \pm 0.5\%$ and $0.43\% \pm 0.03\%$ vs $0.08\% \pm 0.04\%$ for the 2-year design storm and 10-year design storm respectively, compared to SR5. SR5 is a highly urbanized watershed with few locations suitable for rain garden implementation. Since the volume of the two design storms is large, and the total area that is suitable for GI implementation is relatively small, the reduced portion of stormwater volume and peak flow is also relatively small. Also, as mentioned previously, IDEAS is also capable of air pollutant deposition and life cycle cost estimation. Appendix E contains results for these parameters for all design scenarios presented in Table 3.3.

Table 3.3. Performance of different rain garden scenarios for stormwater capture and treatment in each of the two case study watersheds at their respective watershed outlets (Number in parenthesis is the percentage reduction in comparison to the baseline.)

DR5						
	2-year storm lasting for 120 minutes (4.3 cm of the rainfall)			10-year storm lasting for 120 minutes (6.6 cm of the rainfall)		
Percentage rain garden coverage	Peak flow Reduction [m ³ s ⁻¹] (%)	Total volume reduction [m ³] (%)	Total nitrogen load reduction (gr)	Peak flow Reduction [m ³ s ⁻¹] (%)	Total volume reduction [m ³] (%)	Total nitrogen load reduction (gr)
100	0.151 (4.93)	870 (5.49)	63.3 ± 15.1	0.248 (0.48)	1653 (5.43)	124.8 ± 31.6
75	0.144 (4.68)	826 (5.21)	64.4 ± 16.8	0.234 (0.46)	1568 (5.15)	126.5 ± 35.0
64	0.140 (4.56)	805 (5.07)	66.1 ± 16.0	0.228 (0.44)	1530 (5.03)	129.9 ± 33.2
50	0.136 (4.42)	780 (4.92)	66.7 ± 19.7	0.220 (0.43)	1482 (4.87)	130.6 ± 40.5
32	0.130 (4.23)	744 (4.70)	66.1 ± 19.3	0.210 (0.41)	1419 (4.66)	129.2 ± 39.7
16	0.124 (4.03)	708 (4.46)	67.6 ± 21.00	0.200 (0.39)	1357 (4.46)	131.7 ± 42.7
Baseline Scenario	Peak flow [m³s⁻¹] 3.072	Total volume [m³] 15846	Total nitrogen load (gr) 3931.2	Peak flow [m³s⁻¹] 51.622	Total volume [m³] 30450	Total nitrogen load (gr) 5768.7
SR5						
100	0.007 (1.44)	28 (1.03)	9.0 ± 3.6	0.011 (0.14)	60 (1.24)	16.2 ± 6.6
75	0.008 (1.56)	22 (0.82)	9.2 ± 3.7	0.008 (0.10)	58 (1.21)	16.5 ± 6.7
64	0.006 (1.32)	18 (0.65)	9.0 ± 3.8	0.007 (0.08)	58 (1.21)	16.0 ± 6.9
50	0.004 (0.91)	14 (0.51)	9.3 ± 3.8	0.006 (0.08)	57 (1.20)	16.4 ± 6.8
32	0.002 (0.44)	8 (0.29)	9.3 ± 4.0	0.004 (0.05)	57 (1.19)	16.5 ± 7.0
16	0.001 (0.30)	5 (0.17)	9.4 ± 4.2	0.003 (0.03)	57 (1.20)	16.6 ± 7.4
Baseline Scenario	Peak flow [m³s⁻¹] 0.482	Total volume [m³] 2740	Total nitrogen load (gr) 314.5	Peak flow [m³s⁻¹] 7.909	Total volume [m³] 4825	Total nitrogen load (gr) 461.5

Next, to see how these findings translate to real-world conditions, the performance of the GI networks is assessed for continuous rainfall records between 2007 and 2010. The number of Monte Carlo simulations used in this section is the same as for the previous analysis conducted for design storms. Table 3.4 shows the magnitude and percentage of reductions in peak flow, total flow volume, and total nitrogen load at the two watershed outlets for the three-year rainfall period. The percentage reduction in peak flow falls between that of the 2-year and 10-year design storms, suggesting that the most intense storm within the three-year period had an intensity higher than the 2-year storm and lower than the 10-year storm.

Also, similar to the design storms, the percentage of stormwater volume that was reduced via GI is not significant. Although implementation of GI reduces the intensity of peak flow, the stormwater eventually follows its route to the outlet, assuming enough time has passed after the end of rainfall and the time of concentration. On the other hand, the reductions in nitrogen load are more significant than storm water volume and peak flow. This is due to the SWMM model assumption that a nutrient/ pollutant deposited on GI is removed from the system and does not end up in the watershed outlet.

Table 3.4. Performance of different rain garden scenarios for stormwater capture and treatment in each of the two case study watersheds at their respective watershed outlets (Number in parenthesis is the percentage reduction in comparison to the baseline.)

DR5			
Percentage rain garden coverage	Peak flow Reduction [m³s⁻¹] (%)	Total volume reduction [m³] (%)	Total nitrogen load reduction (gr)
100	0.31 (3.1)	178,300 (4.2)	15,600 ± 2,200
64	0.28 (2.8)	172,904 (4.0)	14,690 ± 2,260
32	0.26 (2.6)	88,950 (2.1)	12,450 ± 2,400
Baseline Scenario	Peak flow [m³s⁻¹] 10	Total volume [m³] 4,277,500	Total nitrogen load (gr) 131,720
SR5			
100	0.019 (1.1)	10,600 (3.1)	770 ± 50
64	0.017 (1.0)	8550 (2.5)	720 ± 35
32	0.014 (0.8)	4100 (1.2)	630 ± 20
Baseline Scenario	Peak flow [m³s⁻¹] 1.751	Total volume [m³] 342,200	Total nitrogen load (gr) 10,537

3.5.2. Effect of GI design parameters on simulation results

To assess how the design features that users can specify via GI Designer affect the simulation results, two design scenarios for both trees and rain gardens were created. One design scenario consists of 3900 m² of rain garden coverage across all potential pervious areas in four small subwatersheds in DR5. The second scenario consists of 133 tree installations covering the entire potential pervious area in the same four subwatersheds in DR5. The scenarios, detailed in Appendix F, explore how the soils and stratum parameters affect the design performance. The Jupyter notebook is executed for each scenario and the results are stored as CSV files in the JupyterHub environment. The simulation results at the subwatershed level are summarized in Tables 3.5-3.7 for different types and depths of raingarden soil and different sizes and stratum types for tree installations, respectively. The baseline scenario, in which there are no trees and raingardens inserted, computes flow and nitrogen load throughout the design storm simulation period, in addition to time of concentration, at the four subwatershed outlets.

Table 3.5 shows that the amount of peak flow reduction, stormwater volume reduction, and nitrogen uptake at the four subwatershed outlets does not change significantly among different soil types, even for rain gardens with high hydraulic conductivity soils. Note that when a soil type is changed, all of its parameters, including suction head and hydraulic conductivity, are also changed to generate the results presented in Table 3.5. The table shows the hydraulic parameter values, soil suction head, and initial moisture deficit for each soil type at a soil depth of 0.5 meters, which is the median soil depth among the three depths available in IDEAS_GI (0.25m, 0.5m, 1m).

The only parameter that seems to slightly affect stormwater capture and treatment is the depth of rain gardens, as shown in Table 3.6. To generate Table 3.6, soil depth is varied while soil type is consistent, i.e. clay, across all scenarios. According to the table, an increase in the depth of rain gardens results in a slight increase in stormwater capture and nutrient load reduction. Therefore, it can be concluded that using the presented modelling assumptions and approaches, and more importantly the magnitude of design storms, cumulative benefits even at the subwatershed scale show no significant differences between different soil

types from rain gardens and trees as small GI practices. From another point of view, once GI coverage increases across the watershed, the cumulative effects of the network of GI practices show higher reductions in peak flow and cumulative volume of absorbed stormwater (see DR5 case in Table 3.3).

Comparing the performance of the rain garden installations between the two design storms for each of the soil types (see Table 3.5), it can be noticed that volume and peak flow reductions for the 10-year design storm is almost 1.5 times more than that of the 2-year design storm. However, the percentage reduction in peak flow and cumulative stormwater volume is not significantly different between the two design storms. Note that the reduction in peak flow and storm water volume for the two storms are small even at the subwatershed outlets, meaning that even numerous installations of rain garden and trees do not have significant overall impact for the given design storms.

Table 3.6 shows the results of simulations for different soil depths, again for numerous rain garden installations. The results show a slight dependence of the results, computed at subwatershed scale, on the soil depth of the rain gardens. Rain gardens with a depth of one meter perform slightly better in stormwater capture and treatment in comparison to the rain gardens with lower depths. Despite the fact that the simulation results are compared at the four subwatershed outlets between baseline and design scenarios, and not at the watershed outlet, the impacts of the installations are small. More importantly, the design storms used in this study, although selected based on Maryland design guidelines, have a high rainfall volume. The magnitude and intensity of the rainfalls is a contributing factor in the low performance of small GI practices in capturing and treating stormwater in this case study.

Table 3.7 shows the results of stratum type and tree size on the hydrologic performance of trees for stormwater capture and treatment. The design scenario consists of 133 installations, which is the total number of available locations for tree implementation, of three tree types (deciduous, eucalyptus, and evergreen) across four subwatersheds in DR5 Watershed. The locations of the tree installations can be found in Appendix E. Among the three canopy types that IDEAS_GI is capable of simulating (Leonard et al.

2018), deciduous performs slightly better in comparison to the other species. Deciduous has a higher storage factor, 0.197, in comparison to those of the other two stratum types (0.0094, and 0.0394). As a result, the surrogate rain barrels, designed to represent trees in SWMM 5.0, have a higher storage volume, resulting in significantly larger reductions in stormwater volume.

Also, an increase in tree size generally increases stormwater capture and peak flow reduction, since a larger tree has more leaf surface area to intercept stormwater. However, for such large storms, implementation of GI practices do not result in tangible hydrological benefits. A network of green infrastructure practices merged with conventional gray infrastructure practices may be a more viable solution to mitigate stormwater volume and peak flow reduction (Wang et al. 2013).

Table 3.5. Effect of soil type in stormwater capture and treatment at the DR5 subwatershed outlets in the rain garden scenario (numbers in parentheses show reductions in percentages compared to baseline scenario.)

Soil type [average hydraulic conductivity (cm/hr), average capillary suction head (cm), Initial moisture deficit as fraction]	2-year storm lasting for 120 minutes (4.3 cm depth of the rainfall)			10-year storm lasting for 120 minutes (6.6 cm depth of the rainfall)			
	Peak flow reduction range [m ³ s ⁻¹] (%)	Total volume reduction range [m ³] (%)	Total nitrogen load reduction range (gr)	Peak flow Reduction [m ³ s ⁻¹] range (%)	Total volume reduction range [m ³] (%)	Total nitrogen load reduction range (gr)	
Sand [23.5, 4.9, 0.346]	0.02± 0.01 (1.1± 0.5%)	1.3± 0.6 (1.0± 0.7%)	1.0 ± 0.7	0.03± 0.01 (0.9± 0.4%)	2.4± 1.1 (0.8± 0.4%)	1.7 ± 1.0	
Loamy-Sand [6.0, 6.1, 0.312]	0.02± 0.01 (1.1± 0.5%)	1.3± 0.6 (1.0± 0.7%)	1.0 ± 0.7	0.03± 0.01 (0.9± 0.4%)	2.4± 1.1 (0.8± 0.4%)	1.7 ± 1.0	
Sandy-Loam [2.2, 11.0, 0.246]	0.02± 0.01 (1.1± 0.5%)	1.3± 0.6 (1.0± 0.7%)	1.0 ± 0.7	0.03± 0.01 (0.9± 0.4%)	2.4± 1.1 (0.8± 0.4%)	1.7 ± 1.0	
Silt-Loam [0.68, 16.7, 0.171]	0.02± 0.01 (1.1± 0.5%)	1.3± 0.6 (1.0± 0.7%)	1.0 ± 0.7	0.03± 0.01 (0.9± 0.4%)	2.4± 1.1 (0.8± 0.4%)	1.7 ± 1.0	
Loam [1.3, 8.9, 0.193]	0.02± 0.01 (1.1± 0.5%)	1.3± 0.6 (1.0± 0.7%)	1.0 ± 0.7	0.03± 0.01 (0.9± 0.4%)	2.4± 1.1 (0.8± 0.4%)	1.7 ± 1.0	

Table 3.5 (cont.) Effect of soil type in stormwater capture and treatment at the DR5 subwatershed outlets in the rain garden scenario (numbers in parentheses show reductions in percentages compared to baseline scenario.)

Soil type [hydraulic conductivity (cm/hr), capillary suction head (cm), Initial moisture deficit]	2-year storm lasting for 120 minutes (4.3 cm depth of the rainfall)			10-year storm lasting for 120 minutes (6.6 cm depth of the rainfall)		
	Peak flow reduction range [m ³ s ⁻¹] (%)	Total volume reduction range [m ³] (%)	Total nitrogen load reduction range (gr)	Peak flow Reduction [m ³ s ⁻¹] range (%)	Total volume reduction range [m ³] (%)	Total nitrogen load reduction range (gr)
Sandy-Clay-Loam [0.3, 21.9, 0.143]	0.02± 0.01 (1.1± 0.5%)	1.3± 0.6 (1.0± 0.7%)	1.0 ± 0.7	0.03± 0.01 (0.9± 0.4%)	2.4± 1.1 (0.8± 0.4%)	1.7 ± 1.0
Clay-Loam [0.2, 20.1, 0.146]	0.02± 0.01 (1.1± 0.5%)	1.3± 0.6 (1.0± 0.7%)	1.0 ± 0.7	0.03± 0.01 (0.9± 0.4%)	2.4± 1.1 (0.8± 0.4%)	1.7 ± 1.0
Sandy-Clay [0.12, 23.9, 0.091]	0.02± 0.01 (1.1± 0.5%)	1.3± 0.6 (1.0± 0.7%)	1.0 ± 0.7	0.03± 0.01 (0.9± 0.4%)	2.4± 1.1 (0.8± 0.4%)	1.7 ± 1.0
Silty-Clay-Loam [0.2, 27.3, 0.105]	0.02± 0.01 (1.1± 0.5%)	1.3± 0.6 (1.0± 0.7%)	1.0 ± 0.7	0.03± 0.01 (0.9± 0.4%)	2.4± 1.1 (0.8± 0.4%)	1.7 ± 1.0
Clay [0.06, 31.6, 0.079]	0.02± 0.01 (1.1± 0.5%)	1.3± 0.6 (1.0± 0.7%)	1.0 ± 0.7	0.03± 0.01 (0.9± 0.4%)	2.4± 1.1 (0.8± 0.4%)	1.7 ± 1.0
Silt-Clay [0.1, 29.2, 0.092]	0.02± 0.01 (1.1± 0.5%)	1.3± 0.6 (1.0± 0.7%)	1.0 ± 0.7	0.03± 0.01 (0.9± 0.4%)	2.4± 1.1 (0.8± 0.4%)	1.7 ± 1.0

Table 3.6. Effect of soil depth in stormwater capture and treatment at the DR5 subwatershed outlets in the rain garden scenario (numbers in parentheses show reductions in percentages compared to baseline scenario.)

Depth (Meter)	Peak flow reduction range [m³s⁻¹] (%)	Total volume reduction range [m³] (%)	Total nitrogen load reduction (gr)	Peak flow reduction range [m³s⁻¹] (%)	Total volume reduction range [m³] (%)	Total nitrogen load reduction range (gr)
0.25	0.02± 0.01 (1.1± 0.5%)	1.3± 0.6 (1.0± 0.7%)	1.0 ± 0.7	0.03± 0.01 (0.9± 0.4%)	2.4± 1.1 (0.8± 0.4%)	1.7 ± 1.0
0.5	0.02± 0.01 (1.1± 0.5%)	1.3± 0.6 (1.0± 0.7%)	1.0 ± 0.7	0.03± 0.01 (0.9± 0.4%)	2.4± 1.1 (0.8± 0.4%)	1.7 ± 1.0
1	0.02± 0.01 (1.1± 0.5%)	1.3± 0.6 (1.0± 0.7%)	1.2 ± 0.5	0.03± 0.01 (0.9± 0.4%)	2.4± 1.1 (0.8± 0.4%)	2.0 ± 1.0

Table 3.7. Effects of stratum type and tree size on stormwater capture and treatment at the DR5 subwatershed outlets in the tree scenario (numbers in parentheses show reductions in percentages compared to baseline scenario.)

	2-year storm lasting 120 minutes (4.3 cm rainfall depth)		10-year storm lasting 120 minutes (6.6 cm rainfall depth)	
Stratum type	Peak flow Reduction [m³s⁻¹] (%)	Total volume reduction [m³] (%)	Peak flow Reduction [m³s⁻¹] (%)	Total volume reduction [m³] (%)
Evergreen	0.02± 0.01 (1.1± 0.5 %)	1.0± 0.7 (0.9± 0.7%)	0.02± 0.02(0.8± 0.5%)	1.8± 1.4 (0.7± 0.4%)
Eucalypt	0.02± 0.01 (1.1± 0.5 %)	1.0± 0.7 (0.9± 0.7%)	0.02± 0.02(0.8± 0.5%)	1.8± 1.4 (0.7± 0.4%)
Deciduous	0.03± 0.01 (1.6± 0.5 %)	1.0± 0.7 (0.9± 0.7%)	0.03± 0.02(1.2± 0.5%)	1.8± 1.4 (0.7± 0.4%)
Tree size (radius)	Peak flow Reduction [m³s⁻¹] (%)	Total volume reduction [m³] (%)	Peak flow Reduction [m³s⁻¹] (%)	Total volume reduction [m³] (%)
Large (4 ft)	0.02± 0.01 (1.1± 0.5 %)	1.0± 0.7 (0.9± 0.7%)	0.02± 0.02(0.8± 0.5%)	1.8± 1.4 (0.7± 0.4%)
Medium (2 ft)	0.02± 0.01 (1.1± 0.5 %)	1.0± 0.7 (0.9± 0.7%)	0.02± 0.02 (0.8± 0.5%)	1.8± 1.4 (0.7± 0.4%)
Small (1 ft)	0.02± 0.01 (1.1± 0.5 %)	1.0± 0.7 (0.9± 0.7%)	0.02± 0.02(0.8± 0.5%)	1.8± 1.4 (0.7± 0.4%)

3.6. Summary of the case study results

Several sets of simulations were conducted to assess the sensitivity of the simulation results to GI parameters, as well as the difference in simulation results across the two case studies in portions of Stoney Run and Dead Run Watersheds in Baltimore City and County, respectively. The results show that variations in soil depth and rain garden parameters do not lead to tangible reductions in peak flow and cumulative flow at the DR5 outlet for the design storms specified by the government design manuals used in this study. Also, the choice of storm event frequency greatly affects the significance of GI design, even after implementing GI at all potential locations across a watershed, to the extent that the GI installations might not show promising stormwater volume and peak flow reduction under some design storms. Therefore, future research can further investigate the magnitude of design storms that are most suitable and practical in the design guidelines for small GI practices.

Comparing the simulation results for both design storms and continuous rainfall records in SR5 and DR5 watersheds, the effects of GI practices in SR5, which is smaller and highly urbanized, are not as significant as in DR5, even after implementation in all potential locations across the watershed. DR5 is a semi-urbanized watershed with considerably more suitable area to implement GI practices, which enables higher benefits. Future research is needed to further investigate the impacts of different types of GI, including larger-scale and networks of GI, in other types of watersheds and for different design storms.

Moreover, the overall percentages of reductions in peak flow and stormwater volume for continuous rainfall records are not significantly higher than those for the design storms. This observation suggests that the rainfalls within the three-year simulation period were similar to the design storms and that most of the stormwater captured across the watershed via GI eventually finds its way to the watershed outlet. However, nitrogen load reduction shows more promise over the long term, suggesting that more focus should be given to design for stormwater quality improvement via GI practices.

The next chapter explores the stormwater-related performance and other benefits/costs associated with different GI networks at different spatial scales in more depth. IDEAS_GI is used for detection of potential locations for GI implementation and preliminary assessment of GI performance prior to a more detailed design and planning process.

3.7. IDEAS_GI capabilities and future development directions

The IDEAS_GI software provides an interface for interactive modelling of GI practices at site to watershed scales. Considering the scope and features, Table 3.8 summarizes how IDEAS_GI can address specific needs of different types of users.

Table 3.8. Potential IDEAS_GI users for different applications

User	Application
Stormwater engineers and planners	Initial off-site assessment of GI installation feasibility
Property owners	Preliminary analysis of GI-provided costs and benefits, previews of GI appearance after installation
Municipalities as potential large-scale planners	Simulation of watershed behavior after implementation of numerous GI practices throughout the network of subwatersheds. Identification of the most promising areas for more detailed investigations of GI suitability.

IDEAS_GI is open source and allows users to upload datasets and models of any watershed, navigate to the latitude and longitude of interest, insert GI practices, and obtain preliminary estimates of costs and benefits of such practices. The software also provides a framework for other modelling practices to be merged with the Google™ Satellite-view and Google™ Street-view editors.

IDEAS_GI provides a reasonable representation of estimated hydrographs based on selections of routing time steps, routing method, infiltration method, resolution of subwatersheds, and parameters used for each subwatershed. Therefore, IDEAS_GI users must calibrate and verify their models to address these factors prior to uploading to the Jupyter environment. The hydrologic/hydraulic models that are coupled with IDEAS_GI can vary in terms of execution time, spatial and time scale, routing and infiltration approaches, and rainfall duration. Therefore, IDEAS_GI can assist hydrologists, engineers, and practitioners as a flexible modeling package with an interactive representation of landscapes that can be shared with stakeholders to support GI implementation. IDEAS_GI can also provide a comparative estimation of how GI design scenarios perform in terms of stormwater quantity reduction and quality improvement in comparison to other scenarios.

IDEAS_GI was presented at a workshop entitled “IDEAS_GI Software: Interactive Visual Design Tool for Exploring Green Infrastructure Potential at Neighborhood to Watershed Scales” in April 2017 at the USGS Center in Catonsville, MD. The workshop involved practitioners and stormwater engineers, mostly from the Baltimore area. Participants found the tool useful in providing insights on cost/benefit assessments of future GI practices. One future direction, based on the feedback received from participants, is to demonstrate the degree of mitigation in flood hazard potential and associated costs for each type of GI design. Rivera (2018) used data-driven approaches to assess changes in flash and river flooding potential, considering social vulnerability and urban heat island. Future versions of the software can incorporate such approaches.

Attendees were also interested in adding a feature to assess the impervious area treated for each design. According to Maryland Department of Environment regulations, property owners are required to allocate 20% of their pervious land to GI practices in order to treat their respective impervious land, thus satisfying a municipal separate storm sewer system (MS4) permit (Maryland Department of the Environment 2009). Thus, attendees wanted to see if the IDEAS_GI tool can specify geographic areal boundaries of the area treated for each GI practice. Leonard et al. (2019) introduced the IDEAS_GI version merged with

RHESSys, which provides a high-resolution patch-based map in which contributing cells to every patch have already been assigned. Future versions of the software would integrate the two modelling approaches to address this need.

IDEAS_GI can also be used to investigate whether candidate designs will help municipalities meet stormwater-related objectives or regulations, e.g. Total Maximum Daily Load (TMDL) management. Incentives (e.g., stormwater trading permits, taxes, or rebates) can be applied at neighborhood or watershed scales to encourage sufficient GI installation. Therefore, one future software development path would add a capability in IDEAS_GI to examine whether GI designs are complying with regulations. Considering the ranges of uncertainties that IDEAS_GI provides for every design scenario, the software could provide a probability that a given scenario will meet environmental regulations in the case study area. IDEAS_GI could also be adapted to assess the impacts of proposed regulations on GI installation and performance.

Lastly, workshop attendees discussed that more realistic representations of rain gardens and bioswales could encourage users, particularly homeowners, to implement GI. Regarding co-benefits, sustainability offices and advocates as well as capital investors might also be interested to use IDEAS_GI to justify their investments. Having a more realistic representation of GI implementations in neighborhoods should assist decision makers and planners in assessing and communicating the benefits of proposed installations, thus facilitating GI installation at larger scales. This can then support more detailed design studies at the most promising locations.

Chapter 4: Spatial Scale Effects on Uncertainty and Sensitivity in Green Infrastructure Cost/Benefit Assessment

4.1. Introduction

GI has been implemented increasingly throughout the US as an environmental amenity, mostly as individual projects by the private sector (i.e., property owners), rather than integrated, community-wide efforts (Young 2011). One significant barrier to community-wide planning is the lack of standardized modeling approaches as well as consideration of uncertainty (Nylen and Kiparsky 2015). As mentioned in Chapter 1, there are a myriad of tools to address GI design and performance assessment, each having their own specific features and limitations (Zoppou 2001; Elliott and Trowsdale 2007; Jayasooriya and Ng 2014). These tools don't assess co-benefits or cost/benefit impacts at multiple scales to assess whether GI investment is financially justifiable. Also, since they use deterministic simulation models, they do not assess how uncertainties inherent in the modeling approaches affect their results (CNT 2010; Environmental Protection Agency 2014). More detailed cost/benefit analyses are needed to better inform practitioners of the outcomes of their investments and potentially lead to more use of GI (Vandermeulen et al. 2011). These shortcomings are some of the reasons that such tools are not widely used for real-world decision-making.

In the peer-reviewed literature, Niu et al. (2010) have analyzed benefits and costs of green roof technologies, with more focus on energy savings, relative to conventional roof systems in Washington DC. Liu et al. (2016) have also conducted a cost-benefit analysis of different green infrastructure options in a case study in Beijing. However, neither of these studies considered the impacts of uncertainty and spatial scales. Clark et al. (2008) performed a probabilistic economic analysis of the environmental benefits of green roofs, but focused solely on a single installation. Kousky et al. (2013) estimated avoided flood damages in a case study in Wisconsin, and concluded that with careful placing of green infrastructure in a watershed, benefits can exceed costs. However, they did not address uncertainty and focused solely on flooding reduction. Some other studies have primarily focused on comparative trade-off analyses between green and gray (i.e. conventional drainage and pipe system) stormwater infrastructure using a regret-based

approach and life cycle assessment (Casal-Campos et al. 2015; Wang et al. 2013). These studies demonstrate that combinations of gray and green infrastructure provide a more robust option for combined sewer overflow (CSO) reduction and water quality improvement compared to using each option individually.

To build on this work, this study analyzes the uncertainty of GI benefits and costs at multiple spatial scales (i.e. household, subwatershed and watershed scales) for the DR5 case study watershed described in Chapter 2. To compute benefits and costs of GI practices, two analysis metrics are used: Benefit-Cost Ratio (BCR) and nutrient removal costs from stormwater. It is worth noting that the definition of the BCR metric is one of the contributions of this study. This metric facilitates comparison of different GI practices' stormwater treatment efficiency by using treated volume of stormwater, which is determined based on design guidelines.

This chapter specifically focuses on rain gardens and permeable pavements as small-scale practices that can be used throughout a watershed, typically on residential properties and parking lots, respectively. The methodology section highlights the rationale for selecting raingardens and permeable pavements as the GI practices, the categories of benefits and costs considered, the approaches used for modeling costs and benefits, and how uncertainties are quantified. In the results section, cumulative density functions of BCRs and nutrient removal costs, referred to as analysis metrics/ metrics, are presented at household, subwatershed and watershed scale via two different scenarios of uncertainty quantification approaches. The effect of uncertain parameters, as well as subwatershed-related parameters, on the analysis metrics is also investigated. Finally, in the discussion and conclusions section, the findings are summarized and suggestions for future research are provide.

4.2. Case study watershed

The case study area is the DR5 watershed (Fig. 4.1), located in Gwynns Falls Watershed in Baltimore County, Maryland (MD), that was described in Chapter 2. To identify locations suitable for GI

implementation, IDEAS_GI (Chapter 3) is used as an initial assessment tool. To model stormwater flow across the watershed, the SWMM numerical model is used (Rossman 2004) as in the previous chapter. To add rain garden practices to the SWMM 5.0 model, a percentage of potential candidate pervious area is assigned to rain gardens, referred to as the GI design scenario. To add permeable pavement, a percentage of impervious parking area is assigned for the GI design scenario. Then, the GI practices are modelled using the LID module in SWMM. The module assumes each practice consists of several layers, including surface and soil layers for rain gardens and surface, pavement, storage and seepage layers for permeable pavements (Rossman and Huber 2016).

Also, the models were calibrated for the nutrient loads, meaning that to create baseline scenarios with respect to nutrient load, there is a need to create baseline water quality scenarios based on the subwatershed and conveyance network arrangements. Literature review and probabilistic Monte Carlo simulations to assign SWMM input values to the layers for all GI practices were conducted. More details will be thoroughly explained in the next sections. Also, in the later sections, the details of results are presented with respect to four randomly selected subwatersheds that are shown in Fig. 4.1.

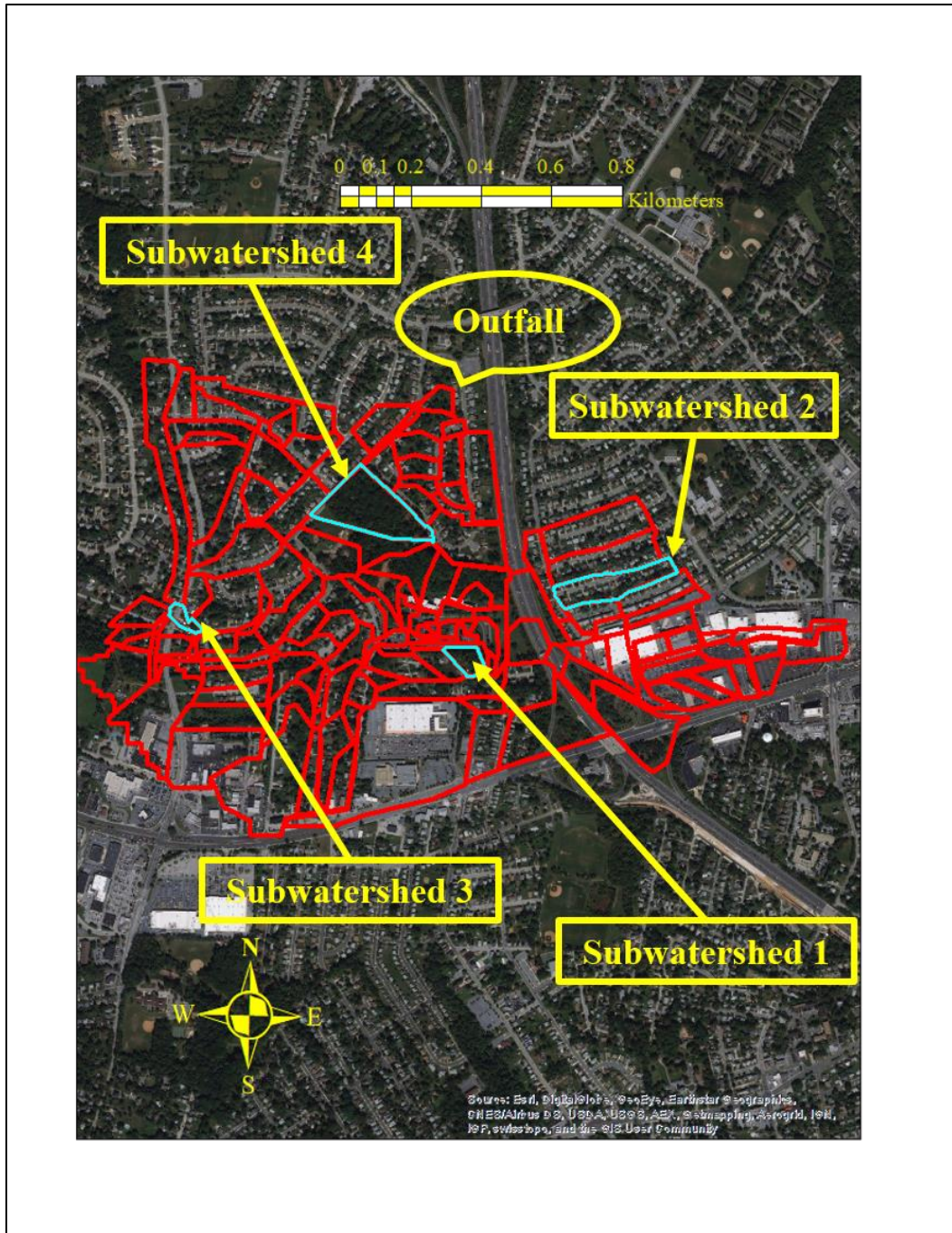


Fig. 4.1. Boundaries of DR5 Watershed and its subwatersheds as modeled in SWMM with four randomly selected subwatersheds

4.3. Methodology

This section elaborates on the methods and assumptions used in this chapter. First, justification for the types of GI practices is provided. Then, the categories of benefits and costs are specified, along with the two

analysis metrics, BCR and nutrient removal costs. Next, the details on the deployed models, the types and uncertainty bounds of the modeling parameters from the literature, and the economic valuation of environmental benefits are presented. Finally, how the uncertainty analysis is conducted and how the effects of the uncertain parameters on the final results are assessed at the three spatial scales (household, subwatershed, and watershed) are discussed. Fig. 4.2 summarizes the overall steps of the methodology, which can be applied to any case study. The first main step in the methodology is (a) the selection of GI types, relevant benefits and costs along with their assessment models, analysis metrics, uncertain modelling parameters, and economic valuation methods. This step allows the analysis to be customized to a particular case study. The second main step (b) involves uncertainty quantification. The last major step (c) consists of different methods to analyze the factors affecting analysis metric distributions. Later in this section, details about each of these steps are presented in more detail and descriptions of how each step has been applied to this case study are given.

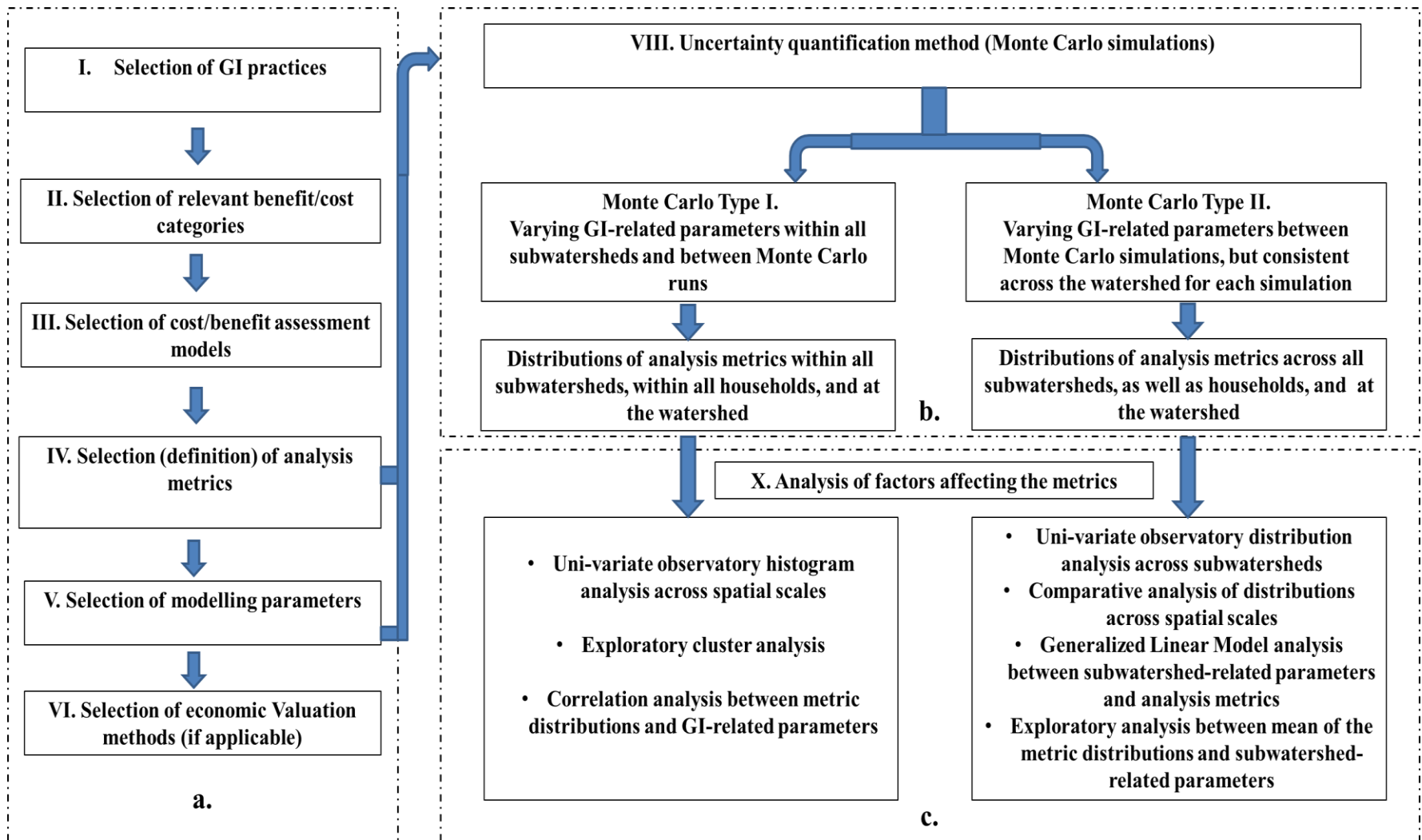


Fig. 4.2. Flow chart describing steps of the methodology

4.3.1. Selection of GI practices

Implementation of small GI practices needs to consider environmental feasibility and meet regulatory standards, which are specific to the case study area. Since environmental concerns in different urban environments vary, municipalities tend to emphasize types of GI practices that meet their environmental goals (Zuniga-Teran et al. 2019). Thus, city- and state-level regulations can significantly change the choice of GI practices in any given environment.

For this case study, Dead Run 5 Watershed (DR5) is semi-urbanized, hence most of its land cover consists of residential and commercial buildings and the types of feasible GI practices are limited. Retention ponds require a minimum contributing area of ten acres, according to Maryland guidelines (Maryland Department of Environment 2009), which is greater than the contributing areas of potential GI locations in the watershed. However, since there are 280 residential properties in Dead Run, numerous rain gardens could be implemented throughout the watershed on residential properties.

Furthermore, there are multiple commercial buildings within the watershed. Each commercial building in the case study area provides an opportunity for two types of GI: green roofs and permeable pavements. Implementation of other GI practices, rain gardens and bioswales, are not well-suited within the boundaries of commercial buildings in this case study, since the available area to implement such practices does not abide by the state of Maryland regulations for GI installations (Maryland Department of Permitting Services 2012). Green roofs, despite reducing peak flows from storm events, have not shown promising performance in reducing stormwater nutrients and pollutants (Berndtsson 2010b; Teemusk and Mander 2007). Thus, the focus is solely on permeable pavements and rain gardens as target GI practices in this study.

4.3.2. Selection of benefit categories

The benefits associated with GI implementation are not limited to stormwater management and air quality improvement. In fact, GI practices have been shown to have social benefits, which are not easily quantified, including community cohesion, stress and anxiety reduction, educational benefits, etc. (Li and Sullivan

2016; Holtan, et al. 2015; Hartig et al. 2014; Jiang et al. 2014). Among the quantifiable categories of benefits and costs, some are highly uncertain. For example, property value increase may be a quantifiable benefit, but there is no consensus in the literature to assess its impact (Adelaja et al. 2008; McConnell and Walls 2005). Furthermore, there has been extensive research to quantify the impacts of green space on urban heat mitigation (Rivera 2018; Zhang et al. 2017). However, assessing impacts on urban heat requires extensive data and computational power to address the complexities of the urban environment. Therefore, this study focuses on stormwater quality improvement, life cycle cost, and air pollutant deposition throughout the life cycle of GI practices. These categories are quantifiable and the literature supports quantification of their benefits and associated uncertainties. The reason stormwater quantity is excluded from the benefits is that monetary valuation methods typically rely on water treatment and water quality volume (WQV) instead of flash flooding (Weiss et al. 2007). More importantly, Total Maximum Daily Load (TMDL) for water quality improvement is one of the most important considerations for the case study watershed, which ultimately drains into Chesapeake Bay (Linker et al. 2013). The importance of TMDL highlights why water quality treatment has the highest priority in comparison to other environmental objectives in the case study area.

It is worth noting that the focus on water quality is due to TMDL concerns in the Chesapeake Bay. In fact, any given case study might have a unique environmental priority and objective, ranging from biodiversity preservation to pluvial flooding. Therefore, the category of benefit and costs, and subsequently the choice of modelling approach, will be specific to the case study.

4.3.3. Selection of cost/benefit assessment models

Similar to the selection of benefit categories, the choice of modelling approach is tailored to the scope, location, spatial scale and other specific properties associated with each case study. As mentioned in Section 4.2, in this study SWMM 5.0 is used to simulate stormwater quantity and quality before and after GI implementation at different spatial scales. As GI is inserted into the model, stormwater volume for the simulation period is generated. Then, masses of nutrients at watershed and subwatershed outlets throughout

the entire continuous rainfall period are compared to baseline scenario, in which there is no GI present. The baseline models, which were provided to us, were calibrated to mimic the hydrograph at the watershed outlet throughout the continuous simulation period. Therefore, the model did not account for nutrient load in the stormwater. To create baseline scenarios for nutrient loads at the subwatershed outlet, a series of probabilistic baseline simulations are executed without addition of GI. The probabilistic baseline simulations follow 750 Monte Carlo simulations that will be discussed in the “Uncertainty quantification” section, with the exception that GI practices are not included in the SWMM models. The SWMM model requires format of equation for nutrient build-up and wash-off during dry and wet periods of the simulation. The probabilistic parameters that are used to generate these scenarios are build-up constants applied in a power function for the nutrients during dry periods, wash-off constants applied in an event mean concentration formulation for nutrients during wet periods, and concentration of the nutrient in the rainfall. The specific ranges of these parameters are listed in Appendix G. It is worth noting that the three sets of aforementioned parameters are independent of each other.

To determine the life cycle cost of GI practices, the WERF SELECT model is used (WERF 2015). The model provides a framework in which maintenance and life cycle costs of GI practices can be computed by entering user-specified parameters (e.g., installation level, maintenance frequency, and unit construction cost). Since the model follows engineering economics concepts and is flexible, it was decided to extract its framework from spreadsheets, and write it in several Python scripts for its different modules, each associated with one of its life cycle elements.

To determine the extent of air pollutant deposition, empirical deposition equations from i-Tree Street Model (Soares et al. 2011) were used. This model estimates the mass of air pollutants that potentially deposit over the leaf area of GI practices throughout the simulation period. As with the cost estimation model, the equations used in the model were extracted and implemented in a Python script, which provides the range of ozone (O_3), particulate matter ($PM_{2.5}$), sulfur dioxide (SO_2), nitrogen dioxide (NO_2), and carbon monoxide (CO) throughout the entire simulation period. For each day within the simulation time period,

average daily concentrations of each pollutant are computed assuming the concentrations are uniformly distributed throughout the day. Then, using empirical models from the i-Tree Streets model (Nowak et al. 2006), the amount of air pollutant deposition over leaf surface area of rain gardens is computed for each scenario. In reality, such air pollutants that are deposited throughout the dry period over leaf area of rain gardens and vegetated surfaces are washed off during rainfall events and advected to downstream water bodies. However, since many of these air pollutants are not primary nutrients in stormwater quality monitoring and are not heavily regulated from a regulatory standpoint, soluble air pollutants are not traced in stormwater runoff downstream. Thus, in this study, only the monetary benefits of air pollutant deposition over leaf area of rain gardens are considered with regard to air pollutant deposition.

4.3.4. Selection of analysis metrics

To account for the benefits and costs mentioned in Section 4.3.3, two metrics are used in this study: nutrient removal cost and Benefit-Cost Ratio (BCR). BCR is highly dependent on the volume of treated water as a primary design criterion based on state of Maryland guidelines (Maryland Department of the Environment 2009). Volume of treated water is the storage needed to capture and treat the runoff from most of the average annual rainfall. The volume of treated water generally relies on subwatershed contributing area and its runoff coefficient, and assumes that GI designs should treat a certain depth of each rainfall and that the rest is left untreated (Weiss et al. 2007). Therefore, its computation might not represent real-world physical behavior of the watershed during every rainfall event. In this analysis, for each design scenario, depending on the area of GI practices and their contributing area, the depth of rainfall that is supposed to be treated according to the guidelines published for residents in nearby counties (Department of Environmental Protection 2017) were computed, as no rain garden installation guidelines were found for the residents in the Baltimore county. Using the depth of treated stormwater along with the area of the subwatershed, runoff coefficients of the subwatersheds, and rainfall records of the continuous simulation period, the average annual amount of rainfall volume that is supposed to be treated, i.e. volume of treated water, is computed.

Then, the equivalent treatment technology, chosen from sand filters, dry basins, and wetlands (as large concentrated GI practices) to treat the same volume of water (Weiss et al. 2007), is compared.

Then annualized life cycle cost of the technology is computed for its entire life cycle [assumed to be 25 years as in the WERF SELECT model (WERF, 2012)] using the methods explained in the previous section. However, since the BCRs are designed as comparative metrics between benefits and costs, it was assumed that the annualized life cycle cost is consistent throughout the simulation period (for this case study, 2007-2010). The computed cost for the simulation period is equivalent to avoided cost or monetary benefit for stormwater treatment and is used as the monetary benefit in the BCR analysis. Therefore, there is no need to simulate the watershed and GI behavior in treating stormwater to compute the BCRs. More details on the approach are provided in the “Selection of economic valuation method” section below.

Next, nutrient removal costs are computed as the second analysis metric by first calculating pollutant mass at each outlet within the watershed. Each outlet corresponds to either a subwatershed, a household, or watershed outlet. One assumption, which is made in the models developed for this study, is that once nutrients are removed from the watershed, they are not transported back into surface water through subsurface flow. As a result, the nutrients deposited at any locations within the watershed are not considered at subsequent subwatershed outlets. The computed areas under pollutographs, i.e. graphs representing the concentration of a certain pollutant over time, are generated for the GI design scenario. Then the average of the baseline scenarios, in which there is no GI present, are compared to obtain the reduced concentrations after GI implementation. Then, the differences are divided by the life cycle cost of GI technology used in the household, subwatershed, or entire watershed for each GI design scenario to achieve their corresponding removal costs. It is worth noting that air pollutant deposition is only used to compute BCR values and not the nutrient removal costs, since BCRs compute the comparative benefits of small GI technologies in comparison to other conventional large-scale practices. On the other hand, nutrient removal costs consider the effects of GI practices in relation to implementation locations across a watershed.

To compute BCR at watershed scale, the volume of treated water in the watershed needs to be determined. To do so, it was assumed that the depth of water treated by a rain garden is an uncertain parameter consistent throughout the watershed, bounded by minimum and maximum depth of stormwater that can be treated via GI practices according to state guidelines (for this case study, 0.2 and 5 inches respectively). This allows computation of the cost of equivalent wetland technology to achieve the same volume of treated water. However, the nutrient removal costs at the watershed scale are simulated the same way as those at the subwatershed scale.

4.3.5. Selection of modeling parameters

Appendix G gives detailed parameter uncertainty bounds for continuous parameters and Appendix H gives the categories of values used for categorical variables used in this study, along with literature sources. If a specific distribution is not available in the literature, a triangular distribution is used to define minimum, median, and maximum values. These values were extracted from the literature and are specified in Appendices G and H.

4.3.6. Selection of economic valuation methods

Once the volume of treated stormwater and deposited air pollutants are estimated, their magnitudes are translated into monetary benefit through economic valuation. The valuation method used in this study is the avoided cost method (Farber et al. 2006), which computes how much cost will be avoided through the environmental benefits that GI provides. For the water quality portion of the benefits, the volume of treated stormwater for each GI installation across the subwatersheds is first determined. Upon calculation of the volume of treated stormwater for each GI design scenarios for every subwatershed, the cost of equivalent stormwater treatment technology is calculated to treat equivalent stormwater volume (Weiss et al. 2007). The life cycle costs of such technologies are assumed to be monetary benefit, i.e. avoided costs of water treatment. The parameters used for avoided cost computations are also probabilistic (Weiss et al. 2007).

To account for uncertainties in the modelling parameters, Monte Carlo simulations are conducted to determine ranges of BCR values for all GI design scenarios (see Appendices G and H). Weiss et al. (2007) have found that the cost of stormwater treatment depends on the GI practice used to treat stormwater. They developed equations to estimate life cycle cost of sand filters, dry basins, bioretention filters, wetlands, and infiltration trenches for different ranges of the volume of treated stormwater. For all of the equations, the volume of treated stormwater is the only independent variable. The equations use the volume of treated stormwater in a power function, with a given ranges of multiplier (B_0) and power (B_1) values. To use the equations, first the equivalent technology to achieve the same volume of treated water as GI design scenarios is computed. Then, the life cycle cost of the equivalent technology is determined as the avoided cost, i.e. monetary benefit of stormwater treatment.

To conduct valuation of air pollutant deposition, the cost of air pollutant removal from power plants is used with the parameters and uncertainty bounds listed in Appendices G and H.

Once these monetary benefits are calculated, Benefit Cost Ratios (BCRs) are computed using the following equations:

$$BCR_{rain\ garden} = \frac{Benefit_{stormwater\ treatment} + Benefit_{air\ pollutant\ removal}}{Life\ cycle\ cost} \quad (Eq. 4.1)$$

$$BCR_{permeable\ pavement} = \frac{Benefit_{stormwater\ treatment}}{Life\ cycle\ cost} \quad (Eq. 4.2)$$

where $Benefit_{annual\ stormwater\ treatment}$ is equal to the annualized avoided cost of a comparable technology to treat the same volume of stormwater and $Benefit_{annual\ air\ pollutant\ removal}$ is equal to the annualized avoided cost of the same magnitude of air pollutants.

4.3.7. Integration of modeling approaches

As models and parameters are selected, they need to be integrated to conduct further analysis. Modeling approaches for air pollutant deposition and life cycle estimation, extracted from i-Tree and WERF models, are used in a series of python scripts. Then, SWMM models for the watershed are created using SWMM

package (Pathirana 2018). Also, a random number generator function is assigned to each uncertain parameter. For each set of random values for uncertain parameters, inputs to cost and air pollutant deposition models are modified and input SWMM files for the case study are overwritten.

An important aspect of the analysis is the coverage and contributing area of GI practices for each set of Monte Carlo simulations. To account for these two parameters, the areal coverage of GI, i.e. GI design scenario, is changed for each set of Monte Carlo simulations. Specifically, for each GI design scenario the coverage of GI is assumed to be equal to 32%, 64%, and 100% of suitable GI locations for all subwatersheds. Also, to account for GI contributing area, two cases in this study for each GI coverage scenario are designed. One case assumes that the entire subwatershed impervious area contributes to GI practices in the subwatershed and the other assumes that a proportional portion of the subwatershed is contributing to each GI coverage case. For example, for a design scenario in which it was assumed that GI coverage is 32% of the entire possible locations for all subwatersheds throughout the watershed, Monte Carlo simulations are executed assuming that both 32% and 100% of impervious area across all subwatersheds are contributing to GI practices. The two types of simulations are referred to as “variable” and “fixed” contributing area allocation scenarios, respectively. These two types of simulation are designed to address the lack of availability of routing information within each subwatershed by considering two extents of the contributing impervious area.

This type of multi-coverage scenario analysis is not considered for permeable pavement, which can only be allocated to a few candidate locations with known GI coverage and known contributing area. Therefore, “fixed” and “variable” contributing area scenarios are only for rain gardens. The SWMM models used in this work were originally prepared at subwatershed and watershed scales. The models were then modified to simulate the household scale. A new SWMM model is created for each household, assuming that the households as small independent subwatersheds, each having their own outlet. For the case study considered herein, 280 households have land area suitable for implementation of GI practices and hence 280 subwatersheds are modeled. Since these household-level models are constructed to assess the level of

highly local nutrient removal, the routing between the households is ignored. In fact, the only sets of distributions that are used are those at the single household level, each acting independently from the other households. For all households, baseline scenarios are run, GI installations are assigned, and Monte Carlo simulations are executed. At the household scale, the contributing area is set to the entire land area of the household; thus, fixed and variable contributing area are not executed at this scale.

4.3.8. Uncertainty quantification

The Monte Carlo simulations to compute BCR and nutrient removal cost are conducted with two types of uncertainty assessments:

Monte Carlo Type I. *Varying GI-related parameters within all subwatersheds and between Monte Carlo runs*

In this set of Monte Carlo simulations, parameters pertaining to subwatershed configurations (i.e. area, imperviousness ratio, percentage of pervious area suitable for GI) are fixed throughout the simulations and only uncertain parameters related to GI practices are changed. This enables the effects of uncertainty in GI parameters on total BCR and nutrient removal at all spatial scales to be quantified. To also consider the importance of GI area for each subwatershed, each rain garden Monte Carlo scenario is evaluated with different area coverages using “fixed” and “variable” contributing area, as explained previously.

750 iterations of Monte Carlo Type I simulations were conducted for both rain gardens and permeable pavements. This minimum number of iterations was selected by simulating 100, 250, 500, 750, 1000, 1250, 1500, and 2000 Monte Carlo iterations for one individual subwatershed and observing the minimum value when the distribution of nutrient removal costs and BCRs stabilized.

Monte Carlo Type II. *Varying GI-related parameters between Monte Carlo simulations, but consistent across the watershed for each simulation*

In this type of simulation, GI-related parameters are fixed and identical throughout the watershed, including all subwatersheds, for each iteration. As a result, the only parameters that vary from one subwatershed to another during each iteration are those pertaining to subwatershed properties (i.e. area, imperviousness ratio, percentage of pervious area suitable for GI, and distance to watershed outlet). The subwatershed properties vary from one subwatershed to another but are not changed from one Monte Carlo iteration to the next. On the other hand, the GI-related parameters, while fixed throughout the watershed for one simulation, are changed from one iteration to the next one. This type of analysis identifies the effects of subwatershed-related parameters on overall rain garden BCR and nutrient removal costs, highlighting which subwatersheds show more efficiency in stormwater treatment. Since only a handful of subwatersheds have potential locations for permeable pavements, Monte Carlo Type II does not apply to permeable pavements. The same number of Monte Carlo iterations, 750, were used for Type I as Type II. This was the minimum number of simulations to stabilize the distributions of the metrics for this case study.

For better clarity, Fig. 4.3 summarizes the different design scenarios analyzed in this study. Please note that the two types of Monte Carlo simulations are not in the order of complexity.

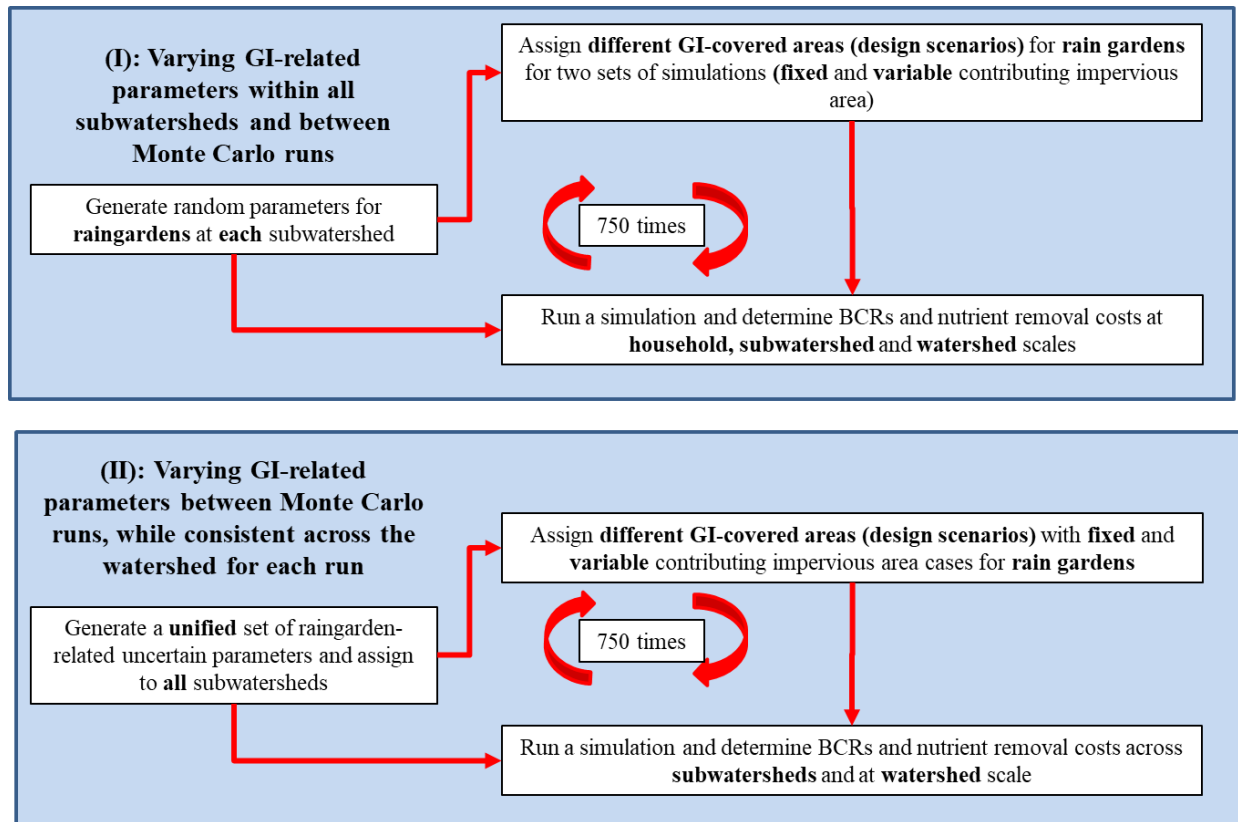


Fig. 4.3. Flow chart of the design scenarios showing the two types of Monte Carlo simulations

4.3.9. Analysis of the factors affecting the metrics

Once distributions of the BCRs and nutrient removal costs are computed using Monte Carlo Type I, the distributions across the different design scenarios shown in Fig. 4.3 are compared in order to assess the effects of uncertain parameters, as well as GI coverage, on each metric's distributions. Also, to determine which rain garden-related parameters have the most impact on the metric distributions, individual subwatersheds, and their metric's distributions generated under Monte Carlo Type I are investigated. Then, the effects of any of the categorical parameters, listed in Appendix I, on classification of the distribution of the metrics are explored. Possible correlations between uncertain numerical parameters, listed in Appendix G, and metrics across all subwatersheds are also investigated. Moreover, as the distributions of the metrics at subwatershed scale are compared, the corresponding distribution of the metrics at watershed scale is also computed. Doing so, the distributions can be compared and checked for any emerging patterns using

univariate cumulative distribution function (CDF) comparisons (for reference, see Taylor 1990). The same type of analysis is conducted at the household scale. Doing so, the distributions of the metrics at household scale can be computed and compared to the metric distributions at the other spatial scales.

To identify numeric rain garden-related parameters that contribute the most to cost-benefit metrics, Pearson correlation analysis is conducted between uncertain numeric input parameters listed in Appendix I and metrics in all of the subwatersheds for all Monte Carlo Type I simulations. P-values and R-coefficients result from correlation analysis between independent uncertain parameters (for reference, see Taylor 1990). If the p-value is less than the significance level (usually 0.05) then the model fits the data well and the null hypothesis that the slope of the regression model is not statistically different from zero can be rejected. R-coefficients measure the level of variation in the analysis metrics that can be explained by the linear model generated from uncertain parameters within all subwatersheds that have candidate feasible locations for GI implementation.

By running Monte Carlo Type II, the effect of subwatershed-related parameters on each metric's distributions is analyzed. Subwatershed-related parameters include subwatershed area, imperviousness ratio, area of rain garden candidates, distance from subwatershed outlet to the watershed outlet along the stream, runoff coefficient for the continuous rainfall period, and Shreve order number.

For each set of simulations, the value of the metrics across all subwatersheds are computed and then Pearson correlations are calculated between the subwatershed-related parameters and the metrics (Pearson 1895). Any emerging patterns across the subwatersheds are also checked to see if any hypotheses can be developed. To do so, the distributions of the metrics over all Monte Carlo simulations for all subwatersheds are compared to distributions at the watershed scale using two-sample Kolmogorov-Smirnov tests for each of the three design scenario cases. The test is a nonparametric test of the equality of two distributions with two resulting parameters: D statistic and a p-value (Marsaglia et al. 2003). D statistic shows the absolute

maximum vertical distance between the cumulative distribution functions of the two samples, and thus represents similarity of the two CDFs.

4.4. Results and discussion

Each sub-section below presents results for one type of uncertainty and parameter significance analysis (rain garden Type I, Section 4.4.1, and Type II, Section 4.4.2; permeable pavements, Section 4.4.3) at subwatershed, watershed, and household scales. The significance of each uncertain parameter in relation to BCR values is also analyzed.

4.4.1. Results for uncertainty assessment with rain-garden-related parameters (Type I)

Fig. 4.4 shows the cumulative density function (CDF) of BCRs generated from Monte Carlo Type I simulations for four randomly-selected subwatersheds, each showing three different GI design scenarios (i.e. GI coverages): 32, 64, and 100 percent. Properties of the four subwatersheds, presented in Fig. 4.1, are detailed in Table 4.1. Table 4.1 also summarizes the averages of BCR distributions, as well as nutrient removal costs that are presented in subsequent figures, for the four subwatersheds across all design scenarios.

Table 4.1. Properties and mean of analysis metrics of the randomly selected subwatersheds

Properties/ mean of simulation results		Subwatershed 1	Subwatershed 2	Subwatershed 3	Subwatershed 4
Area (hectares)		1.26	1.51	3.43	1.05
Imperviousness ratio (%)		29.1	30.8	73.9	22.5
Percentage of pervious area for GI (%)		4.1	12.7	31.3	35.9
Distance to watershed outlet (m)		606	417	1302	471
Mean of BCRs	32% GI coverage -fixed contributing area	52.9	17.9	31.5	5.2
	32% GI coverage -variable contributing area	47.3	18.2	34.5	5.4
	64% GI coverage -fixed contributing area	25.2	9.1	17.2	2.6
	64% GI coverage -variable contributing area	25.5	9.4	16.4	2.6
	100% GI coverage	17.1	6.0	10.6	1.8
Mean of phosphorous removal costs (\$/kg)	32% GI coverage -fixed contributing area	2.5	4.0	45.5	17.2
	32% GI coverage -variable contributing area	2.8	4.0	42.2	16.3
	64% GI coverage -fixed contributing area	5.2	8.1	83.0	34.4
	64% GI coverage -variable contributing area	5.2	7.7	87.3	35.2
	100% GI coverage	8.2	12.3	140.1	54.9
Mean of nitrogen removal costs (\$/kg)	32% GI coverage -fixed contributing area	1.2	1.1	23.7	7.5
	32% GI coverage -variable contributing area	1.3	1.0	20.1	7.3
	64% GI coverage -fixed contributing area	2.2	2.1	36.4	14.4
	64% GI coverage -variable contributing area	2.4	2.0	42.0	15.1
	100% GI coverage	3.3	3.2	57.0	21.6

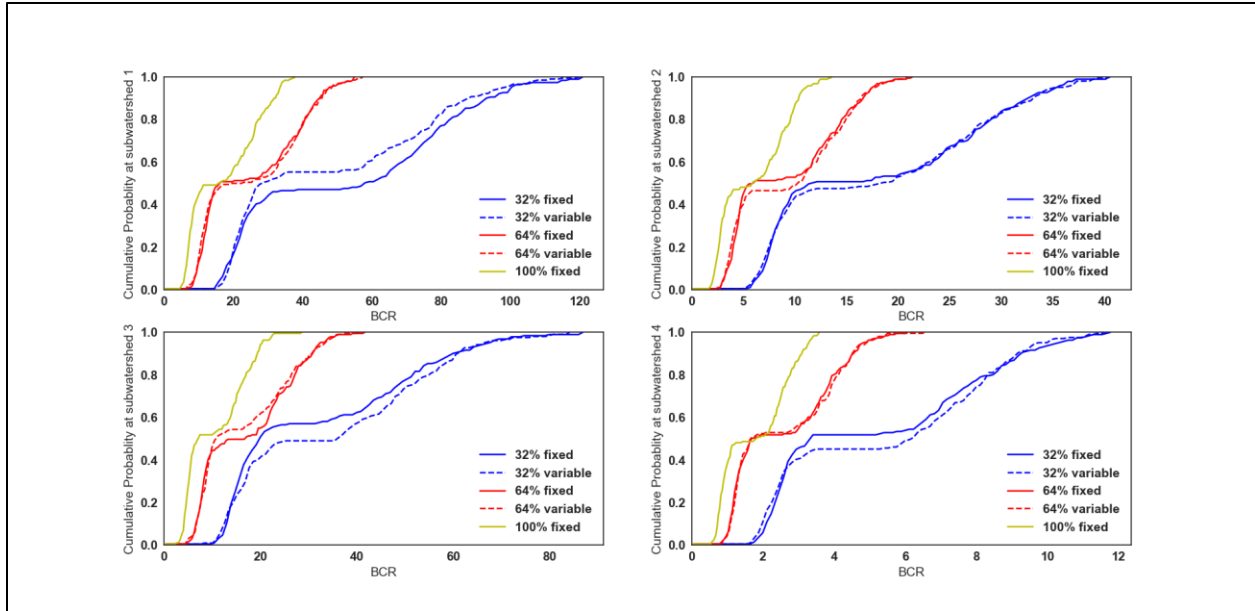


Fig. 4.4. CDFs of BCR for four subwatersheds in Dead Run showing GI design scenarios for 32%, 64%, and 100% under both contributing impervious area scenarios (fixed and variable)

According to Table 4.1, the mean BCR value is considerably greater than one for most of the subwatersheds. Since the BCR values defined in this study heavily rely on comparisons of rain gardens or permeable pavements to other technologies that, according to the guidelines, are expected to treat the same WQV volume, exceeding one does not mean that the investments will result in monetary return. Rather, it can be concluded that implementation of small GI practices is more cost effective in comparison to more concentrated alternative GI practices, i.e. dry and wet basins, for the given subwatershed.

In Fig. 4.4, the range of BCRs changes from one subwatershed to the next, meaning that, regardless of the uncertainty in rain garden parameters, some subwatersheds show more benefits than others. Moreover, as rain garden coverage increases, BCRs tend to show less uncertainty (i.e., the CDF shows less variability), as well as lower mean values for all subwatersheds.

To understand these results, recall that the BCR calculation considers avoided water quality treatment costs under the WQV concept, as explained under section “Economic Valuation”. As rain garden area increases under higher design scenarios, WQV is also increasing. As a result, the avoided cost of the comparable technology providing the WQV (sand filter, dry basin, or wet basin) is also increasing. Although the cost

of dry and wet basins increases with higher capacity, the rate of their increase is not as high as those for rain gardens. In other words, the economies of scale associated with the avoided costs of wet and dry basins show that more rain garden coverages do not necessarily result in higher efficiency stormwater treatment.

For all subwatersheds, the BCR values show that the avoided cost of using comparable WQV treatment for all subwatersheds is higher than the rain garden life cycle cost, meaning that rain gardens are more cost efficient than basins and ponds for semi-urbanized subwatersheds modeled with the assumptions used in this study (routing, depth of treated rainfall for raingardens, lack of exchange between stormwater and underground water tables, etc.).

Figs. 4.5 and 4.6 show the CDFs of nutrient removal costs for the same four subwatersheds. These Figs show that the comparative trend between nutrient cost removal in the four subwatersheds differs significantly from the trend for BCRs. For instance, based on Fig. 4.4, Subwatershed 3 should be the most suitable location for GI installation, as it has the highest BCR values. However, based on Figs 4.5 & 4.6, Subwatershed 2 is the most suitable area. More details on how subwatershed-related parameters affect metrics, and why this shift in suitable subwatersheds occurs when the metrics change, will be presented in the section on Monte Carlo Type II results and discussions below.

According to Figs 4.5 and 4.6, there is a general increase in nutrient removal cost as GI coverage increases from 32% to 100% in different subwatersheds. The results show that accumulated nutrient removal masses do not increase at the same rate as the life cycle cost of rain gardens installed to treat nutrients at the examined GI coverage ranges. Similar to trends observed for BCRs, because higher mean values correspond to higher standard deviations, the uncertainty in nutrient removal costs is highest for maximum GI coverage.

Also, the results show that fixed versus variable contributing area (e.g., 100% vs 32% of impervious area for the 32% GI design scenario), does not change the distribution of BCRs and nutrient removal costs significantly for most subwatersheds. This implies that whether the rain garden is receiving water from a portion of the subwatershed or the entire subwatershed, the installation cost affects nutrient removal costs

more than the amount of nutrients removed. Another important factor is that even for the variable GI coverage scenario, the amount of nutrient removal is reaching the maximum treatment capacity, most likely because the available candidate area for the subwatershed is a relatively small portion of the impervious area for all subwatersheds (see Table 4.1). Therefore, further increases in the contributing area do not significantly improve nutrient reduction during the simulation period (in this case, from 2007 to 2010).

Comparing ranges of nitrogen vs phosphorous removal costs (Figs 4.5& 4.6), note that the costs of phosphorous removal are significantly higher than those of nitrogen. The reason is that the amounts of phosphorous nutrients during rainfall and dry build-up periods are significantly smaller than those of nitrogen.

Comparing Subwatersheds 2 and 4 among Figs. 4.4- 4.6, observe that although their BCRs differ almost by a factor of two, their nutrient removal costs differ by a factor of 14-20. This discrepancy shows that, although commonly used, BCRs based on WQV might not realistically reflect the comparative performance of GI in treating stormwater across a watershed. The WQV calculations assume that a certain depth of rainfall would be treated throughout the watershed, while the simulation results indicate that the concentrations at the subwatershed outlet vary from one subwatershed to the other. These results indicate that the accuracy of GI siting decisions based on BCRs could potentially be affected. More explanation is given in the results section for Monte Carlo Type II simulations.

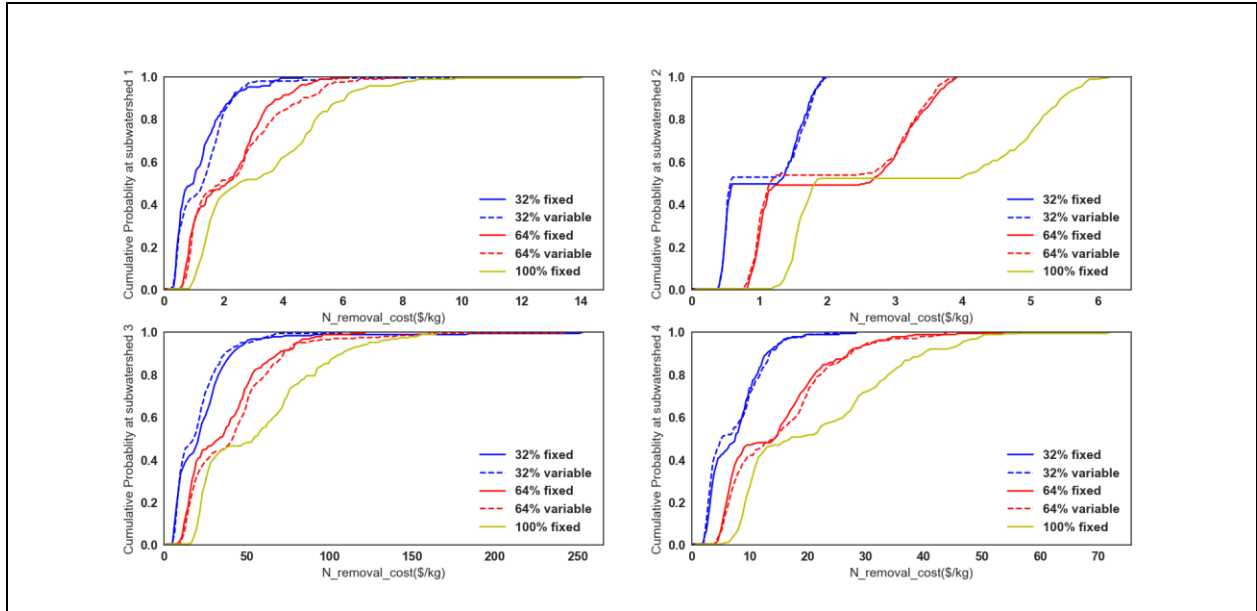


Fig. 4.5. CDFs of total nitrogen removal costs for four subwatersheds under different GI design scenarios with fixed and variable contributing impervious areas

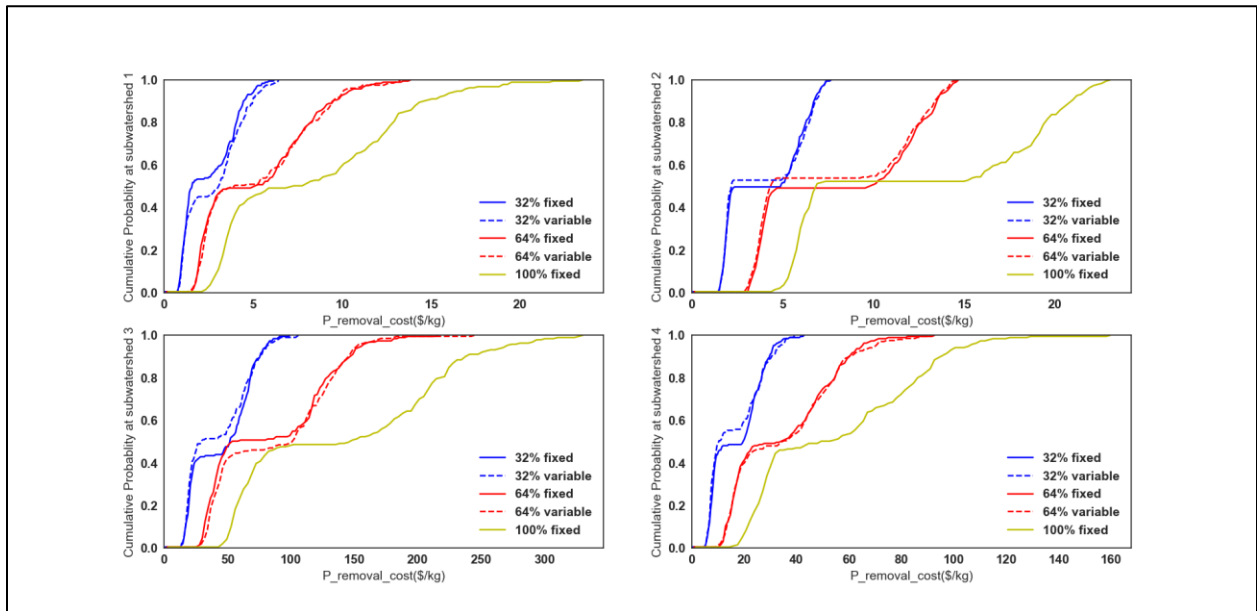


Fig. 4.6. CDFs of total phosphorous removal costs for four subwatersheds under different GI design scenarios with fixed and variable contributing impervious areas

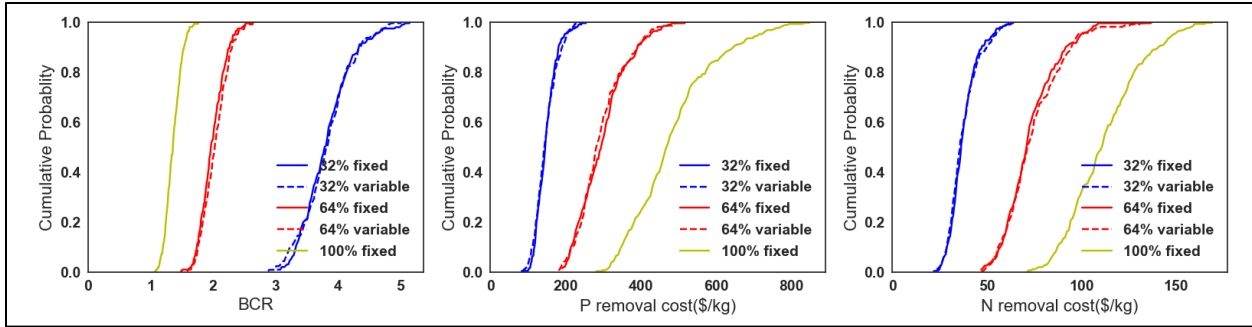


Fig. 4.7. Type I CDFs of BCRs and nutrient removal costs at watershed scale for different GI design scenarios

Fig. 4.7 shows that as the percentage of GI coverage decreases, benefits increase but the results have higher uncertainty. The pattern is similar to those presented in Figs. 4.4 to 4.6 for variations in GI parameters.

To further investigate how the uncertainties in Monte Carlo analysis Type I are generated, the parameters, from all of the rain garden-related parameters, that are contributing the most to BCR and nutrient removal cost uncertainty across all subwatersheds have to be determined. One observation in Figs 4.4 to 4.6 is that the CDFs tend to have inflection points at about 50% cumulative probability, meaning that the distributions are clustered around two different modes, one less and the other more than 50% cumulative probability. These inflection points are the result of bi-modal distributions of the metrics across the two spatial scales, subwatersheds and household.

Analyzing the results against all independent categorical variables (see Appendix F), the installation option for rain gardens (i.e., professional versus self-installation) appears to be a significant factor that divides the simulation results into two clusters (see Fig. 4.8). According to Fig. 4.8, self-installation of GI practices not only decreases the cost of nutrient removal, but also increases BCRs. The importance of installation option suggests that promotion of self-installation through different outreach methods could result in significantly lower surface water treatment costs compared to concentrated water treatment technologies such as dry and wet basins. In fact, when restricted by areal limitations to implement GI practices, self-installation seems to be the predominant factor that increases stormwater treatment efficiency. Also, the occurrence of the

inflection points around 50% is the result of assigning equal probabilities, 50%, to the self and professional installations, which is one of the assumptions made in this study (See Appendix F).

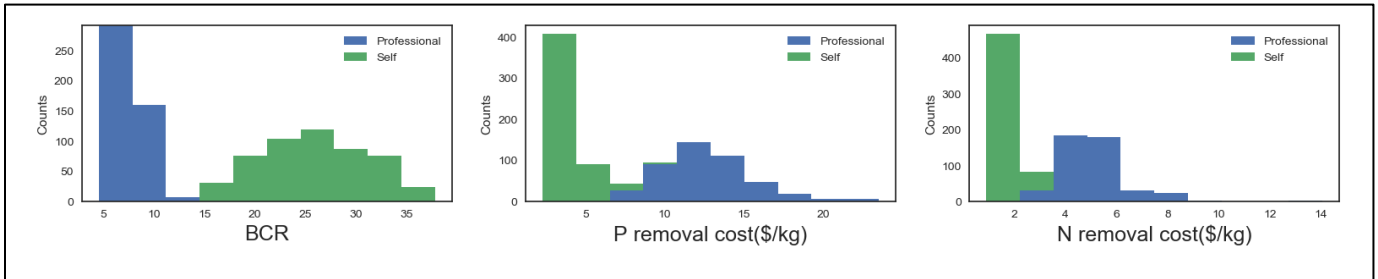


Fig. 4.8. Simulation results vs installation option for a sample subwatershed

Rain garden monetary benefits considered in this study are air pollutant deposition and stormwater treatment benefits. Table 4.2 shows the distribution of monetary benefits associated with air pollutant deposition in the four subwatersheds from Table 4.2 among all Monte Carlo Type I simulations.

Table 4.2 Distribution of the benefits associated with air pollutant deposition across all Monte Carlo Type I simulations for the four randomly selected subwatersheds (Mean percentage ± standard deviation)

Design Scenario	Subwatershed 1	Subwatershed 2	Subwatershed 3	Subwatershed 4
32% with fixed contributing area	0.26± 0.16	0.75± 0.45	0.43± 0.24	2.52± 1.50
32% with variable contributing area	0.25± 0.15	0.73± 0.42	0.41± 0.22	2.54± 1.41
64% with fixed contributing area	0.55± 0.32	1.46± 0.83	0.81± 0.48	4.87± 2.92
64% with variable contributing area	0.54± 0.33	1.40± 0.80	0.80± 0.50	5.25± 3.21
100%	0.78± 0.41	2.22± 1.42	1.24± 0.67	8.13± 4.06

Table 4.2 shows that the share of air pollutant deposition in comparison to water quality benefits is insignificant. Therefore, all of the trends observed for raingarden BCR computations are driven by water quality treatment functionality.

Next, as mentioned in Section 4.3.9, all of the numeric rain garden parameters are investigated to see which have significant correlations with the metric distributions at the subwatershed level. Table 4.3 shows pairs of variables that have P-values less than 0.05.

Table 4.3. Number of subwatersheds (out of 67 subwatershed with candidate locations for rain gardens) with statistically significant correlations (P-values < 0.05) between independent input parameters and analysis metrics under the 100% GI design scenario.

Input parameter \ Metrics	Benefit Cost Ratio	TN removal cost (\$/kg)	TP removal cost (\$/kg)
Interest Rate	60	31	30
Multiplier (B₁) constant for WQV benefit	57		

According to Table 4.3, interest rate has the highest correlation to dependent variables, confirming that cost estimations are highly dependent on interest rates. Constants used for valuation of water quality treatment benefits also tend to have positive correlations with BCRs and nutrient removal costs.

Since the magnitude of monetary benefits associated with total air pollutant deposition is smaller than the stormwater-related benefits, their effects on metrics are negligible. The results, as expected, show that BCR calculations, which rely on monetary valuation of environmental benefits, are mostly sensitive to monetary valuation parameters.

Fig. 4.9 shows the distribution of household-level BCR and pollutant removal costs for all 280 households with candidate GI locations, as well as more detailed results for a randomly selected household. The results show the same trend in reduction of BCRs with coverage, suggesting that the life cycle cost of rain gardens increases at a higher rate in comparison to the life cycle cost of the equivalent technologies to treat the same WQV as rain gardens (i.e. sand filters in this case).

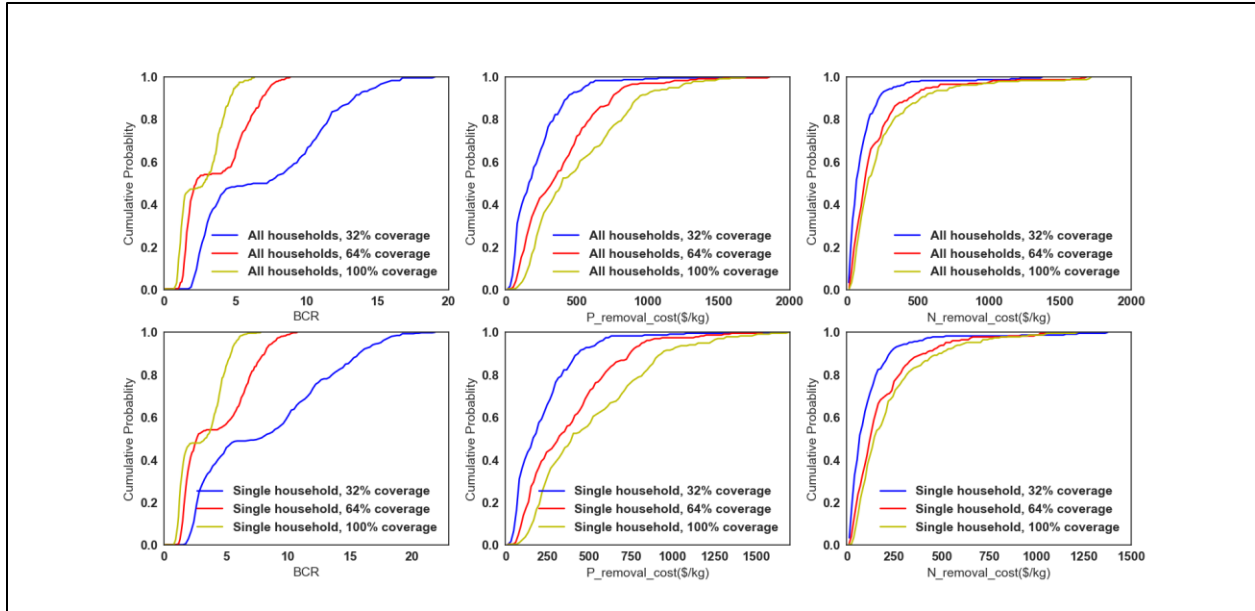


Fig. 4.9. CDFs of BCRs and nutrient removal costs at all households (top row) and a randomly selected individual household with an area equal to average household size in the watershed (bottom row)

The results also show an inflection trend similar to the one observed at the subwatershed scale as a result of the choice between self-installation and professional installation. To draw more conclusions on the effect of household-related parameters on the metrics and decision-making process, more discussions on the comparison between household, subwatershed and watershed are conducted in the sections below. It is worth noting the general pattern that BCRs exceed one, meaning that implementation of residential rain gardens would be more beneficial for stormwater treatment in comparison to sand filters, the equivalent alternative technology. In fact, according to the WQV results, to treat the same level of rainfall at the household level, more sand filter area is needed compared to rain gardens, mostly due to its lower efficiency in stormwater treatment compared to rain gardens, resulting in BCRs exceeding one.

4.4.2. Results of uncertainty assessment for Monte Carlo simulations Type II

In the Monte Carlo Type II uncertainty analysis, rain garden-related parameters are fixed throughout all implemented locations in the watershed for each Monte Carlo simulation, enabling effects of subwatershed parameters on BCRs and nutrient removal costs to be identified. Fig. 4.10 shows the distribution of the mean subwatershed BCR and nutrient removal costs over 750 Monte Carlo simulations.

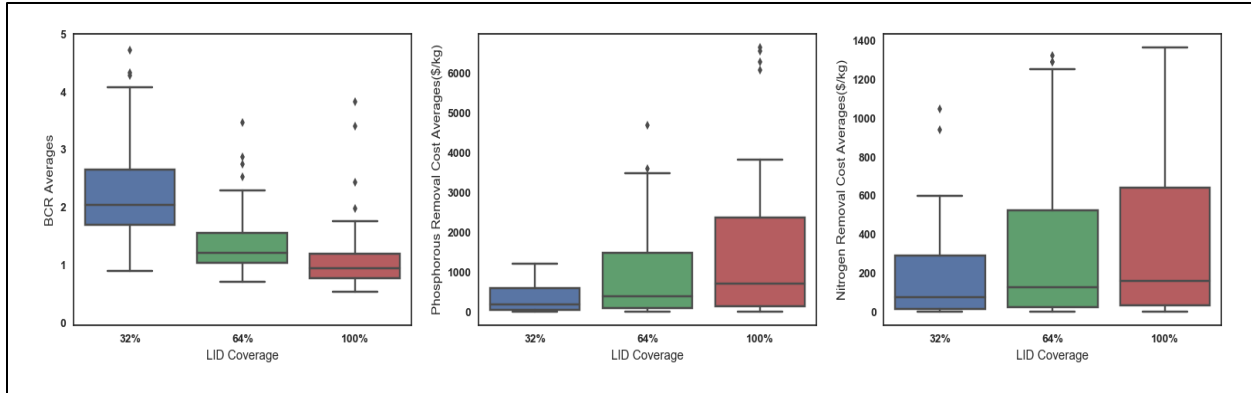


Fig. 4.10. Distribution of simulation results for subwatersheds averaged across all Monte Carlo Type II simulations (the bars represent ranges of distributions across subwatersheds)

Notice that the BCR ranges to decrease once GI coverage increases, which is consistent with the results from Fig. 4.4. The trends for nutrient removal costs are in accordance consistent with Figs 4.5 and 4.6.

Next, the metrics distribution at the subwatershed level is compared to those at the watershed level using the tests explained in Section 4.3.9. Table 4.4 shows the distribution of the D statistic values for all tests. The p-values for all tests are extremely small, less than 0.05, suggesting that the distributions at the subwatershed scales are statistically different from the watershed scale.

Table 4.4. Distributions of D statistics for all comparative Kolmogorov-Smirnov tests between subwatersheds and watersheds

Percentage GI Coverage (%)	Metrics	Mean \pm standard deviation	P-value
32	BCR	0.68 \pm 0.20	<0.00001
32	P removal cost	0.80 \pm 0.26	<0.00001
32	N removal cost	0.79 \pm 0.22	<0.00001
64	BCR	0.67 \pm 0.19	<0.00001
64	P removal cost	0.79 \pm 0.26	<0.00001
64	N removal cost	0.81 \pm 0.20	<0.00001
100	BCR	0.66 \pm 0.18	<0.00001
100	P removal cost	0.78 \pm 0.26	<0.00001
100	N removal cost	0.83 \pm 0.20	<0.00001

To visually compare the metrics' distributions, the mean of the metrics' distributions at subwatershed and watershed levels are presented in Fig. 4.11. Household-scale CDFs based on analysis metrics for 280 households in the case study area are also shown in Fig. 4.11.

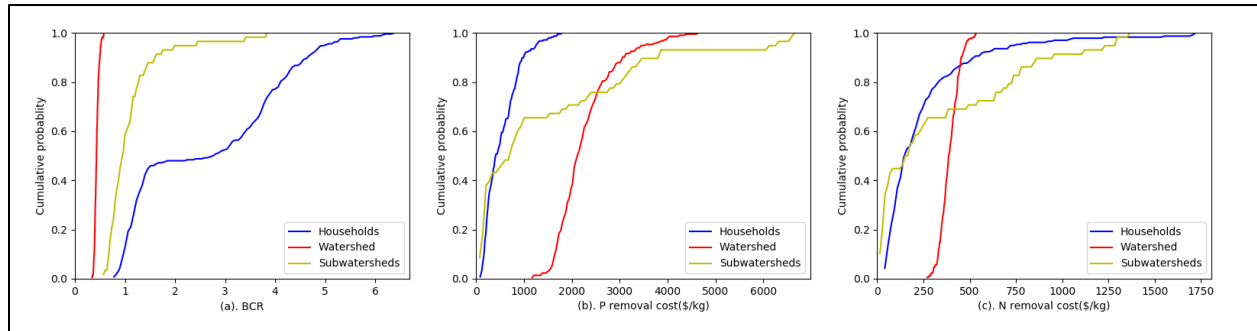


Fig. 4.11. Comparison of CDFs of mean household, subwatershed, and watershed BCRs and nutrient removal costs for 100% GI coverage under the Monte Carlo Type II scenario

Considering Fig. 4.11.a and 4.11.b, the results show that some subwatersheds have average nutrient removal costs lower than the watershed scale. Therefore, these subwatersheds would be the most efficient locations for GI investment across the study area; this result is investigated in more detail later in this section. In fact, the results show that uniform implementation of GI practices across all potential locations in a watershed is not as efficient as targeted implementation in these subwatersheds.

Comparing the CDF of N removal costs for households with the other two scales [Fig. 4.11(c)] shows that some households have removal costs higher and lower than the watershed and subwatershed scale, suggesting that nitrogen removal costs are higher for some households than the average removal costs at the watershed and subwatershed scale. Identifying the specific locations of such households would require further research into optimization of the GI network at patch scales using a model such as RHESys.

On the other hand, the BCR metric results [Fig. 4.11(a)] suggest that GI installation in any of the subwatersheds yields higher average BCR than uniform installation across the entire watershed. Furthermore, GI implementation at any of the households yields higher BCR than at the watershed and subwatershed scales. The results also suggest that rain gardens are more efficient for treating stormwater at

the household scale, while large scale concentrated practices, such as wet and dry basins, are more efficient at the watershed scale.

To determine which subwatershed-related parameters are most influential in providing environmental benefits, the correlations are analyzed between metrics averaged over Monte Carlo Type II runs and independent subwatershed parameter realizations (i.e., area, imperviousness ratio, total GI candidate area, total pervious area, percentage of pervious area that is suitable for GI siting, and distance from each subwatershed outlet to the watershed outlet). The averages of the metrics are right skewed and do not follow a normal distribution. Therefore, a generalized linear model with gamma distribution function, which had the best fit to the metric averages, is used to assess which independent parameters are correlated with the mean of the metrics. Table 4.5 shows the pairs of independent subwatershed parameters and metrics for each design scenario, averaged across all Monte Carlo Type II simulations, that show significant correlations, along with statistics associated with such correlations.

Table 4.5. Pairs with significant correlations in the GLM analysis conducted between metrics averaged across Monte Carlos Type II simulations and across all design scenarios for all subwatershed and subwatershed-related independent parameters

Metrics	Design Scenario	Correlation coefficient	Standard error	z-statistics	P-value
Area (km²) vs. BCR	32%	-9.0727	1.884	-4.817	<0.001
Area (km²) vs. BCR	64%	-20.8303	6.98	-2.984	0.003
Area (km²) vs. BCR	100%	-28.642	8.469	-3.382	0.001
Distance to watershed outlet (m) vs. P removal cost (\$/kg)	64%	-2.58×10 ⁻⁰⁶	1.05×10 ⁻⁰⁶	-2.467	0.014
Distance to watershed outlet (m) vs. P removal cost (\$/kg)	100%	-1.78×10 ⁻⁰⁶	8.80×10 ⁻⁰⁶	-2.027	0.043
Distance to watershed outlet (m) vs. N removal cost (\$/kg)	64%	-8.23×10 ⁻⁰⁶	3.41×10 ⁻⁰⁶	-2.411	0.016

Table 4.5. (cont.) Pairs with significant correlations in the GLM analysis conducted between metrics averaged across Monte Carlo Type II simulations and across all design scenarios for all subwatershed and subwatershed-related independent parameters

Metrics	Design Scenario	Correlation coefficient	Standard error	z-statistics	P-value
Distance to watershed outlet (m) vs. N removal cost (\$/kg)	100%	-7.07×10^{-06}	3.27×10^{-06}	-2.159	0.031

Table 4.5 shows that BCR decreases with subwatershed area regardless of the GI design scenario. This suggests that the ratio of WQV treatment effectiveness using rain garden practices vs large stormwater treatment technologies (i.e. basins) is higher in smaller subwatersheds compared to larger subwatersheds. This observation suggests that more concentrated technologies, such as dry and wet basins, are recommended for planning stormwater treatment at larger scales (i.e. large subwatersheds and watersheds) when using WQV and BCR as analysis metrics. As the area of a subwatershed increases, the technology needed to treat WQV, according to guidelines, requires more areal coverage. Therefore, substitution of numerous rain garden installations with a large concentrated GI is more beneficial if land and resources are available. Furthermore, Table 4.5 shows there is a correlation between distance to watershed outlet and nutrient removal cost. To illustrate this relationship better, Fig. 4.12 shows the distribution of average BCRs and nutrient removal costs for subwatersheds with potential locations to implement GI.

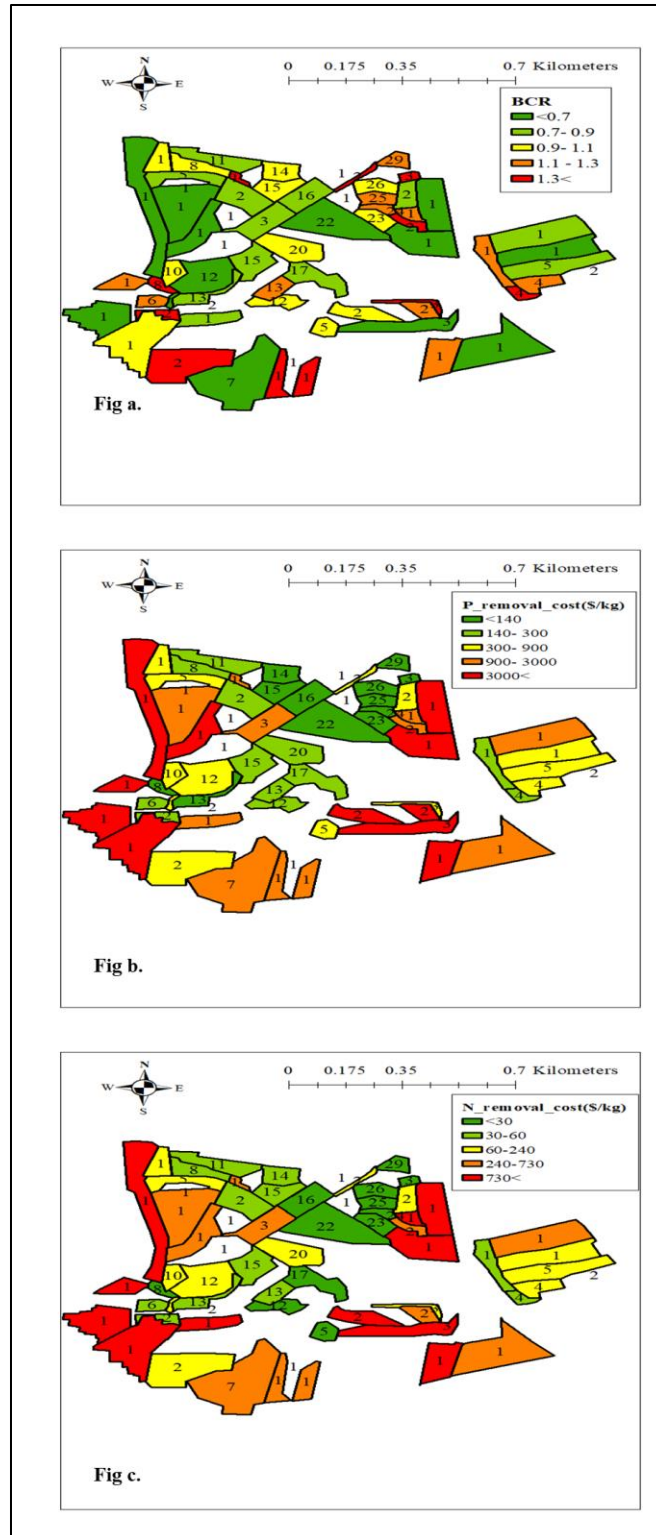


Fig. 4.12. Map of average BCRs and nitrogen and phosphorous removal costs (Figs a, b, and c respectively) for Dead Run subwatersheds with potential locations for GI implementation, under the 100 percent design scenario for Monte Carlo Type II (The numbers within subwatersheds in Figs b and c represent the orders of subwatershed outlets using Shreve stream order.)

One trend that can be observed in Fig. 4.12 is that subwatersheds located on the watershed boundary show higher nutrient removal costs. Fig. 4.12 also shows that subwatersheds receiving run-on from several subwatersheds, those having higher Shreve order numbers (Shreve 1966), have lower nutrient removal costs relative to subwatersheds with low orders.

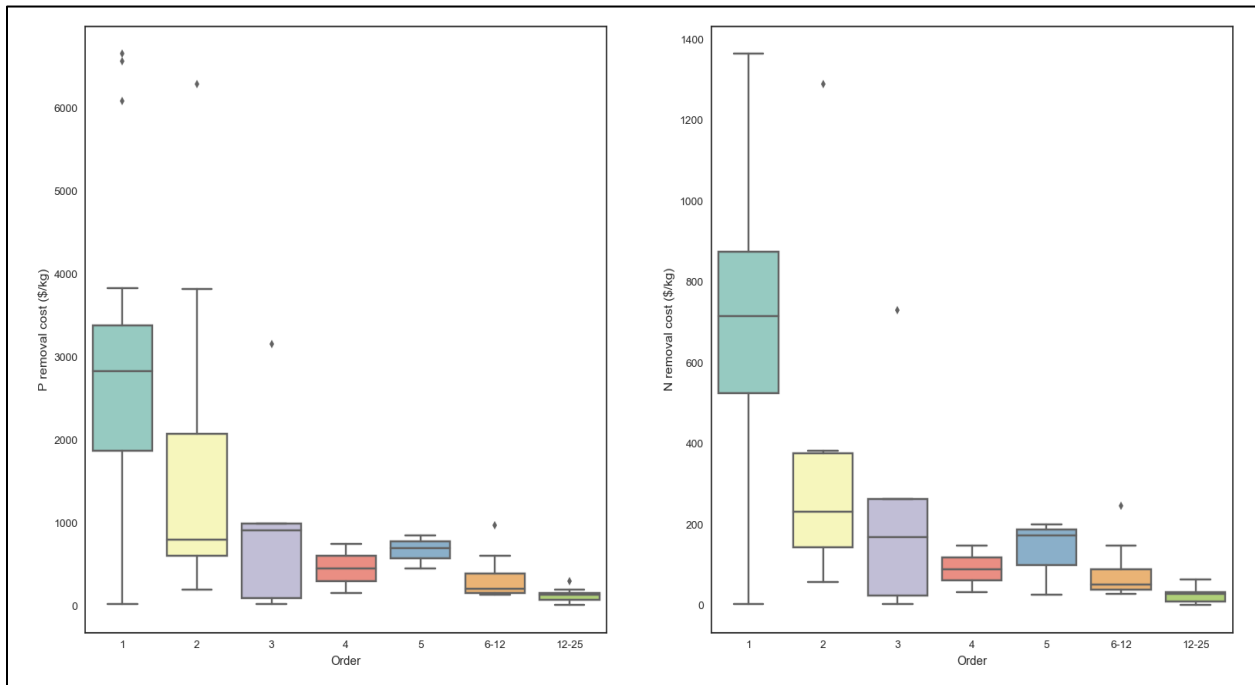


Fig. 4.13. Distribution of the mean nutrient removal costs vs subwatershed Shreve orders numbers in the Dead Run watershed for 100% GI design scenario and Monte Carlo Type II

Fig. 4.13 shows the distribution of nutrient removal costs vs the Shreve order of the 67 subwatershed outlets, which represents the number of subwatersheds contributing to each outlet. Under the watershed modeling assumptions used in this study, the results in Fig. 4.13 indicate that nutrient removal costs are directly affected by subwatershed outlet orders. Since the SWMM modelling framework has no routing capability within the individual subwatersheds, no conclusions can be drawn on how GI should be placed within subwatersheds from this study. However, at the watershed scale, surface water is routed from upstream subwatersheds to downstream subwatersheds using dynamic simulation routing (Rossman 2004). With the current modeling assumptions, nutrients are therefore deposited at upstream/ low-order subwatersheds. Once the pollutants are deposited, they are assumed to be taken out of the system (i.e., subsurface flows are

assumed not to bring nutrients back into downstream flows. Therefore, the concentration of nutrients at downstream subwatersheds' outlets is significantly lower than the baseline. By contrast, upstream subwatersheds experience significantly higher nutrient levels since the nutrients are deposited both within connecting subwatersheds and contributing upstream subwatersheds.

4.4.3. Results of uncertainty analysis for permeable pavement

Among the 138 subwatersheds in Dead Run, only three had potential locations for installing permeable pavement in commercial buildings with parking lots or in vacant parking lots suitable for renovation. Since the number of candidate locations in this case is small, uncertainty assessment is only conducted for permeable-pavement-related parameters using Monte Carlo Type I. Fig. 4.14. shows the CDFs of BCRs and nutrient removal costs at the three subwatershed outlets as well as the entire watershed.

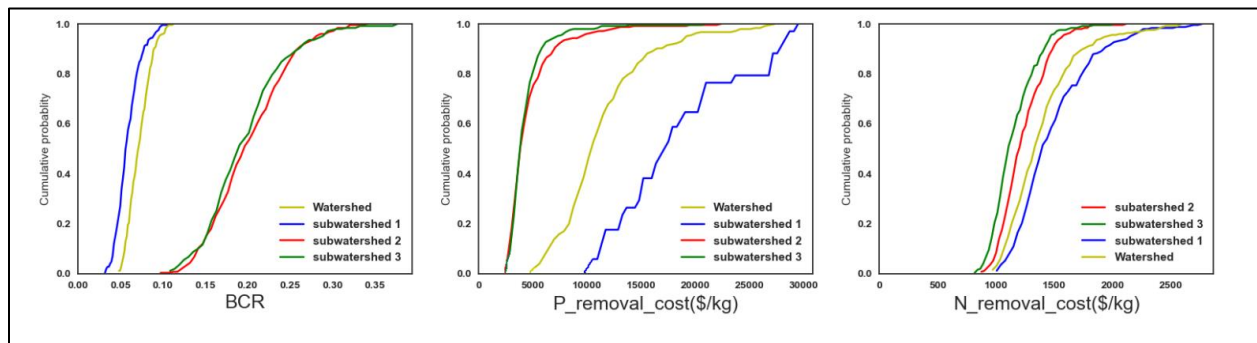


Fig. 4.14. CDFs of BCR and nutrient removal costs using permeable pavement at the subwatershed and watershed levels

Fig. 4.14 shows that BCR values resulting from permeable pavement implementation are significantly lower than those from rain garden installation (See Fig. 4.4). Also, nutrient removal costs are significantly higher than those associated with rain gardens implemented at subwatershed scales (See Figs 4.5, 4.6, and 4.8). There are three primary reasons for such differences. First, construction and maintenance costs for each permeable pavement installation are significantly higher than those of rain gardens (See Appendix H). Second, construction and maintenance of permeable pavements, in contrast to rain gardens, cannot be done using common household practices and requires professional expertise, which is costly. Since there is no self-conducted maintenance and installation, the CDFs in Fig. 4.14 do not have multiple inflection points,

in contrast to the CDFs from the rain garden scenarios (shown in Figs 4.4 to 4.6). Third, nitrogen and phosphorous removal ratios for permeable pavements are generally lower than those of rain gardens, resulting in less nutrient removal and higher nutrient removal costs (See Appendix H).

4.5. Conclusions and discussion

This study investigates and the effects of parameter uncertainty on GI cost/benefit assessment at several spatial scales through Monte Carlo, regression analysis, and Kolmogorov-Smirnov tests of a case study in the state of Maryland. The results showed that higher GI coverage at subwatershed and watershed scales results in lower mean and standard deviation of BCRs. Since avoidance costs from WQV treatment are used to determine BCR and the cost of rain gardens and permeable pavements increase at a higher rate than equivalent technologies (i.e., wet basins, dry basins, and sand filters), higher coverages result in lower BCRs. However, BCRs are generally larger than one, suggesting that using rain gardens is more beneficial than large-scale practices and the benefits exceed the cost. The only scale at which rain garden life cycle costs exceed the benefit is the watershed scale. This suggests that when the GI planning focus is shifted to stormwater treatment and capture at the watershed outlet, implementation of large-scale and concentrated practices is more efficient if land and resources are available. The results also show that areal coverage of GI is more influential than GI contributing area on overall BCRs and nutrient removal costs.

The BCR results suggest that at the household scale, rain garden practices are more efficient for stormwater treatment, while at the watershed scale concentrated dry/wet basins show more promise for stormwater treatment efficiency. Considering nutrient removal costs, there are households and subwatersheds at which removal costs are less than those at the watershed scale. These results call for a more fine-scale optimization approach to recognize such optimal locations within subwatersheds.

Among rain garden-related parameters, installation option has a significant effect on nutrient removal costs, clustering the results into lower and higher ranges. This indicates that training homeowners to perform self-installation could significantly reduce costs. Second, interest rates show the highest correlation with the GI

performance metrics. Also, the constants used to value stormwater capture are more strongly correlated with BCRs than nutrient removal efficiency, indicating that environmental benefit valuation is an important area for further research to reduce uncertainties. Therefore, there is a need for further research to better monetize such benefits. For example, valuation methods could be improved by tracking water treatment cost vs time and adding avoided costs of water treatment to the monetary benefits of GI installations.

Analyzing BCRs, it is observed that the portion of monetary benefits resulting from air pollutant deposition is significantly smaller than water-quality-related benefits. Therefore, the share and effects of air pollutant deposition parameter uncertainties on the overall BCRs are insignificant. Also, monetary valuation of GI stormwater treatment functionality is far more dominant than air pollutant deposition, due to the low magnitude of total air pollutant deposition over leaf area of rain gardens and their relatively low monetary benefits. These findings suggest that more emphasis should be given to water quality control rather than ambient air health in urban GI design guidelines.

Among physical subwatershed-related parameters, subwatershed area shows a correlation with BCR results. This could be due to the relationship between contributing area and GI: As more area contributes to a rain garden, stormwater treatment benefits increase; however, if the subwatershed is small, the benefits increase even more. Also, the distance to watershed outlet is correlated with nutrient removal costs. The distributions of nutrient removal costs also show that for subwatersheds located on the boundary of the watershed, and those located upstream, the cost of nutrient removal is higher than those located downstream, due to run-on transported from upstream to downstream having already been treated by GI implementation upstream. As a result, GI downstream only needs to reduce nutrient concentrations from already-treated run-on, resulting in lower nutrient removal costs. This result indicates a need for incentive programs (e.g., property tax breaks, GI installation subsidies, or trading programs) that would encourage homeowners, especially those in upstream areas with the highest nutrient uptake costs, to invest in small-scale GI installations. This result is consistent with previous studies that have recommended

implementation of GI practices at upstream subwatersheds (Kuller et al. 2016), as well as the importance of run-on consideration in the GI implementation planning (Miles and Band 2015).

Also, comparing nutrient removal costs between permeable pavements and rain gardens, it is clear that rain garden implementation throughout a watershed is more cost effective than permeable pavement installation in commercial parking lots. This result occurs because construction and maintenance of permeable pavements is considerably more expensive and efficiency of these technologies in treating stormwater is generally lower.

Furthermore, monitoring and data gathering on GI benefits can also significantly reduce results uncertainty. Actual daily loads of nutrients can be monitored, especially at the case study area, at both permeable pavement and rain gardens as well as outlets, along with types, costs, and locations of GI installations to compute actual costs of nutrient load reductions (Mayer et al. 2012; Koch et al. 2014; Miles and Band 2015; Perales-Momparler et al. 2017). This would allow the marginal value of nutrient load reduction cost to be calculated for both practices.

To summarize the conclusions drawn from this study, the following take-aways can be highlighted:

- GI coverage in subwatersheds or in front of households does not guarantee improvement in treatment efficiency. Sand filter, dry basins, or wet basins (as concentrated GI practices) are more beneficial for WQV treatment efficiency under higher coverage scenarios, while rain gardens are better for lower coverage scenarios.
- Contributing area is not as important as GI coverage area for each of the subwatersheds with respect to stormwater treatment efficiency.
- Among the uncertain modeling parameters, installation option affects the metrics greatly, suggesting that more self-installation of GI practices results in higher water treatment efficiency.
- The parameters used for WQV treatment valuation are more crucial in benefit-cost assessment of stormwater treatment efficiency in comparison to other physical simulation-related parameters.

- Some subwatersheds have higher nutrient removal efficiencies and some watersheds have lower removal efficiencies, calling for a systematic way to determine the most suitable subwatershed candidates, as given in the next chapter.
- The choice of metrics changes the selection results. Using BCR and treated WQV as the metric, smaller subwatershed areas are more suitable for rain garden implementation. However, the nutrient removal cost metric suggests that implementation of GI in upstream subwatersheds benefits downstream subwatersheds and results in higher downstream nutrient removal efficiency.
- The benefits at the household scale are similar to the ones at the watershed scale. Therefore, the highest efficiencies can be observed by siting GI in some subwatersheds, and even in a portion of the subwatersheds rather than uniform GI coverage across the entire area. However, the results show that even at the household scale, rain gardens are more cost effective for stormwater treatment than comparable technologies such as sand filters.
- Finally, the results showed that permeable pavements are considerably less effective than rain gardens. Also, considering the few locations in suitable for permeable pavements in semi-urbanized watershed, more emphasis should be given to rain garden practices.

This study uses historical continuous rainfall data in a calibrated hydrologic model, which does not account for longer-term climate change impacts on GI investment effectiveness. Further research with climate change scenarios is needed to determine the most effective long-term GI types and locations for each scenario.

This study uses existing models and literature to estimate environmental benefits and economic costs of GI projects and identify uncertainties in modeling parameters. However, some of the uncertain parameters did not have clear and defined uncertainty boundaries in the literature and simple triangular distributions were used. Further research is needed to develop appropriate distributions for all parameters and assess the impacts of other types of distributions (e.g. uniform, log-normal) on overall costs and benefits.

It is important to note that some benefits/costs may be consequential but are secondary to the primary effects of GI implementation. For instance, if nutrients are extracted from stormwater, stormwater treatment plants downstream that might extract such minerals and use them for energy recovery may lose some of their energy sources. Depending on the system boundaries, there could be numerous secondary uncertain effects, such as water treatment plant energy recovery processes and ecosystem stabilization due to nutrient removal, that need additional research.

Finally, further research is needed to quantify and monetize other benefits of GI, such as flood reduction, urban heat island mitigation, noise abatement, changes in real estate values, and micro-climate regulation. This would allow more accurate assessment of the trade-offs between different types of benefits and the optimal arrangement and location of GI for each category of benefits.

Chapter 5: Optimization of green infrastructure networks to maximize stormwater-related benefits and minimize life cycle cost using genetic algorithms and surrogate models

5.1. Introduction

As mentioned in Chapter 1, there are no clear guidelines on the optimal arrangements of GI practices across a watershed, given all of the installation and placement limitations. In fact, there is no consensus on a generalizable practical and quantitative framework to recognize optimum candidate locations for GI placement across a watershed. Most of the frameworks that are proposed in this domain, primarily in the scientific community, are subjective, not comprehensive, or do not provide quantifiable guidelines. One of the generalizable quantitative approaches is optimization.

Optimization has been conducted for many different purposes in water resources planning and management (Nicklow et al. 2010; Reed et al. 2013). Specifically, the EPA-SUSTAIN model for stormwater management can do LID optimization utilizing GIS information (Lee et al. 2012). The tool is a decision support system developed to evaluate alternative plans for stormwater quality management and flow abatement techniques in urban and developing areas. The tool uses a multi-objective optimization model, scatter search + Non-dominated Sorting Genetic Algorithm-II (NSGA-II), to locate optimal locations and types of GI.

Ciou et al. (2012) used a GA optimization model for the optimal placement of GI practices at the watershed scale to achieve water quality objectives at a downstream reservoir. Karamouz et al. (2010) developed a cost-effective GA optimization model with coupled watershed-reservoir and water quality models to design GI strategies. Kaini et al. (2012) used GA with a semi-distributed hydrologic model, Soil and Water Assessment Tool (SWAT), to find optimum GI networks for water quality goals at the watershed scale. Maringanti et al. (2009) used GA for BMP network optimization to control nonpoint source pollutant, with a specific focus on pesticides. Damodaram and Zechman (2013) developed a methodology to select sites

for placing LID practices by merging a GA with a hydrologic model, a hydraulic model, and curve-number-based models for peak flow reduction under different monetary budget scenarios.

Zhang and Chui (2018) have conducted a comprehensive review of existing spatial allocation optimization tools and strategies for GI placement in different catchments. According to their review, most studies have not addressed uncertainty in GI performance and its impact on optimal siting. Despite inherent uncertainties in parameter estimation for all of the models used in these studies, there has been no research published on how uncertainties affect GI placement. Uncertainty in system performance prediction has been a topic of considerable research on other water resources management problems, however. One of the first approaches to address uncertainty in optimization is the chance-constrained optimization approach (Charnes and Cooper 1959). The method has been applied to many different water resource management applications, including aquifer remediation planning (Wagner and Gorelick 1989), ground-water contamination prevention planning (Gailey and Gorelick 1993), reservoir planning for water supply and shortage (Houck 1979; Mariño and Simonovic 1981; Feiring, Sastri, and Sim 1998), and integrated agricultural and water resources management (Lu et al. 2016). The approach requires computing the deterministic equivalents of the constraints, which simplifies the optimization process but is only feasible for normal- or log-normal-distributed parameters.

Another common strategy to address uncertainty is the scenario-based optimization approach, which involves generating numerous parameter realizations from the prior distribution and evaluating the objective function for each sampled realization. This method has been applied in many water resources applications, including watershed management (Yong Liu et al. 2007) and monitoring network design for a contaminated site (Gopalakrishnan, et al. 2003; Chadalavada et al. 2011).

One scenario-based stochastic optimization approach, which is adopted in this research, is the noisy genetic algorithm (noisy GA). Noisy GAs use the traditional GA concepts to handle nonconvex, discrete problems, such as the GI application considered in this study. Noisy GAs are designed to maximize the fitness function

expectation by sampling from several realizations of the objective function for each solution throughout the optimization process. The technique has been applied to different applications such as groundwater remediation design (Gopalakrishnan, et al. 2003; Singh and Minsker 2008; Yan and Minsker 2011) and water allocation during extreme events (Zhao 2017). The method requires extensive sampling and realization evaluations to evaluate each solution over multiple parameter realizations, although low numbers of samples per realization (e.g., 5 per realization) are possible due to the population-based GA convergence process (Gopalakrishnan, et al. 2003). Since the GA does not analytically guarantee convergence to global optimal solutions, we refer to the solutions found in this study as preferable solutions.

To address and overcome the computationally-intensive sampling of noisy heuristic optimizations, surrogate objective functions or constraint models have been extensively proposed and used (Yan and Minsker 2006; Razavi, Tolson, and Burn 2012). In water resources management, surrogate models have been extensively used (Aly and Peralta 1999; Baú and Mayer 2006; Yan and Minsker 2006, 2011; Zhao 2017).

This chapter is the first study to develop and apply noisy heuristic optimization with surrogate models to GI design. A multi-objective, noisy genetic algorithm framework is developed to identify preferable GI networks that maximize environmental benefits and minimize economic costs. The environmental benefits include total runoff reduction and stormwater treatment, but the approach can be generalized with the addition of models of other types of benefits. The economic objectives include life cycle cost of the GI network.

One of the objectives of this study is to determine preferable patterns of GI networks across a watershed. SWMM models are coupled with a noisy multi-objective GA that trains data-driven machine learning algorithms as surrogate models. This approach helps validate the conclusions drawn from previous chapters and, more importantly, assists in driving the simulation-optimization results in a more efficient manner. It also helps to recognize patterns of preferable GI practices that can be used as implementation guidelines.

This chapter also applies post-optimization analytics techniques to investigate the patterns and parameters that indicate preferability of a subwatershed in siting GI practices. Several studies have used various post-optimization approaches to investigate the trade-offs between different solutions on the Pareto frontier (Reed and Minsker 2004; Antipova et al. 2015; Bandaru et al. 2017; Z. Wang and Rangaiah 2017). This study divides solutions among four budgetary scenarios and uses decision trees to classify each group of solutions, and their corresponding decision variables, based on subwatershed-related features. Decision trees and other data mining techniques have been applied to Pareto optimal solutions in the manufacturing domain (Dudas et al. 2015). Several green infrastructure optimization studies have focused either on “what-if” scenarios to meet stormwater treatment and management goals as well as regulatory needs (Neilson and Turney 2010; Liu et al. 2016), or on the choice between green and grey stormwater infrastructure (Lucas and Sample 2015; Alves et al. 2016). Therefore, post-optimization analytics to recognize emerging patterns from the array of potential solutions along a noisy Pareto frontier in the water resources domain is a novel contribution of this study.

In the next section, detailed descriptions of the methodology are presented, including steps required to define the optimization framework, algorithms developed and used, and the surrogate models.

5.2. Methodology

In this section, the case studies and their objective functions are briefly described. Then, the entire optimization framework is explored with a detailed explanation of the probabilistic optimization algorithm. Next, the surrogate modelling framework is presented. And finally, the post-optimization analysis is fully explained and presented. Fig. 5.1 summarizes the overall steps of the methodology, which can be applied to any case study. The first major step in the methodology is (a) correct definition of case study, GI practices, fitness values, objective functions, constraints, and uncertain modelling parameters. The second major step (b) involves application of a noisy genetic algorithm to the problem. The third step (c) is about training, testing, and tuning the surrogate models. The fourth and fifth steps (d and e) include applications of offline and online optimization methods. The last major step (e) involves application of post-optimization

analytics to determine patterns in the configurations of GI coverage across all subwatersheds based on the derived Pareto frontiers.

5.2.1. Case study

The case study watershed considered in this chapter is DR5, which was described in Chapter 2. The modelling parameters, settings, and SWMM models are the same as those discussed in Chapters 2 and 4. In the previous chapters the different distributions of benefits and costs across different spatial scales were presented. In Chapter 3, the impacts of GI practices in a semi-urbanized watershed, such as DR5, were shown for design storms. It was shown in Chapter 3 that, even after full coverage of GI at all potential locations, the magnitudes of the stormwater related benefits during storm events were relatively small. Therefore, in this chapter the focus is on the performance of GI practices during continuous rainfall simulations, using the same continuous rainfall records as in Chapter 4.

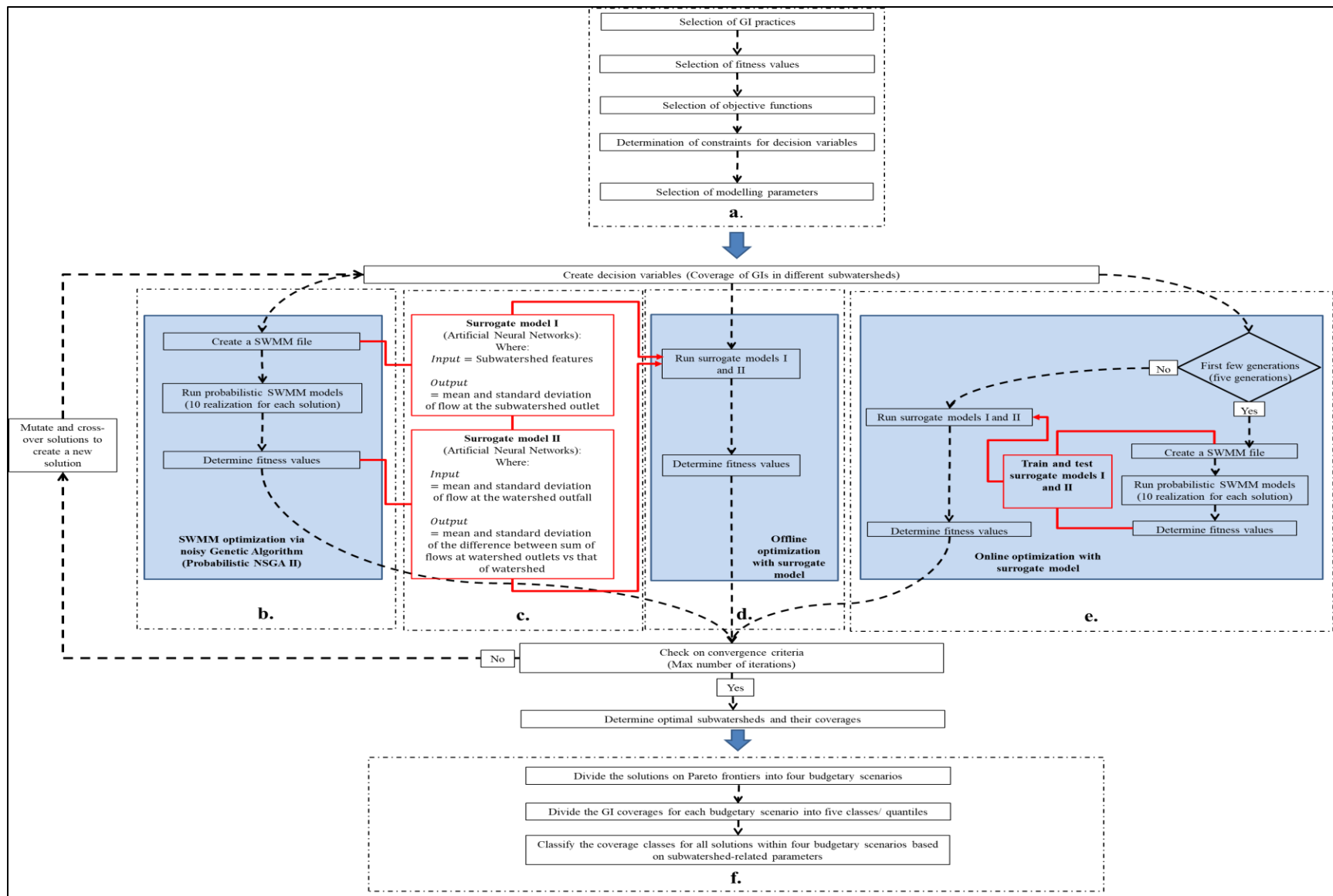


Fig. 5.1. Flow chart describing steps of the methodology

5.2.2. Optimization formulation and algorithms

To find preferable GI networks for the DR5 watershed, it is necessary to see the performance of each proposed network/arrangement (i.e., solution) in terms of its objective function value (or fitness function value in GA terminology). To determine a set of fitness values that encompass stormwater capture, treatment, and life cycle cost associated with each design, GI coverage and nutrient load and stormwater volume reduction costs are considered, same as the analysis metrics in Chapter 4.

Fig. 5.2 shows the nutrient load reductions and stormwater volume reduction costs at the DR5 outlet resulting from 500,000 realizations of GI coverage throughout the watershed. These results were generated using the same methodology as in Chapter 4, Monte Carlo Simulation Type I. Fig 5.2. shows that these two metrics are highly correlated, with a correlation coefficient of 0.96. Therefore, only cumulative flow reduction and life cycle cost are used as the two fitness values for each potential solution within the optimization framework.

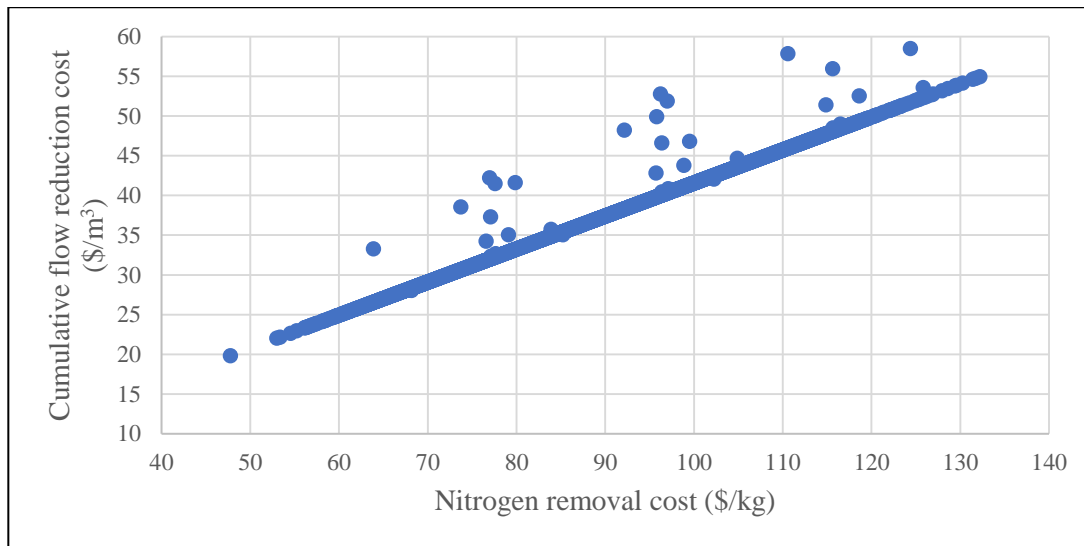


Fig. 5.2. Nitrogen removal cost vs cumulative flow reduction costs for numerous realizations of GI coverage scenarios

To evaluate the fitness of each solution, the same models were used as in Chapter 4 (i.e. WERF SELECT model to determine life cycle cost of GI projects and SWMM 5.0. to determine cumulative flow reduction).

This optimization problem does not have a linear objective function. In fact, the relationship between inputs and outputs is complex due to uncertainties inherent in the modeling process (See Appendix I). As a result, linear or non-linear optimization approaches cannot be applied to this problem without sacrificing accuracy. Therefore, running a meta-heuristic noisy genetic algorithm is a suitable strategy to optimize the watershed for GI coverage.

Noisy GA is a stochastic optimization algorithm that uses traditional GA mechanisms (selection, crossover, and mutation) in a noisy environment for fitness functions that are prone to uncertainty (Fitzpatrick and Grefenstette 1988). Noisy GAs are designed to maximize the conditional fitness expectation for each solution via realization sampling and averaging the fitness values. The number of samples used for fitness averaging is a factor that dictates optimization robustness and efficiency. Even a low sampling number, e.g. as low as five, has been shown to be sufficient for discovery of a reliable solution using noisy GA (Gopalakrishnan et al. 2001). This efficiency occurs because the population contains many individual solutions; as the population converges, multiple samples of a particular solution's fitness will eventually be found in the population. Therefore, even with noise, any individual solution that fails under different sampled conditions will be excluded in the evolution process.

Selection is an important mechanism in this process. Tournament selection, a common practice in GA applications, consists of comparative assessment of two or more solutions, based on fitness value, to select the fittest for the mating mechanisms (i.e., crossover). For this application, each population generated in each generation of the GA process has individual solutions whose fitness function is computed via numerical simulation models, trained surrogate models, or a mix of both simulation and surrogate models. The three categories described above are referred to as the scenario without surrogate models, the scenario with surrogate model trained offline, and the scenario with surrogate models trained online, respectively.

Equations 5.1 to 5.2 show the two fitness (objective) function formulations for the GI optimization model, F_1 and F_2 . The decision variable in this portion of the study is A_i – ratio of GI area over total candidate area

in the i -th subwatershed. Since SWMM is a lumped parameter model, these sets of decision variables determine the portion of the subwatershed allocated to GI implementation.

$$F_1 = \min \left(\sum_{i=1}^{n_{subwatershed}} \frac{\sum_{s=1}^{n_{simulations}} cost_{i,s}}{N} \right) \quad (\text{Eq. 5.1})$$

$$F_2 = \min \left(\sum_{i=1}^{n_{subwatershed}} \frac{\sum_{s=1}^{n_{simulations}} R_{i,s}}{N} \right) \quad (\text{Eq. 5.2})$$

Where:

$cost_{i,s}$: Life cycle cost of GI implementation in i -th subwatershed generated from s -th simulation (Indirect function of A_i ; For more details on this relationship, see Appendix I.

$R_{i,s}$: Total runoff volume at i -th subwatershed outlet throughout rainfall period generated from s -th SWMM simulation (Indirect function of A_i)

N : Number of realizations for each solution

This objective function formulation accounts for uncertainty in probabilistic uncertain parameters used in the SWMM and WERF models (listed in the case study Section 5.2.1) by taking simple averages of several simulations for each fitness evaluation. In other words, as new sets of solutions are generated (i.e., GI coverage in different subwatersheds), the SWMM model is executed multiple times and use the average/expected values of their solutions in Equations 5.2 and 5.3. The multi-objective optimization formulation used in this study is a classic Non-dominated Sorting Genetic Algorithm (NSGA), which creates an archive of the solutions evolved throughout the simulation period and compares each new solution to the best points in the archive (Deb et al. 2000; Singh and Minsker 2008).

To set up the noisy NSGA-II platform, “deap” package was used and modified to include uncertainty in the objective functions (Fortin et al. 2012). For mutation and crossover algorithms, polynomial mutation and simulated binary crossover methods are used, respectively (Deb and Agrawal 1995; Liagkouras and Metaxiotis 2013). The algorithms enable the use of real numbers as decision variables and have been shown to outperform many alternatives (Liagkouras and Metaxiotis 2013). Based on GA guidelines (Minsker 2005), the mutation and crossover probabilities were set at 0.9 and 0.01, respectively, for this case study.

The population size and number of GA generations have been decisive factors in the computational burden of the optimization process (Gibbs et al. 2006). For this case study, the population size was set to 100 based on a trial and error process in which several population sizes (10, 25, 50, 100, and 200) were tested and their corresponding evolved Pareto frontiers were compared. In the first three trials, the small population size resulted in drift and lack of solution exploration. The population sizes of 100 and 200 resulted in similar Pareto fronts. Due to lower computational time, the results associated with a population size of 100 is presented in this chapter. Through trial and error with the population size of 100, the maximum number of generations was set to 3000, which was sufficient for convergence of the Pareto front.

Also through trial and error, the number of realizations for each solution was set to 10 to provide sufficient but not excessive samples to train the surrogate models and generate the uncertainty bounds that are used for probabilistic selection in the multi-objective noisy GA. Multiobjective GAs explore the fitness function response surface and find the Pareto optimal solutions, for which any of the objective functions cannot be improved without compromising improvements in others. To do so, individual solutions are compared to all others in the population and ranked based on their level of nondominance. The overall goal of the NSGA-II multiobjective GA used in this work is to minimize the overall rank of the solutions (Deb et al. 2000). For noisy GAs, hypothesis testing is used for the comparison to give a higher level of confidence for the dominance ranking process (Singh and Minsker 2008). In this study, the confidence level for the hypothesis test, i.e. student’s t- test, is set to 0.95. Also, the noisy GA was executed on a GPU NVIDIA M5000 node with 36 cores and 256 GB of memory using high-performance computing (HPC) capabilities on a SLURM system at SMU.

5.2.3. Surrogate models to quantify uncertainties in stormwater capture at subwatershed and watershed levels

As mentioned, the watershed optimization under uncertainty is a computationally-intensive process. Two computationally intensive modules in the proposed framework contribute to this burden. The first computationally-intensive process is quantification of uncertainties in stormwater capture and cost of each set of GI coverages at the subwatershed level, which result from uncertainties in rain garden modeling parameters. In Chapter 1, these uncertainties are quantified for limited coverage ratios. However, within the optimization process, these uncertainties have to be quantified for any given set of GI coverages, as explained in Section 4.2. Also, after quantifying the stormwater capture and life cycle cost for all subwatersheds, there is a need to compute their corresponding values at the watershed outlet. Although the life cycle costs at the subwatershed level can simply be added together to obtain the corresponding value at the watershed outlet, the same cannot be applied to stormwater capture, which is nonlinear. Therefore, there is a need to train another surrogate model to predict stormwater capture at the watershed outlet given the stormwater capture in each subwatershed.

The second computationally intensive process is genetic algorithm optimization to determine preferable subwatersheds and their GI coverages using the SWMM simulation models. This process requires numerous realizations of the SWMM model, each generating different sets of GI coverages. Considering the computational time required for every simulation, as well as the probabilistic nature of genetic algorithm convergence to preferable solutions, the multi-objective GA requires significant computational time to generate a probabilistic Pareto frontier.

Considering all of these processes, the entire framework is extremely computationally intensive. For the case study considered here, each SWMM simulation requires up to 20 minutes to generate one evaluation of a fitness function. Conducting the evaluations for numerous realizations to generate a posterior distribution of the fitness function therefore requires significant computational power. Furthermore, the meta-heuristic nature of the optimization framework relies on numerous population generations of

generating the fitness function's posterior distribution. For this case study, approximately 1,500,000 fitness function evaluations are required in total, which is 790 hours, assuming that the computational scripts are not parallelized.

Therefore, despite the generalizability of the simulation-optimization framework, the imposed computational burden is likely to hinder application of the framework to real-world case studies. In this chapter, we explore the use of surrogate models to reduce computational time by decreasing executions of the SWMM model.

Feedforward artificial neural networks (ANNs), especially multilayer perceptrons (MLPs), are flexible models that are commonly used as surrogate models (Maier et al. 2010). The models rely heavily on the number of hidden layers, number of perceptrons within the layers, and the type of transfer function, which are specific to the case study and need to be selected by the user. Neural networks are capable of emulating and approximating any function, given that the network features are set appropriately (Maier and Dandy 2000; Maier et al. 2010) However, creating an exact emulator is not usually the primary focus of most surrogate model users, especially when data contain uncertainty and the number of input features is relatively large.

ANN have been extensively used in the field of hydrology as surrogates for physics-based numerical models (Khu and Werner, 2003; Riad et al. 2004; Zou, Lung, and Wu 2007; Behzadian et al. 2009; Kourakos and Mantoglou 2009; Broad 2014), primarily for watershed-level responses to rainfall events. The proposed methodology works at a smaller scale, i.e., subwatershed. Also, input parameters in the models developed here are subwatershed features, which are different from rainfall input used in the reviewed literature. Specifically, the surrogate models are designed to predict the mean and standard deviation of cumulative flow reductions at the subwatershed level. As mentioned in Section 5.2.3, the surrogate models require training and validation using the archives of fitness values and their corresponding decision variables. The Scikit-learn ANN package is used for this, with sigmoid activation functions and constant learning rate of

0.0001. The remaining parameters that must be tuned are: number of hidden layers, number of perceptrons, and the number of iterations for backpropagation training. To determine the minimum number of training iterations at which the testing errors would be minimized, the mean squared errors (MSEs) of model training and testing are plotted against different maximum numbers of training iterations for a simple network with one hidden layer and 20 perceptrons. Fig. 5.3. shows the MSE versus the total number of iterations to predict the mean cumulative flow reduction at the subwatershed level.

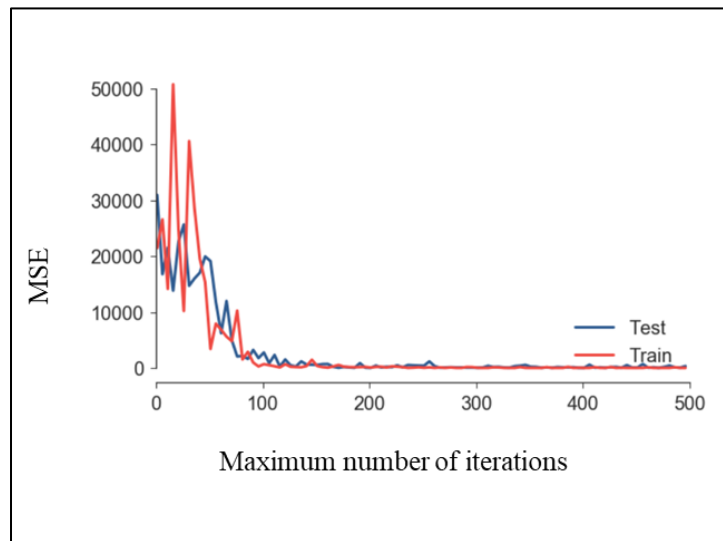


Fig. 5.3. MSE vs. maximum number of iterations for ANN training and testing to predict the mean cumulative flow reductions at the subwatershed level

The figure shows that 100 iterations is sufficient for the ANN to converge and stabilize. To be conservative, 200 iterations are used to tune the other two parameters. Fig. 5.4. shows the MSE for different layer sizes with 200 training iterations.

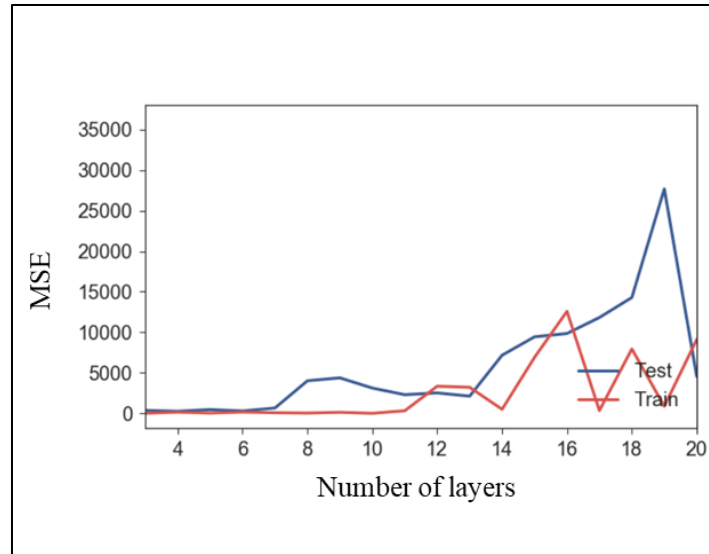


Fig. 5.4. MSE vs. different layer sizes for 200 iterations of ANN training

The MSEs for 200 iterations tend to be stable and close to zero for six layers or less. However, as the number of layers exceeds six, the MSE, especially during testing, tends to increase significantly, suggesting the ANN model is overfit to the training dataset. Therefore, a network of six layers is used to tune the model for the optimal number of perceptrons.

Through grid search, available on Scikit-learn package in python, a “fit” and “score” method is implemented that optimizes the hyper-parameter by cross-validated search over a parameter grid with an interval of one. This search indicated that the optimal number of perceptrons in each layer for this case study is 20, while the other two parameters, i.e. number of layers and number of iterations, were fixed. Fig. 5.5. shows the resulting MSE plots for training and testing datasets to predict the mean flow reductions at the subwatershed level with six layers and 20 perceptrons. After 200 iterations, the training MSE is 0 and the testing MSE is 3.5 m^3 (2.1% of the average of mean flow reductions at the subwatershed level).

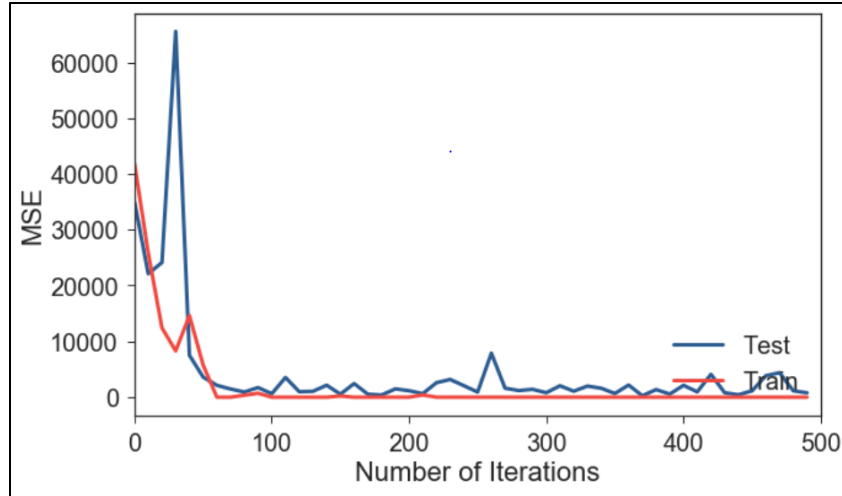


Fig. 5.5. MSE vs. maximum number of iterations for ANN training and testing to predict mean cumulative flow reductions at the subwatershed level (network with six layers and 20 perceptrons)

As mentioned previously, the cumulative flow reduction at the watershed outlet, which is one of the fitness function values, is not equal to a linear summation of the reductions at the subwatershed levels based on the assumptions used in this study. Thus, two alternative indicators for the prediction of cumulative flow reduction at the watershed outlet via surrogate models are compared: cumulative flow reduction at the watershed outlet and the difference between the sum of subwatershed cumulative flow reductions and the cumulative flow reduction at the watershed outlet.

After tuning the ANN models for the two metrics, the R^2 values associated with the cumulative flow reduction at the watershed outlet and the difference between the sum of subwatershed and watershed flow reductions are 0.80 and 0.96, respectively. The higher prediction accuracy associated with the second metric suggests that predicting the difference between the sum of subwatershed and watershed flow reductions is more accurate than predicting watershed flow reduction directly. Therefore, the surrogate models are trained to predict the mean and standard deviation of the flow reductions at the subwatershed levels, use the predicted values to calculate the mean and standard deviation of the summation of the flow reductions at the subwatershed level, and finally predict the mean and standard deviation of the difference between the summation and flow reductions at the watershed outlet.

The ANN models developed in this work are black-box tools for the SWMM models that can be used to rapidly predict uncertainty ranges for subwatershed simulation results for a given storm or a continuous rainfall record. The ANN models assist the optimization process via the following approaches, as explained briefly in Section 5.2.2:

1. *Offline surrogate models:*

In this approach, the surrogate models are pre-trained and pre-tested using the database archive generated during execution of the noisy GA without surrogate. These models then substitute for the numerical simulations in predicting the mean and standard deviations of the fitness values throughout the noisy GA execution.

2. *Online surrogate models:*

In this approach, for the first five generations of the noisy GA process, only the numerical simulation model is used for evaluating fitness. After the first 5 generations, with each generation having a population of 200 individuals and each individual having 10 realizations to quantify uncertainties, the online surrogate model is trained and tested. The features for the online surrogate model are similar to the ones used for the offline version (i.e., the same number of layers, same number of perceptrons, and same number of iterations). Five generations were selected as the surrogate training threshold because the resulting 5,000 available simulation runs ($5 \times 100 \times 10$) ensures that every potential percentage GI coverage within any subwatershed is 99% likely to occur. Eq.5.3 shows how this number is computed, assuming that percentage coverages are rounded to integer variables.

$$P(o) = 1 - P(no) = 1 - n * P(r_{no})^r \quad (\text{Eq. 5.3})$$

Where:

$P(o)$: probability of a particular coverage occurring within the first five generations

$P(no)$: probability of a particular coverage not occurring within the first five generations

n : number of potential solutions (100 for this case study)

$P(r_{no})$: probability of a solution not occurring within each run (0.99)

r : total number of simulation runs (5,000 for this case study)

After five generations, just the surrogate models are used for the remaining generations.

5.2.4. Post-optimization analytics

As the optimization converges to preferable solutions, GI coverages in different subwatersheds for each point on the Pareto frontier are determined. By dividing the Pareto frontier into several sections and sorting the sections by life cycle cost from low to high, average coverages for sets of budgetary scenarios can be determined. Then, for each budgetary scenario, the distribution of GI coverage scenarios can be determined by computing decision variable statistics for each solution. Doing so, the watersheds can be classified into five categories, based on mean preferable GI coverage, for each budgetary scenario. Then, supervised classification methods, specifically decision trees, are used to assess the importance of different watershed-related features on GI coverage within each of the four budgetary scenarios.

Decision trees are structures where each node pertains to a test on an attribute, each branch represents the outcome of the test, and each leaf node holds a subset of data categories. The criterion to construct the trees is Gini impurity, i.e. the probability of incorrectly classifying a randomly chosen element in the dataset if it were randomly labeled according to the class distribution in the dataset. Eq. 5.4. shows the Gini impurity equation.

$$G = \sum_{i=1}^C P_i(1 - P_i) \quad (\text{Eq. 5.4})$$

Where:

C : number of classes

P_i : the probability of randomly picking an element of class i

To construct the decision trees, the objective is to find the best split of the dataset by maximizing the Gini Gain, which is computed by subtracting the weighted impurities of the branches from the original impurity (Coppersmith et.al. 1999). In this case study, for each budgetary scenario, the prediction classes are the GI coverage classes of the solutions. The attributes are subwatershed-related parameters, which were discussed in Section 4.3.9. The decision trees are constructed using “Scikit-learn” package in python. Also, the maximum depth of the decision trees is set to three to identify only the most predictive subwatershed-related parameters in determining the five categories of preferable GI coverages for each budgetary scenario.

5.3. Results

In this section, the results of the genetic algorithm without surrogate models are first presented in Section 5.3.1 as a benchmark, as well as to explore how levels of GI investment affect GI siting across the watershed. Then the focus in Section 5.3.2 is shifted to comparative results from the two surrogate modeling approaches considered in this study.

5.3.1. Noisy multi-objective genetic algorithm results

Fig. 5.6. shows the Pareto frontier of the preferable GI strategies found among 3,000,000 evaluations (equivalent to 3000 generations, each with a population size of 200 individuals and 10 realizations for each individual) after 35 days of computing time. This Pareto frontier is treated as a benchmark case for the other optimization scenarios.

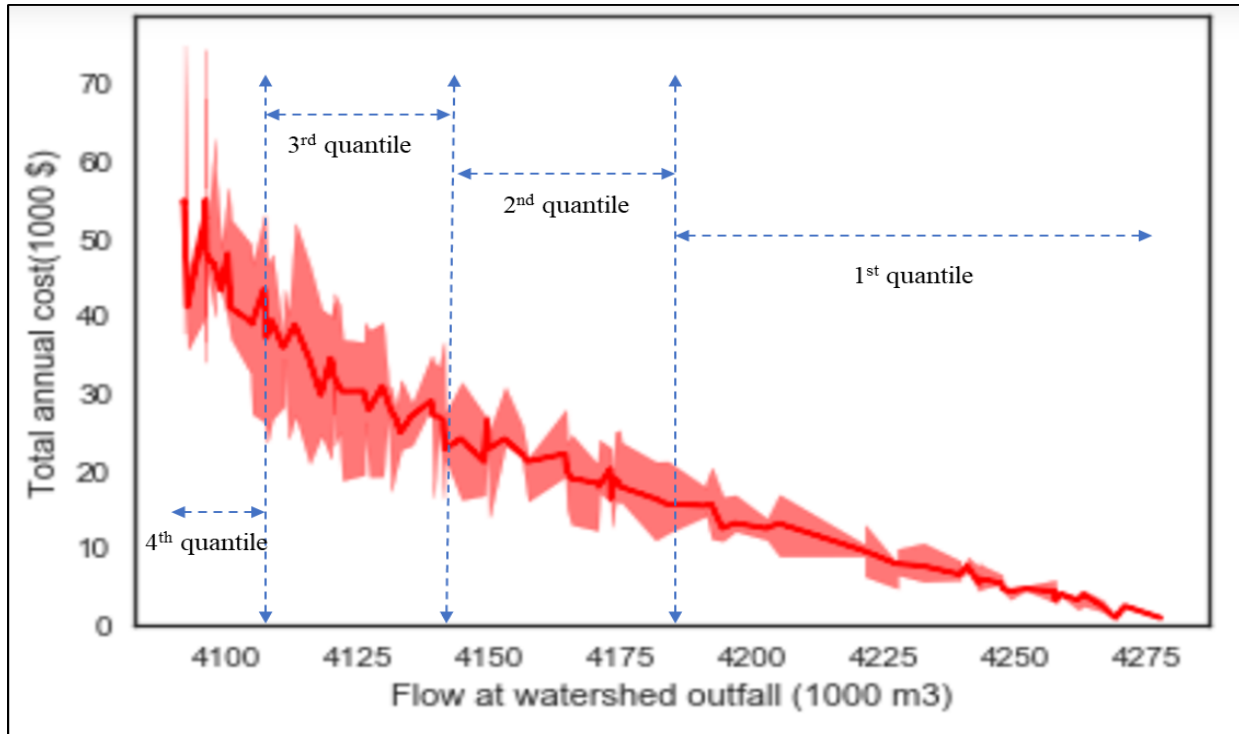


Fig. 5.6. Pareto frontier generated via noisy multi-objective GA for DR5 watershed

The preferable patterns of GI coverage across the watershed are investigated by dividing the solutions on the Pareto frontier into four budgetary scenarios representing the four quantiles of life cycle cost shown in Fig. 5.6. Fig. 5.7 shows the average coverage of GI among the solutions on the Pareto frontier for each budgetary scenario. The maximum GI coverage among the subwatersheds changes from 37% to 99%, comparing Fig 5.7.a to Fig. 5.7.d, as the investment budget increases. The coverage classes for the subwatersheds also change, implying that the preferable coverage of GI within subwatersheds depends on budgetary constraints.

Next, the effects of subwatershed-related features (subwatershed area, imperviousness ratio, area of rain garden candidates, distance from subwatershed outlet to the watershed outlet along the stream, runoff coefficient for the continuous rainfall period, and Shreve order number) on the level of GI coverage in Pareto frontier solutions is investigated. For each budgetary scenario, the preferable GI coverage is divided into five quantiles, sorted based on GI coverage from low to high. The ranges of the classes for the four budgetary scenarios are presented with different colors in Fig. 5.7. Then, decision trees (described in

Section 5.2.3.) were created to determine the effects of subwatershed-related parameters on the coverage classes for each of the four budgetary scenarios given in Section 5.2.2.

Fig. 5.6 shows the four classification trees generated for the four budgetary scenarios. Within each node, except for nodes at the end of branches, five rows of information show the criteria for subsequent branches: (1) the sample attribute (i.e., subwatershed characteristic) used for branching and the threshold for branching, (2) the Gini value for the node, (3) total number of samples (subwatersheds) that are classified into the node, (4) number of samples in each of the five coverage classes for that node, and (5) coverage class in which the samples can be classified. If an ending node, i.e. a leaf, has a Gini value of zero then its samples (subwatersheds) in brackets (third row) can no longer be classified into different coverage classes and they all belong to the coverage class associated with that leaf. For any node that does not have a Gini value of zero, the classification associated with the node, and the number of samples in brackets for the five coverage classes (row 3 or 4), have to be further classified in order to reliably select a coverage class. Note that, because the trees are limited to three levels to reduce model complexity, some leaf nodes do have non-zero Gini values and could be split further on other attributes if a more complex model is desired.

Fig. 5.8 suggests that for the highest (Fig. 5.8d) and lowest (Fig. 5.8a) budgetary scenarios, the distance to watershed outlet is the decisive factor in GI siting. When the budgetary scenario is lowest, GI practices should be installed only in subwatersheds closest to the watershed outlet. When the budgetary scenario is highest, GI is sited across the watershed but highest priority is still given to subwatersheds closest to the watershed outlet.

On the other hand, according to Figs 5.8.b and 5.8.c, the importance of total distance to the watershed outlet is lower for the middle budgetary scenarios. In fact, the impacts of different features for preferable GI coverage for these solutions are more complex, don't follow a consistent pattern, and require more depth for their corresponding classifier decision trees.

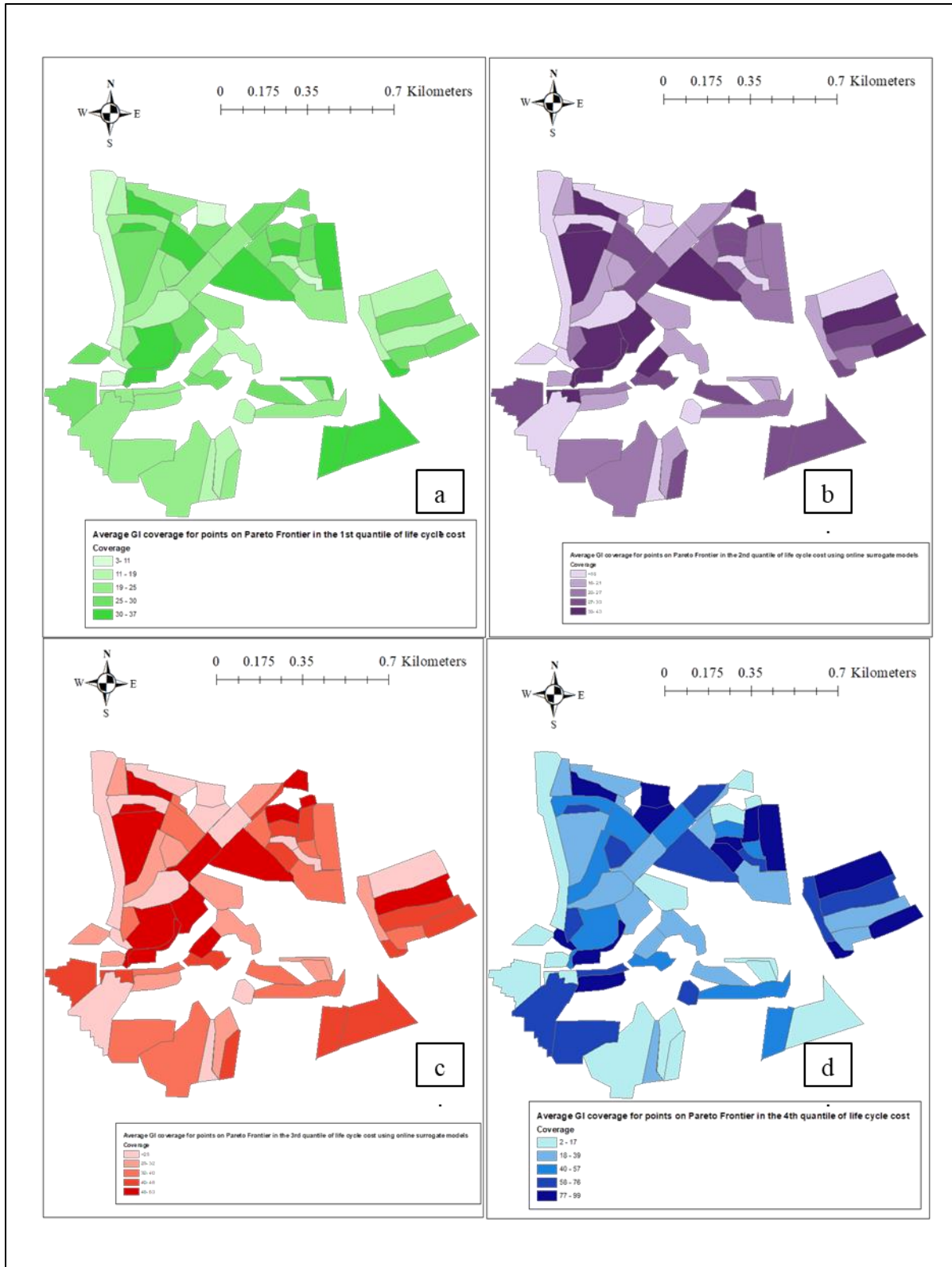


Fig. 5.7. Average GI coverage for points on the Pareto frontier in the (a) first, (b) second, (c) third, and (d) fourth quantile of life cycle cost.

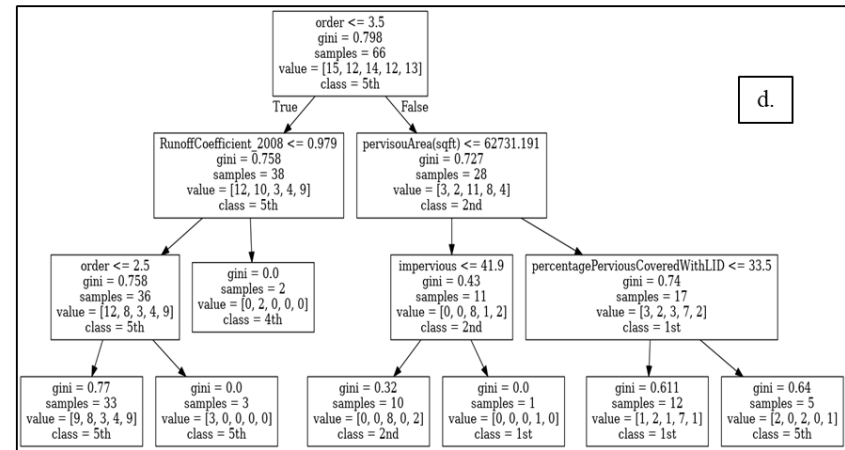
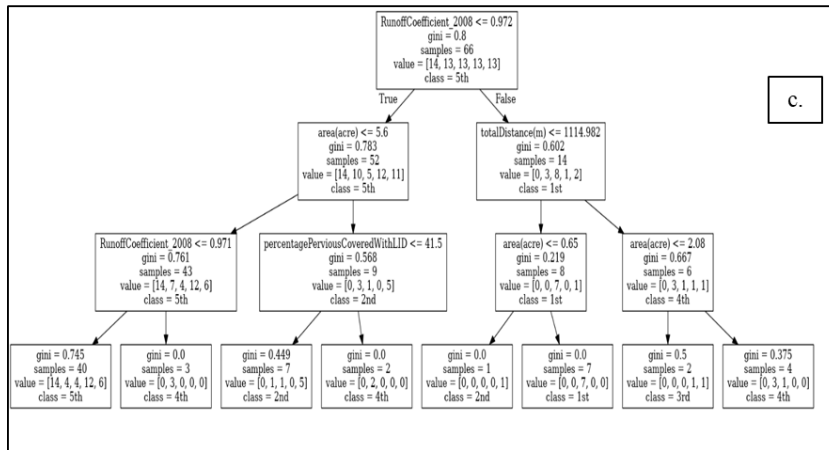
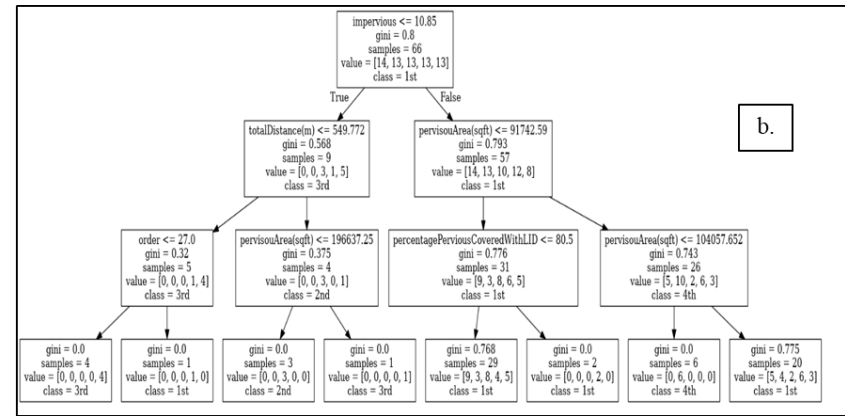
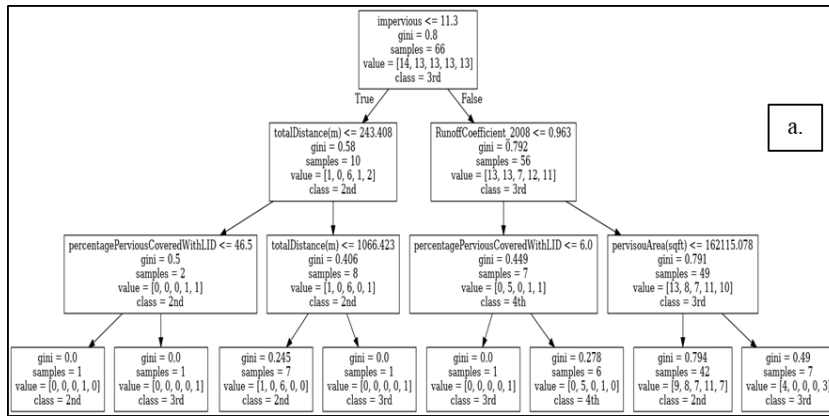


Fig. 5.8. Decision trees to classify subwatersheds based on GI coverage classes within (a) 1st life cycle quantile, (b) 2nd life cycle quantile, (c) 3rd life cycle quantile, (d) and 4th life cycle quantile budgetary scenarios

5.3.2. Results of optimization with offline and online surrogate models

This section compares results from the offline and online surrogate models, described in Section 5.2.3, with the benchmark results from the previous section that used the computationally-intensive numerical model.

The computation time for the offline surrogate model was 0.85 days, as compared to 35 days for the benchmark case without the surrogate. Fig. 5.7 compares the Pareto frontier generated with the offline surrogate model to the benchmark case without the surrogate model. To ensure comparability of the two Pareto fronts, the surrogate solutions were evaluated with the numerical model after the optimization was completed.

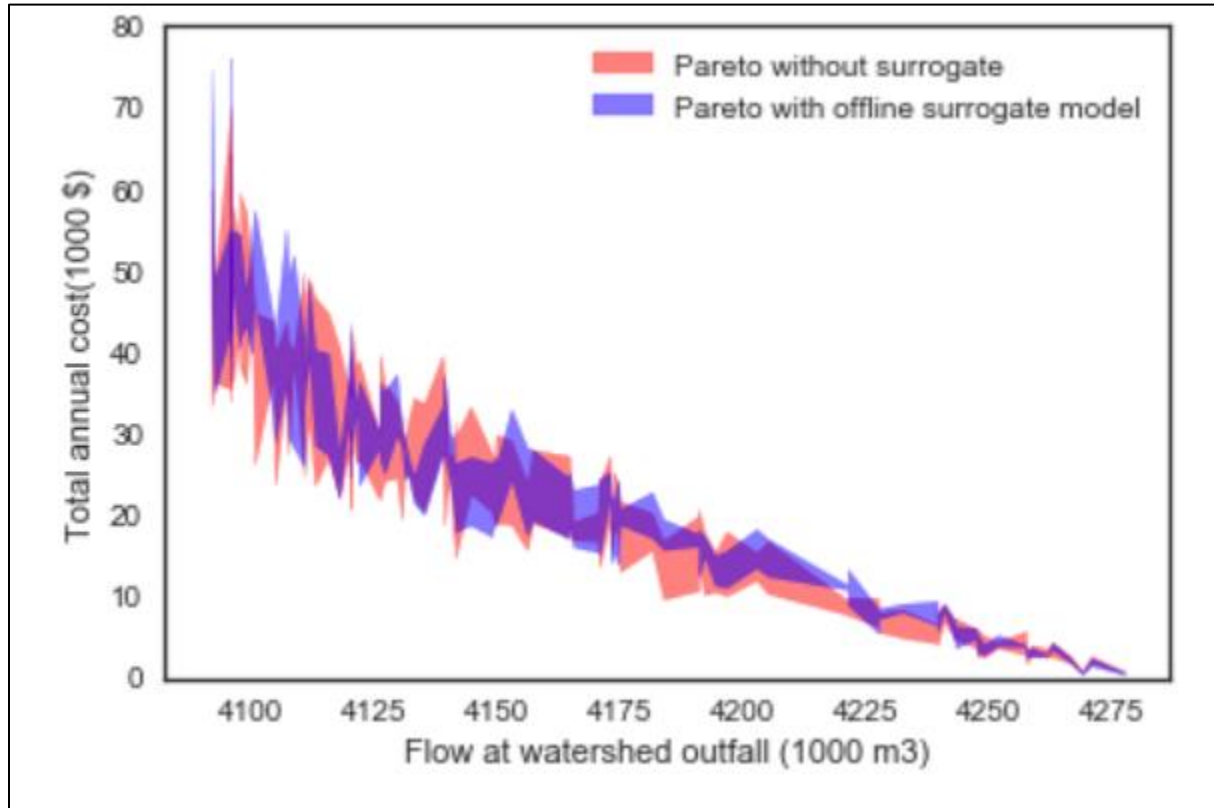


Fig. 5.9. Comparison of Pareto frontiers generated from noisy GA without the surrogate models and with the offline surrogate model. The solutions on both frontiers are evaluated using the numerical model. (The band shows the 90% confidence interval of the ten realizations associated with each solution.)

According to Fig. 5.9, the fitness values from the surrogate models are similar to those found by the noisy

GA without the surrogate models. A 2-D Kolmogorov-Smirnov test for similarity of the two distributions

of fitness values resulted in D statistics and p-value of 0.06 and 0.67 respectively. This means that the two Pareto frontiers are statistically similar at a confidence level of 99%. Table 5.1. shows the mean and standard deviation of the differences in preferable GI coverages from the noisy GA with and without offline surrogate models in each of the four quantiles of life cycle cost and five categories of subwatershed coverages (shown in Fig. 5.5).

Table 5.1. Mean and standard deviation of differences in preferable GI coverage from Noisy GA to offline surrogate model (positive sign in parentheses shows an increase in mean coverage compared to the noisy GA without surrogate models.)

	1 st coverage class	2 nd coverage class	3 rd coverage class	4 th coverage class	5 th coverage class
1 st quantile of life cycle cost	(+) 2%± 2%	(+) 3%± 2%	(+) 4%± 2%	(+)3%± 3%	(+) 3%± 2%
2 nd quantile of life cycle cost	(+) 2%± 2%	(+) 3%± 2%	(+) 3%± 2%	(+) 4%± 2%	(+) 4%± 1%
3 rd quantile of life cycle cost	(+) 5%± 3%	(+) 5%± 3%	(+) 6%± 4%	(+) 5%± 3%	(+) 6%±3%
4 th quantile of life cycle cost	(+) 7%± 2%	(+) 7%± 2%	(+) 6%± 3%	(+) 7%± 3%	(+) 8%± 4%

Table 5.1 shows that the most significant differences are observed in the 4th quantile category. The coverages in the first and second quantiles did not change significantly, meaning that the preferable locations for GI installations and the order of GI coverage across subwatersheds did not change significantly with implementation of the offline surrogate model compared to the benchmark case.

The online surrogate model also significantly reduced computational time, from 35 days to 1.9 days, but not as much as the offline surrogate, which required 0.85 days. However, to be comparable, time spent generating the training set for the offline surrogate must be considered, which was 35 days. Overall execution time for the online surrogate model was thus significantly lower than the offline surrogate model.

Fig. 5.10 compares the Pareto frontier generated by the online surrogate model with the benchmark case without surrogate model. Another 2-D Kolmogorov-Smirnov test of the similarity of the two distributions of fitness values was conducted and the resulting D statistics and P-value were 0.1 and 0.74 respectively, suggesting that there the two distributions are not statistically different from each other with 99% confidence.

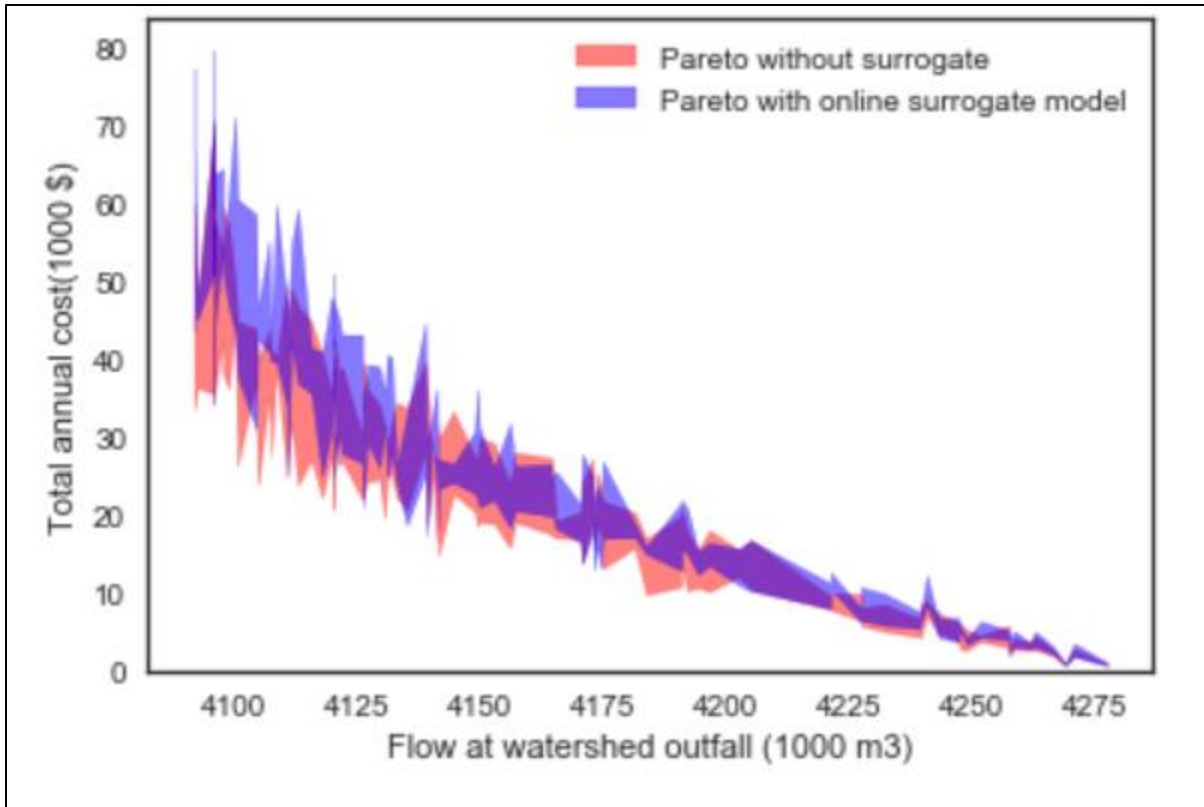


Fig. 5.10. Comparison of Pareto frontiers generated from noisy GA with and without the online surrogate models

Fig. 5.11 shows the average GI coverage identified with the online surrogate model for the four budgetary scenarios. The patterns of preferable GI coverage across the subwatersheds remain the same as those presented in Fig 5.7.

Table 5.2 compares the GI coverages across subwatersheds between the noisy GA with and without online surrogate models in the four quantiles of life cycle cost and five categories of coverages. The positive sign in parentheses shows an increase in coverage compared to the noisy GA without surrogate models in Table 5.2. As with the offline surrogate results in Table 5.1, the largest differences can be observed in the 2nd and 3rd quantile categories, especially in the subwatershed with the highest coverage (i.e., the 5th coverage class).

However, the results consistently show that regardless of the method used, i.e. noisy GA with no surrogate, online surrogate model, or offline surrogate model, the distributions of preferable coverages, comparing

Fig. 5.11 to Fig. 5.7, within the four different budgetary scenarios remain the same. Consequently, the decision trees created for this optimization scenario would be the same as the ones presented in Fig. 5.6 without surrogate models. This observation suggests that both surrogate models perform accurately enough to identify the preferable arrangement patterns of GI coverages across the watershed, despite the differences observed in Tables 5.1 and 5.2.

Table 5.2. Differences in preferable GI coverage across subwatersheds from Noisy GA to online surrogate model

	1 st coverage class	2 nd coverage class	3 rd coverage class	4 th coverage class	5 th coverage class
1 st quantile of life cycle cost	(+) 3%± 3%	(+) 4%± 2%	(+) 4%± 2%	(+) 4%± 2%	(+) 4%± 3%
2 nd quantile of life cycle cost	(+) 5%± 4%	(+) 4%± 3%	(+) 5%± 2%	(+) 7%± 2%	(+) 4%± 3%
3 rd quantile of life cycle cost	(+) 5%± 3%	(+) 6%± 4%	(+) 5%± 5%	(+)8%± 4%	(+) 6%±2%
4 th quantile of life cycle cost	(+) 10%± 2%	(+) 8%± 4%	(+) 8%± 5%	(+) 10%± 4%	(+) 8%± 4%

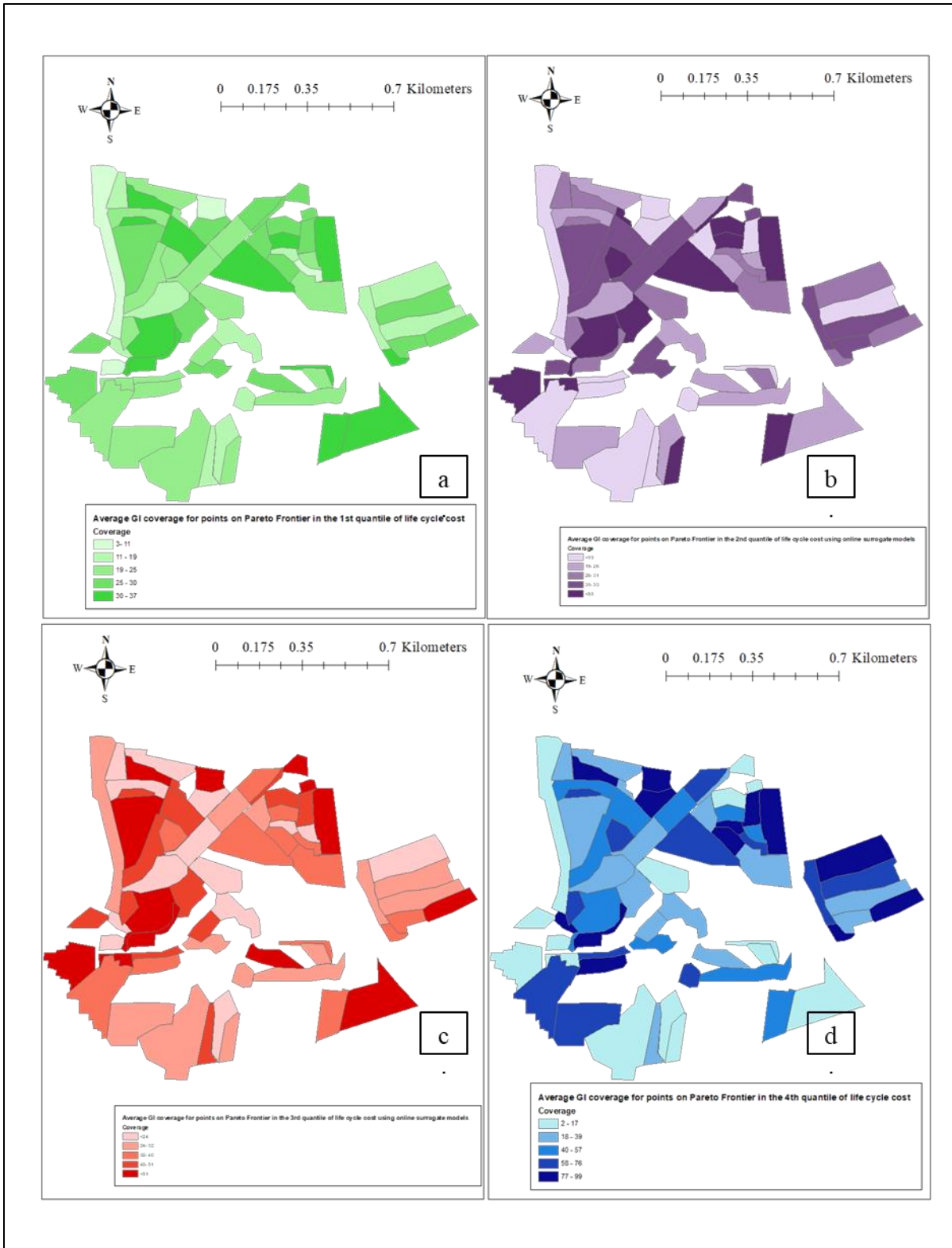


Fig. 5.11. Average GI coverage for solutions on the Pareto frontier found via online surrogate models in the (a) first, (b) second, (c) third, and (d) fourth quantile of life cycle cost

5.4. Conclusions and future work

This chapter presented an optimization framework for planning green infrastructure networks considering for stormwater and life cycle objectives. The optimization process involves a multi-objective, noisy genetic algorithm that accounts for uncertainties associated with GI modeling parameters. The approach integrates two simulation models (i.e., SWMM and WERF), which work at subwatershed scales to predict the cumulative flow at the watershed outlet, with three different optimization algorithms: noisy NSGA-II without surrogate models, noisy NSGA-II with offline surrogate models, and noisy NSGA-II with online surrogate models.

Classifying the preferable GI coverages obtained without surrogate models via decision trees shows that for the budgetary scenario with the highest and lowest budgets, distance to the watershed outfall is the most important factor in GI siting. In the lowest budgetary scenario, the decision trees suggest that the highest (and perhaps only) investments should be allocated to subwatersheds closest to the watershed outlet. The highest budgetary scenario also gives highest priority to this region, but GI is sited in other subwatersheds as well, with the lowest priority given to subwatersheds with the highest distance to the watershed outlet.

Other studies have also found that implementation of GI practices would be most beneficial at downstream subwatersheds closest to the watershed outlet (Di Vittorio and Ahiablame 2015; Giacomoni and Joseph 2017). However, there has not been a consensus on best locations for GI implementation, and Zhen et al. (2004) have argued that catchment characteristics and environmental goals should be taken into consideration. The framework developed in this study would facilitate further optimization-simulation analysis for diverse watersheds and environmental goals in order to investigate what GI siting arrangement/network is the most beneficial for a given case study.

Obtaining these results with the noisy GA without surrogate model is extremely computationally demanding. Therefore, surrogate models were created using ANNs to reduce the computational effort. The online and offline surrogate models, which rely on archives of decision variable inputs and fitness value

outputs, were able to predict the mean and standard deviation of cumulative flow reductions at the subwatershed and watershed outfall with R^2 of 80% and 96%, respectively. Both online and offline surrogate models required 95% to 97% less computational effort during the optimization process and generated Pareto frontiers that were statistically similar to the benchmark noisy GA without surrogate models at a 95% confidence level. Furthermore, the preferable patterns of GI coverages across subwatersheds, despite having different ranges of GI coverages, remained the same across the three types of fitness functions (no surrogate, online surrogate, and offline surrogate). However, the offline surrogate required pre-training of the ANN with a prior noisy GA execution, and hence the overall computational savings is not significant unless multiple GA executions are needed (e.g., for many design scenarios). Therefore, the online surrogate approach is recommended for the greatest overall computational savings without significant loss of accuracy.

In this chapter, the best-performing values for the ANN hyper-parameters (number of hidden layers, number of perceptrons, and number of iterations of backpropagation) were determined using an archive of decision variables and their corresponding fitness values from a prior noisy GA execution. We then used the same model parameters in both the online and offline surrogate models. Therefore, the successful execution of both the offline and online methods relied on the initial computationally demanding noisy GA optimization execution. Future research should optimize the hyperparameters of the online surrogate after the first few generations of the online optimization process to ensure the model is truly independent of prior executions.

For future research, other novel neural network platforms and packages, such as keras (Chollet 2015) and tensor flow (Abadi et al. 2015), could be explored to further increase the accuracy and robustness of the predictive surrogate models. Executing individual fitness evaluations in parallel would reduce overall clock time to identify the Pareto frontier, with and without the surrogate models.

Other future research could focus on multi-scale optimization of GI networks considering other objectives. Distributed hydrologic models (e.g., RHESSys, Tague and Band 2004) would more accurately capture

patch-by-patch performance of GI for water quality treatment and water quantity management and identify preferable locations of GI practices at smaller scales (individual plot to patch). Doing so, the importance of different patch-related features in the preferable subwatersheds can be investigated, thus providing guidelines on the best types of patches for GI implementation. The optimization framework developed in this work could easily be extended to evaluate such more complex scenarios, although the computational effort would be considerably higher and the surrogate models would be even more important.

Chapter 6: Conclusions and future research

This dissertation creates a decision-making framework to assist decision makers with recognition of the potential locations for small GI practices in urban/ semi-urbanized watersheds, and conducts quantitative analysis on the functionality of the GI practices with respect to spatial scale and uncertainty in their performance. This dissertation specifically focuses on rain gardens as small-scale practices that can be implemented across two case study watersheds, DR5 and SR5 in the state of Maryland. Numerical simulation models, uncertainty quantification methods, meta-heuristic optimization methods, and data-driven machine learning methods are used to determine where GI practices should be placed.

After presenting the details of the case studies, the third chapter of this dissertation highlights the capabilities of a software platform developed to allow practitioners to interactively identify and evaluate the performance of small GI practices using hydrologic models. The online Cloud-based interactive tool — called IDEAS_GI, or Interactive DEsign and ASsessment of GI — assesses GI performance using hydrologic and empirical models to estimate cost, stormwater volume reduction and treatment, and air pollutant deposition. The tool is designed to be used as an initial screening platform to identify potential locations for GI implementation across case study watersheds and to provide an overview of GI performance across spatial scales, as well as its inherent uncertainties.

IDEAS_GI provides a reasonable representation of estimated hydrographs based on selections of routing time steps, routing method, infiltration method, resolution of subwatersheds, and parameters used for each subwatershed. The hydrologic/hydraulic models that are coupled with IDEAS_GI can vary in terms of execution time, spatial and time scale, routing and infiltration approaches, and rainfall duration. Therefore, IDEAS_GI can assist hydrologists, engineers, and practitioners as a flexible modeling package with an interactive representation of landscapes that can be shared with stakeholders to support GI implementation.

The IDEAS demonstrated the sensitivity of the simulation results to GI parameters as well. The results showed that soil depth and type of rain garden installations do not lead to tangible reductions in peak flow

and cumulative flow reduction at the DR5 outlet for the design storms specified by government design manuals. Instead, increasing the coverage in all subwatersheds with potential locations for GI, i.e. a network of GI practices, will result in slightly higher performance in stormwater capture and treatment. Also, the choice of storm event frequency greatly affected the overall performance of GI networks.

Future research can further investigate the level of significance and magnitude of stormwater-related functionalities (e.g. stormwater volume reduction, peak flow reduction and nutrient removal) associated with GI designs in different watersheds with respect to different design storms, and not the only ones from the design manuals. In fact, assessing the magnitude of design storms that is most appropriate for small GI practices for different climates, given different environmental goals, could significantly improve understanding of their performance, thus reducing the uncertainty in predicting GI performance assessment for design and planning purposes.

Comparing the results of simulations between two case study watersheds, SR5 and DR5, the effects of GI practices in SR5, which is smaller and highly urbanized, is not as promising as those of DR5, even after implementation at all potential locations across the watershed. DR5 is a semi-urbanized watershed with a considerably larger suitable area to implement GI practices, which enables higher impacts. Also, looking at the performance of GI for the design storms and continuous rainfall records, the results show that the percentage decrease in nitrogen reduction is higher than that of stormwater volume and peak reductions. More investigations are needed to assess the impacts of other factors, such as relative locations within a subwatershed, connectivity to impervious contributing area, or land use type, on the performance of GI practices.

In Chapter 4, the stormwater-related performance of GI practices and other benefits/costs associated with different GI networks at different spatial scales were analyzed. IDEAS_GI was used for detection of potential locations for GI implementation and facilitation of initial off-site assessment of GI practices. Based on the results from Chapter 2, the focus of Chapter 3 shifted to GI functionality during continuous

rainfall records. The chapter demonstrated how the scale of implementation (i.e., household, sub-watershed, or watershed), affects the cost and benefits of GI, focusing on rain gardens and the uncertainties inherent in estimation of their performance. This chapter assessed the extent of GI implementation and its effects on overall cost/benefit assessments of GI.

The chapter concluded that GI coverage in subwatersheds or in front of households does not guarantee improvement in treatment efficiency. Sand filter, dry basins, or wet basins (as concentrated GI practices) are more beneficial for WQV treatment efficiency under higher coverage scenarios, while rain gardens are better for lower coverage scenarios. It was also found that contributing area is not as important as GI coverage area for each of the subwatersheds with respect to stormwater treatment efficiency, based on the assumptions used in SWMM 5.0. Also, among the uncertain modeling parameters, installation option affects the metrics greatly, suggesting that more self-installation of GI practices results in higher water treatment efficiency. Furthermore, the parameters used for WQV treatment valuation are more crucial in benefit-cost assessment of stormwater treatment efficiency in comparison to other physical simulation-related parameters.

The chapter also showed that the choice of metrics changes the selection results. Using BCR and treated WQV as the metric, smaller subwatershed areas are more suitable for rain garden implementation. However, the nutrient removal cost metric suggests that implementation of GI in upstream subwatersheds benefits downstream subwatersheds and results in higher downstream nutrient removal efficiency.

The benefits at the household scale are similar to the ones at the watershed scale. Therefore, the highest efficiencies can be observed by siting GI in some subwatersheds, and even in a portion of the subwatersheds rather than uniform GI coverage across the entire area. However, the results show that even at the household scale, rain gardens are more cost effective for stormwater treatment than comparable technologies such as sand filters.

The chapter used historical continuous rainfall data in a calibrated hydrologic model, which does not account for longer-term climate change impacts on GI investment effectiveness. Further research with climate change scenarios is needed to determine the most effective long-term GI types and locations for each scenario.

The chapter also used existing models and literature to estimate environmental benefits and economic costs of GI projects and identify uncertainties in modeling parameters. However, some of the uncertain parameters did not have clear and defined uncertainty boundaries in the literature and simple triangular distributions were used. Further research is needed to develop appropriate distributions for all parameters and assess the impacts of other types of distributions (e.g. uniform, log-normal) on overall costs and benefits.

It is important to note that some benefits/costs may be consequential but are secondary to the primary effects of GI implementation. For instance, if nutrients are extracted from stormwater, stormwater treatment plants downstream that might extract such minerals and use them for energy recovery may lose some of their energy sources. Depending on the system boundaries, there could be numerous secondary uncertain effects, e.g. ecosystem stabilization due to nutrient removal, that need additional research.

Moreover, further research is needed to quantify and monetize other benefits of GI, such as flood reduction, urban heat island mitigation, noise abatement, changes in real estate values, and micro-climate regulation. This would allow more accurate assessment of the trade-offs between different types of benefits and the preferable arrangement and location of GI for each category of benefits.

Finally, the chapter showed that some subwatersheds have higher nutrient removal efficiencies and some watersheds have lower removal efficiencies, calling for a systematic way to determine the most suitable subwatershed candidates, which is partially addressed in the Chapter 5.

The fifth chapter provides a framework for identifying preferable locations to place GI. This chapter shows locations where subwatersheds are more suitable for GI placement from the standpoints of water quantity, and life cycle cost. The chapter uses noisy meta-heuristic optimization algorithms, noisy GA, to find the preferable arrangement and location of GI practices in a semi-urbanized watershed. To optimize the network in an efficient manner and to overcome the computational burden of the optimization process, the optimization algorithms were merged with surrogate machine learning models, in this case artificial neural networks. The surrogate models are trained to replace the computationally-intensive numerical models using datasets generated during and after the optimization process, referred to as online and offline noisy GA respectively.

The optimization with noisy GA without surrogate model was extremely computationally demanding. As a result, the Pareto frontier generated from this approach was used as a baseline to compare the performance of the other two optimization methods. Noisy GA without offline surrogate model, resulted in a similar Pareto frontier in which the majority of points, after accounting for their uncertainties and their equivalent fitness values using the SWMM model, did not have statistically different fitness values. However, using noisy GA with online surrogate model the Pareto frontier of the solutions was statistically different from the baseline Pareto frontier. After classifying and ranking the preferable fitness values and their corresponding decision variables, the results showed that, the patterns of GI coverages remained the same across the three optimization scenarios. Thus, the results suggested that the optimization process has investigated the solution space thoroughly and has reached a global optimal.

Classifying the preferable GI coverages across the subwatersheds via decision trees, showed that for the budgetary scenario with the highest and lowest budget, distance to the watershed outfall is an important factor. In fact, in the lowest budgetary scenario, the results suggest that the highest investments, and potentially all of the investments, should be allocated to the subwatersheds closest to the watershed outlet. In the highest budgetary scenario, the results also suggest that the highest investments should be made

closest to the watershed outlet, but GI is also sited in other subwatersheds, with the lowest investments in the subwatersheds with the highest distance to watershed outlet.

Additional noisy GA runs can ensure that the optimal solution has been reached and the solution spaces has fully been investigated. There is also an immediate potential to apply the optimization techniques to the other case study, e.g. SR5 watershed. Doing so, the conclusions drawn from emerging preferability patterns can be justified.

Finally, this study demonstrates the need for future research that focuses on increasing the optimization resolution via distributed hydrologic modeling to capture cell-by-cell performance of GI for water quality treatment and water quantity management. For more generalizable recommendations, there is a need for optimization frameworks that identify preferable locations of GI practices at small scales using distributed hydrologic models.

References

- Abadi, Martin, Ashish Agarwal, Paul Barham, Eugene Brevdo, Zhifeng Chen, Craig Citro, Greg S. Corrado, et al. 2015. "Tensorflow: An Open Source Machine Learning Framework for Everyone." Github. <https://github.com/tensorflow/tensorflow>.
- Adelaja, Soji, Yohannes Hailu, Rachel Kuntzsch, Mary Beth Lake, Max Fulkerson, Charles McKeown, Laila Recevskis, and Nigel Griswold. 2008. "Comprehensive Study on Economic Valuation, Economic Impact Assessment, and State Conservation Funding of Green Infrastructure Assets in Michigan Shaping the Future from the Ground Up." <https://www.mml.org/pdf/information/msulandpolicyreport.pdf>.
- Alves, Alida, Arlex Sanchez, Zoran Vojinovic, Solomon Seyoum, Mukand Babel, and Damir Brdjanovic. 2016. "Evolutionary and Holistic Assessment of Green-Grey Infrastructure for CSO Reduction." *Water* 8 (9): 402. <https://doi.org/10.3390/w8090402>.
- Aly, Alaa H., and Richard C. Peralta. 1999. "Optimal Design of Aquifer Cleanup Systems under Uncertainty Using a Neural Network and a Genetic Algorithm." *Water Resources Research* 35 (8): 2523–32. <https://doi.org/10.1029/98WR02368>.
- Antipova, E., C. Pozo, G. Guillén-Gosálbez, D. Boer, L.F. Cabeza, and L. Jiménez. 2015. "On the Use of Filters to Facilitate the Post-Optimal Analysis of the Pareto Solutions in Multi-Objective Optimization." *Computers & Chemical Engineering* 74 (March): 48–58. <https://doi.org/10.1016/J.COMPCHEMENG.2014.12.012>.
- Bandaru, Sunith, Amos H.C. Ng, and Kalyanmoy Deb. 2017. "Data Mining Methods for Knowledge Discovery in Multi-Objective Optimization: Part A - Survey." *Expert Systems with Applications* 70 (March): 139–59. <https://doi.org/10.1016/J.ESWA.2016.10.015>.
- Barbosa, A.E., J.N. Fernandes, and L.M. David. 2012. "Key Issues for Sustainable Urban Stormwater Management." *WATER RES* 46 (20): 6787–98. <https://doi.org/10.1016/J.WATRES.2012.05.029>.
- Baú, Domenico A., and Alex S. Mayer. 2006. "Stochastic Management of Pump-and-Treat Strategies Using Surrogate Functions." *Advances in Water Resources* 29 (12): 1901–17. <https://doi.org/10.1016/J.ADVWATRES.2006.01.008>.
- Behzadian, Kouros, Zoran Kapelan, Dragan Savic, and Abdollah Ardeshir. 2009. "Stochastic Sampling Design Using a Multi-Objective Genetic Algorithm and Adaptive Neural Networks." *Environmental Modelling & Software* 24 (4): 530–41. <https://doi.org/10.1016/J.ENVSOFT.2008.09.013>.
- Berg, Agnes E van den, Sander L Koole, and Nickie Y van der Wulp. 2003. "Environmental Preference and Restoration: (How) Are They Related?" *Journal of Environmental Psychology* 23 (2): 135–46. [https://doi.org/10.1016/S0272-4944\(02\)00111-1](https://doi.org/10.1016/S0272-4944(02)00111-1).
- Berndtsson, Justyna Czemieli. 2010a. "Green Roof Performance towards Management of Runoff Water Quantity and Quality: A Review." *ECOL ENG* 36 (4): 351–60. <https://doi.org/10.1016/j.ecoleng.2009.12.014>.
- . 2010b. "Green Roof Performance towards Management of Runoff Water Quantity and Quality:

- A Review.” *ECOL ENG* 36: 351–60. <https://doi.org/10.1016/j.ecoleng.2009.12.014>.
- Bicknell, Brian R, John C Imhoff, John L Kittle Jr., Anthony S Donigian Jr., Robert C Johanson, and Thomas O Barnwell. 1996. “HYDROLOGICAL SIMULATION PROGRAM - FORTRAN USER’S MANUAL FOR RELEASE 11.” Athens, Georgia. http://sdi.odu.edu/mbin/hspf/dos/hspf_v11_entirety.pdf.
- Brezonik, Patrick L, and Teresa H Stadelmann. 2002. “Analysis and Predictive Models of Stormwater Runoff Volumes, Loads, and Pollutant Concentrations from Watersheds in the Twin Cities Metropolitan Area, Minnesota, USA.” *WATER RES* 36 (7): 1743–57. [https://doi.org/10.1016/S0043-1354\(01\)00375-X](https://doi.org/10.1016/S0043-1354(01)00375-X).
- Broad, Darren Ross. 2014. “Water Distribution System Optimization Using Metamodels.” Stochastic sampling design using a multi-objective genetic algorithm and adaptive neural networks. <https://digital.library.adelaide.edu.au/dspace/bitstream/2440/98139/2/02whole.pdf>.
- Brown, Rebekah R. 2005. “Impediments to Integrated Urban Stormwater Management: The Need for Institutional Reform.” *Environmental Management* 36 (3): 455–68. <https://doi.org/10.1007/s00267-004-0217-4>.
- California Department of Transportation. 2014. “Pervious Pavement Design Guidance.” Sacramento, California. <http://www.dot.ca.gov/hq/oppd/stormwtr/>.
- Cameron, Ross W.F., Tijana Blanuša, Jane E. Taylor, Andrew Salisbury, Andrew J. Halstead, Béatrice Henricot, and Ken Thompson. 2012. “The Domestic Garden – Its Contribution to Urban Green Infrastructure.” *URBAN FOR URBAN GREE* 11 (2): 129–37. <https://doi.org/10.1016/J.UFUG.2012.01.002>.
- Casal-Campos, Arturo, Guangtao Fu, David Butler, and Andrew Moore. 2015. “An Integrated Environmental Assessment of Green and Gray Infrastructure Strategies for Robust Decision Making.” *ENVIRON SCI TECHNOL* 49 (14): 8307–14. <https://doi.org/10.1021/es506144f>.
- Center for Neighborhood Technology. 2006. “Green Values National Stormwater Management Calculator.” 2006. <http://greenvalues.cnt.org/national/calculator.php>.
- Chadalavada, Sreenivasulu, Bithin Datta, Ravi Naidu, S Chadalavada, · R Naidu, and B Datta. 2011. “Uncertainty Based Optimal Monitoring Network Design for a Chlorinated Hydrocarbon Contaminated Site The Uncertainty in Estimating The.” *Environ Monit Assess* 173: 929–40. <https://doi.org/10.1007/s10661-010-1435-2>.
- Charnes, A., and W. W. Cooper. 1959. “Chance-Constrained Programming.” *Management Science* 6 (1). <https://doi.org/https://doi.org/10.1287/mnsc.6.1.73>.
- Chiew, F H S, and L Siriwardena. 2005. “Estimation Of SIMHYD Parameter Values For Application In Ungauged Catchments.” In . www.toolkit.net.au/rrl.
- Chini, Christopher, James Canning, Kelsey Schreiber, Joshua Peschel, Ashlynn Stillwell, Christopher M. Chini, James F. Canning, Kelsey L. Schreiber, Joshua M. Peschel, and Ashlynn S. Stillwell. 2017. “The Green Experiment: Cities, Green Stormwater Infrastructure, and Sustainability.” *Sustainability* 9 (1): 105. <https://doi.org/10.3390/su9010105>.
- Chollet, François. 2015. “Keras.” Github. <https://github.com/keras-team/keras>.

- Chow, Ven Te. 1959. *Open Channel Hydraulics*. McGraw-Hill Book Company, Inc; New York.
- Ciou, Shih-Kai, Jan-Tai Kuo, Pin-Hui Hsieh, and Gwo-Hsing Yu. 2012. "Optimization Model for BMP Placement in a Reservoir Watershed." *Journal of Irrigation and Drainage Engineering* 138 (8): 736–47. [https://doi.org/10.1061/\(ASCE\)IR.1943-4774.0000458](https://doi.org/10.1061/(ASCE)IR.1943-4774.0000458).
- Clark, Corrie, Peter Adriaens, and F Brian Talbot. 2008. "Green Roof Valuation: A Probabilistic Economic Analysis of Environmental Benefits." *ENVIRON SCI TECHNOL* 42 (6): 2155–61. <https://doi.org/10.1021/es0706652>.
- CNT. 2010. "The Value of Green Infrastructure A Guide to Recognizing Its Economic, Environmental and Social Benefits." Chicago, IL. http://www.cnt.org/sites/default/files/publications/CNT_Value-of-Green-Infrastructure.pdf.
- Coppersmith, Don, Se June Hong, and Jonathan R.M. Hosking. 1999. "Partitioning Nominal Attributes in Decision Trees." *Data Mining and Knowledge Discovery* 3 (2): 197–217. <https://doi.org/10.1023/A:1009869804967>.
- CUAHSI. 2019. "HydroShare." 2019. <https://www.hydroshare.org/>.
- Damodaram, Chandana, and Emily M. Zechman. 2013. "Simulation-Optimization Approach to Design Low Impact Development for Managing Peak Flow Alterations in Urbanizing Watersheds." *Journal of Water Resources Planning and Management* 139 (3): 290–98. [https://doi.org/10.1061/\(ASCE\)WR.1943-5452.0000251](https://doi.org/10.1061/(ASCE)WR.1943-5452.0000251).
- Davis, Allen. 2008. "Field Performance of Bioretention: Hydrology Impacts." *J. Hydrol. Eng.* 132: 90–95. <https://doi.org/10.1061/ASCE1084-0699200813:290>.
- Deb, Kalyanmoy, Samir Agrawal, Amrit Pratap, and T Meyarivan. 2000. "A Fast Elitist Non-Dominated Sorting Genetic Algorithm for Multi-Objective Optimization: NSGA-II." In *Parallel Problem Solving from Nature PPSN VI.*, 849–58. Springer, Berlin, Heidelberg. https://doi.org/10.1007/3-540-45356-3_83.
- Deb, Kalyanmoy, and Ram Bhushan Agrawal. 1995. "Simulated Binary Crossover for Continuous Search Space." *Complex Systems* 9 (2): 115–48. <https://pdfs.semanticscholar.org/b8ee/6b68520ae0291075cb1408046a7dff9dd9ad.pdf>.
- Denman, L, P B May, and P F Breen. 2006. "An Investigation of the Potential to Use Street Trees and Their Root Zone Soils to Remove Nitrogen from Urban Stormwater." *Australasian Journal of Water Resources* 10 (3): 303–11. <https://doi.org/10.1080/13241583.2006.11465306>.
- Department of Environmental Protection. 2017. "RainScapes: Environmentally-Friendly Landscapes for Healthy Watersheds." <http://www.missutility.net/>.
- Domenico, P.A, and F.W. Schwartz. 1990. *Physical and Chemical Hydrogeology*. New York: John Wiley & Sons.
- Drake, Jennifer, Andrea Bradford, and Tim Van Seters. 2014. "Stormwater Quality of Springesummer-Fall Effluent from Three Partial-Infiltration Permeable Pavement Systems and Conventional Asphalt Pavement." *J ENVIRON MANAGE* 139: 69–79. <https://doi.org/10.1016/j.jenvman.2013.11.056>.
- Duncan, Jonathan M., Lawrence E. Band, and Peter M. Groffman. 2017. "Variable Nitrate Concentration-Discharge Relationships in a Forested Watershed." *HYDROL PROCESS* 31 (9): 1817–24.

<https://doi.org/10.1002/hyp.11136>.

- Duncan, Jonathan M., Claire Welty, John T. Kemper, Peter M. Groffman, and Lawrence E. Band. 2017. "Dynamics of Nitrate Concentration-Discharge Patterns in an Urban Watershed." *WATER RESOUR RES* 53 (8): 7349–65. <https://doi.org/10.1002/2017WR020500>.
- Elliott, A. H., and S. A. Trowsdale. 2007. "A Review of Models for Low Impact Urban Stormwater Drainage." *ENVIRON MODELL SOFTW* 22 (3): 394–405. <https://doi.org/10.1016/j.envsoft.2005.12.005>.
- Environmental Protection Agency, US. 2014. "The Economic Benefits of Green Infrastructure A Case Study of Lancaster, PA About the Green Infrastructure Technical Assistance Program." 2014. https://www.epa.gov/sites/production/files/2015-10/documents/cnt-lancaster-report-508_1.pdf.
- Farber, Stephen, Robert Costanza, Mathew Wilson, Jon Erickson, Dan Childers, S Farber, R Costanza, et al. 2006. "Linking Ecology and Economics for Ecosystem Management Recommended Citation." *BIOSCIENCE* 56 (2): 117–29. http://digitalcommons.fiu.edu/fce_lter_journal_articles.
- Feiring, B.R., T. Sastri, and L.S.M. Sim. 1998. "A Stochastic Programming Model for Water Resource Planning." *Mathematical and Computer Modelling* 27 (3): 1–7. [https://doi.org/10.1016/S0895-7177\(97\)00263-X](https://doi.org/10.1016/S0895-7177(97)00263-X).
- Felson, Alexander J., and Steward TA Pickett. 2005. "Designed Experiments: New Approaches to Studying Urban Ecosystems." *Frontiers in Ecology and the Environment* 3 (10): 549–56. [https://doi.org/10.1890/1540-9295\(2005\)003\[0549:DENATS\]2.0.CO;2](https://doi.org/10.1890/1540-9295(2005)003[0549:DENATS]2.0.CO;2).
- Fitzpatrick, J. Michael, and John J. Grefenstette. 1988. "Genetic Algorithms in Noisy Environments." *Machine Learning* 3 (2–3): 101–20. <https://doi.org/10.1007/BF00113893>.
- Fortin, Félix-Antoine, Ulavalca Marc-André Gardner, Marc Parizeau, and Christian Gagné. 2012. "DEAP: Evolutionary Algorithms Made Easy François-Michel De Rainville." *Journal of Machine Learning Research* 13: 2171–75.
- Gailey, Robert M., and Steven M. Gorelick. 1993. "Design of Optimal, Reliable Plume Capture Schemes: Application to the Gloucester Landfill Ground-Water Contamination Problem." *Groundwater* 31 (1): 107–14.
- Giacomini, M. H., and John Joseph. 2017. "Multi-Objective Evolutionary Optimization and Monte Carlo Simulation for Placement of Low Impact Development in the Catchment Scale." *Journal of Water Resources Planning and Management* 143 (9): 04017053. [https://doi.org/10.1061/\(ASCE\)WR.1943-5452.0000812](https://doi.org/10.1061/(ASCE)WR.1943-5452.0000812).
- Gibbs, M.S., H.R. Maier, G.C. Dandy, and J.B. Nixon. 2006. "Minimum Number of Generations Required for Convergence of Genetic Algorithms." *2006 IEEE International Conference on Evolutionary Computation*, 565–72. <https://doi.org/10.1109/cec.2006.1688360>.
- Gill, S.E, J.F Handley, A.R Ennos, and S Pauleit. 2007. "Adapting Cities for Climate Change: The Role of the Green Infrastructure." *Built Environment* 33 (1): 115–33. <https://doi.org/10.2148/benv.33.1.115>.
- Gopalakrishnan, Gayathri, Barbara Minsker, and David E. Goldberg. 2001. "Optimal Sampling in a Noisy Genetic Algorithm for Risk-Based Remediation Design." *J. Hydroinf.* 5 (1): 11–25.

[https://doi.org/10.1061/40569\(2001\)94](https://doi.org/10.1061/40569(2001)94).

- Gopalakrishnan, Gayathri, Barbara S. Minsker, and David E. Goldberg. 2003. "Optimal Sampling in a Noisy Genetic Algorithm for Risk-Based Remediation Design." *Journal of Hydroinformatics* 5 (1): 11–25. <https://doi.org/10.2166/hydro.2003.0002>.
- Hartig, Terry, Richard Mitchell, Sjerp de Vries, and Howard Frumkin. 2014. "Nature and Health." *ANNU REV PUBL HEALTH* 35 (1): 207–28. <https://doi.org/10.1146/annurev-publhealth-032013-182443>.
- Hartig, Terry, Richard Mitchell, Sjerp De Vries, and Howard Frumkin. 2014. "Nature and Health." *ANNU REV PUBL HEALTH* 35 (1): 207–28. <https://doi.org/10.1146/annurev-publhealth-032013-182443>.
- Heidari, Bardia, Lorne Leonard, Band. Lawrence E, and Barbara S. Minsker. 2017. "IDEAS for GI_Deadrun | HydroShare." HydroShare. <https://www.hydroshare.org/resource/75dfc27015f1467388d712b562657835/>.
- Heidari, Bardia, Ankit Rai, and Barbara Minsker. 2016. "Optimization of Green Infrastructure Network at Semi-Urbanized Watersheds to Manage Stormwater Volume, Peak Flow and Life Cycle Cost: Case Study of Dead Run Watershed." In *Abstract (H51A-1425) Presented at 2016 AGU Fall Meeting*. San Francisco, CA, 12-16 Dec. <https://agu.confex.com/agu/fm16/meetingapp.cgi/Paper/126807>.
- Heidari, Bardia, Arthur A Schmidt, and Barbara S Minsker. n.d. "Spatial Scale Effects on Uncertainty and Sensitivity in Green Infrastructure Cost/Benefit Assessment." *J ENVIRON MANAGE*.
- Hirabayashi, Satoshi, Charles N Kroll, and David J Nowak. 2012. "Development of a Distributed Air Pollutant Dry Deposition Modeling Framework." *ENVIRON POLLUT* 171: 9–17. <https://doi.org/10.1016/j.envpol.2012.07.002>.
- Holtan, Meghan T., Susan L. Dieterlen, and William C. Sullivan. 2015. "Social Life Under Cover." *ENVIRON BEHAV* 47 (5): 502–25. <https://doi.org/10.1177/0013916513518064>.
- Horsburgh, Jeffery S., Mohamed M. Morsy, Anthony M. Castronova, Jonathan L. Goodall, Tian Gan, Hong Yi, Michael J. Stealey, and David G. Tarboton. 2016. "HydroShare: Sharing Diverse Environmental Data Types and Models as Social Objects with Application to the Hydrology Domain." *J AM WATER RESOUR AS* 52 (4): 873–89. <https://doi.org/10.1111/1752-1688.12363>.
- Houck, Mark H. 1979. "A Chance Constrained Optimization Model for Reservoir Design and Operation." *Water Resources Research* 15 (5): 1011–16. <https://doi.org/10.1029/WR015i005p01011>.
- Janhäll, Sara. 2015. "Review on Urban Vegetation and Particle Air Pollution - Deposition and Dispersion." *ATMOS ENVIRON* 105: 130–37. <https://doi.org/10.1016/j.atmosenv.2015.01.052>.
- Jayasooriya, V. M., and A. W.M. Ng. 2014. "Tools for Modeling of Stormwater Management and Economics of Green Infrastructure Practices: A Review." *WATER AIR SOIL POLL* 225 (8). <https://doi.org/10.1007/s11270-014-2055-1>.
- Jiang, Bin, Chun-Yen Chang, and William C. Sullivan. 2014. "A Dose of Nature: Tree Cover, Stress Reduction, and Gender Differences." *LANDSCAPE URBAN PLAN* 132 (December): 26–36. <https://doi.org/10.1016/J.LANDURBPLAN.2014.08.005>.
- Jiang, Bin, Linda Larsen, Brian Deal, and William C. Sullivan. 2015. "A Dose–Response Curve Describing the Relationship between Tree Cover Density and Landscape Preference." *Landscape and Urban Planning* 139 (July): 16–25. <https://doi.org/10.1016/J.LANDURBPLAN.2015.02.018>.

- Kabir, Md Imran, Edoardo Daly, and Federico Maggi. 2014. "A Review of Ion and Metal Pollutants in Urban Green Water Infrastructures." *SCI TOTAL ENVIRON* 470–471: 695–706. <https://doi.org/10.1016/j.scitotenv.2013.10.010>.
- Kaini, Prakash, Kim Artita, and John W Nicklow. 2012. "Optimizing Structural Best Management Practices Using SWAT and Genetic Algorithm to Improve Water Quality Goals." *Water Resour Manage* 26: 1827–45. <https://doi.org/10.1007/s11269-012-9989-0>.
- Karamouz, Mohammad, Masoud Taheriyoun, Akbar Baghvand, Hamed Tavakolifar, and Farzad Emami. 2010. "Optimization of Watershed Control Strategies for Reservoir Eutrophication Management." *Journal of Irrigation and Drainage Engineering* 136 (12): 847–61. [https://doi.org/10.1061/\(ASCE\)IR.1943-4774.0000261](https://doi.org/10.1061/(ASCE)IR.1943-4774.0000261).
- Khan, Usman, Caterina Valeo, Angus Chu, and Jianxun He. 2013. "A Data Driven Approach to Bioretention Cell Performance: Prediction and Design." *Water* 5 (1): 13–28. <https://doi.org/10.3390/w5010013>.
- Khu, Soon Thiam, and Micha G F Werner. 2003. "Reduction of Monte-Carlo Simulation Runs for Uncertainty Estimation in Hydrological Modelling." *Hydrology and Earth System Sciences* 7 (5): 680–92. <https://pdfs.semanticscholar.org/eac1/d60a21caa61a9093785a1c3b96d6007bf3a8.pdf>.
- Koch, Benjamin J., Catherine M. Febria, Muriel Gevrey, Lisa A. Wainger, and Margaret A. Palmer. 2014. "Nitrogen Removal by Stormwater Management Structures: A Data Synthesis." *JAWRA Journal of the American Water Resources Association* 50 (6): 1594–1607. <https://doi.org/10.1111/jawr.12223>.
- Kourakos, George, and Aristotelis Mantoglou. 2009. "Pumping Optimization of Coastal Aquifers Based on Evolutionary Algorithms and Surrogate Modular Neural Network Models." *Advances in Water Resources* 32 (4): 507–21. <https://doi.org/10.1016/J.ADVWATRES.2009.01.001>.
- Kousky, Carolyn, Sheila M. Olmstead, Margaret A. Walls, and Molly Macauley. 2013. "Strategically Placing Green Infrastructure: Cost-Effective Land Conservation in the Floodplain." *ENVIRON SCI TECHNOL* 47 (8): 3563–70. <https://doi.org/10.1021/es303938c>.
- Kuller, M., P. M. Bach, D. Ramirez-Lovering, and A. Deletic. 2016. "The Location Choice of Water Sensitive Urban Design within a City: A Case Study of Melbourne." In *IWA World Water Congress and Exhibition*.
- Lee, Joong Gwang, Ariamalar Selvakumar, Khalid Alvi, John Riverson, Jenny X. Zhen, Leslie Shoemaker, and Fu hsiung Lai. 2012. "A Watershed-Scale Design Optimization Model for Stormwater Best Management Practices." *ENVIRON MODELL SOFTW* 37: 6–18. <https://doi.org/10.1016/j.envsoft.2012.04.011>.
- Leonard, Lorne, and Band. Lawrence E. 2017. "RHESSys-Jupyter-Notebooks." GitHub. <https://github.com/leonard-psu/RHESSys-Jupyter-notebooks>.
- Leonard, Lorne, Band. Lawrence E, and Laurence Lin. 2017. "Green Infrastructure Designer with RHESSys Workflow." HydroShare. <http://www.hydroshare.org/resource/3f7680cf83dc426e858d5b48cb95a565>.
- Leonard, Lorne, Brian Miles, Bardia Heidari, Laurence Lin, Anthony M. Castronova, Barbara Minsker, Jong Lee, Charles Scaife, and Lawrence E. Band. 2019. "Development of a Participatory Green Infrastructure Design, Visualization and Evaluation System in a Cloud Supported Jupyter Notebook

- Computing Environment.” *ENVIRON MODELL SOFTW* 111 (January): 121–33.
<https://doi.org/10.1016/J.ENVSOFT.2018.10.003>.
- Leonard, Lorne N, Brian Miles, Bardia Heidari, Laurence Lin, Anthony Castronova, Barbara Minsker, and Lawrence E Band. 2019. “Development of a Participatory Green Infrastructure Design, Visualization and Evaluation System in a Cloud Supported Jupyter Notebook Computing Environment.” *ENVIRON MODELL SOFTW*, no. 111: 121–33.
<https://doi.org/https://doi.org/10.1016/j.envsoft.2018.10.003>.
- Li, Dongying, and William C Sullivan. 2016. “Impact of Views to School Landscapes on Recovery from Stress and Mental Fatigue.” *LANDSCAPE URBAN PLAN* 148: 149–58.
<https://doi.org/10.1016/j.landurbplan.2015.12.015>.
- Li, Hui, Masoud Kayhanian, and John T. Harvey. 2013. “Comparative Field Permeability Measurement of Permeable Pavements Using ASTM C1701 and NCAT Permeameter Methods.” *J ENVIRON MANAGE* 118 (March): 144–52. <https://doi.org/10.1016/J.JENVMAN.2013.01.016>.
- Liagkouras, K., and K. Metaxiotis. 2013. “An Elitist Polynomial Mutation Operator for Improved Performance of MOEAs in Computer Networks.” In *22nd International Conference on Computer Communication and Networks (ICCCN)*, 1–5. IEEE. <https://doi.org/10.1109/ICCCN.2013.6614105>.
- Linker, Lewis C., Richard A. Batiuk, Gary W. Shenk, and Carl F. Cerco. 2013. “Development of the Chesapeake Bay Watershed Total Maximum Daily Load Allocation.” *J AM WATER RESOUR AS* 49 (5): 986–1006. <https://doi.org/10.1111/jawr.12105>.
- Liu, Wen, Weiping Chen, Qi Feng, Chi Peng, and • Peng Kang. 2016. “Cost-Benefit Analysis of Green Infrastructures on Community Stormwater Reduction and Utilization: A Case of Beijing, China.” *ENVIRON MANAGE* 58: 1015–26. <https://doi.org/10.1007/s00267-016-0765-4>.
- Liu, Yaoze, Lawrence O. Theller, Bryan C. Pijanowski, and Bernard A. Engel. 2016. “Optimal Selection and Placement of Green Infrastructure to Reduce Impacts of Land Use Change and Climate Change on Hydrology and Water Quality: An Application to the Trail Creek Watershed, Indiana.” *Science of The Total Environment* 553 (May): 149–63. <https://doi.org/10.1016/J.SCITOTENV.2016.02.116>.
- Liu, Yong, A E Huaicheng, Guo Ae, Zhenxing Zhang, A E Lijing, Wang Ae, Yongli Dai, and Yingying Fan. 2007. “An Optimization Method Based on Scenario Analysis for Watershed Management Under Uncertainty.” *Environ Manage* 39: 978–690. <https://doi.org/10.1007/s00267-006-0029-9>.
- Lu, Hongwei, Peng Du, Yizhong Chen, and Li He. 2016. “A Credibility-Based Chance-Constrained Optimization Model for Integrated Agricultural and Water Resources Management: A Case Study in South Central China.” *Journal of Hydrology* 537 (June): 408–18.
<https://doi.org/10.1016/j.jhydrol.2016.03.056>.
- Lucas, William C., and David J. Sample. 2015. “Reducing Combined Sewer Overflows by Using Outlet Controls for Green Stormwater Infrastructure: Case Study in Richmond, Virginia.” *Journal of Hydrology* 520 (January): 473–88. <https://doi.org/10.1016/J.JHYDROL.2014.10.029>.
- Maier, Holger R., Ashu Jain, Graeme C. Dandy, and K.P. Sudheer. 2010. “Methods Used for the Development of Neural Networks for the Prediction of Water Resource Variables in River Systems: Current Status and Future Directions.” *Environmental Modelling & Software* 25 (8): 891–909.
<https://doi.org/10.1016/J.ENVSOFT.2010.02.003>.

- Maier, Holger R, and Graeme C Dandy. 2000. "Neural Networks for the Prediction and Forecasting of Water Resources Variables: A Review of Modelling Issues and Applications." *Environmental Modelling & Software* 15: 101–24. www.elsevier.com/locate/envsoft.
- Maringanti, Chetan, Indrajeet Chaubey, and Jennie Popp. 2009. "Development of a Multiobjective Optimization Tool for the Selection and Placement of Best Management Practices for Nonpoint Source Pollution Control." *Water Resources Research* 45 (6).
<https://doi.org/10.1029/2008WR007094>.
- Mariño, Miguel A., and Slobodan P. Simonovic. 1981. "Single Multipurpose Reservoir Design: A Modified Optimal Control Problem by Chance-Constrained Programming." *Advances in Water Resources* 4 (1): 43–48. [https://doi.org/10.1016/0309-1708\(81\)90007-5](https://doi.org/10.1016/0309-1708(81)90007-5).
- Marsaglia, George, Wai Wan Tsang, and Jingbo Wang. 2003. "Evaluating Kolmogorov's Distribution." *Journal of Statistical Software* 8 (18): 1–4. <https://doi.org/10.18637/jss.v008.i18>.
- Maryland Department of Environment. 2009. "Maryland Stormwater Design Manual, Volume I and II." 2009.
http://mde.maryland.gov/programs/water/StormwaterManagementProgram/Pages/stormwater_design.aspx.
- Maryland Department of Permitting Services. 2012. "RAIN GARDEN (RG)." Rockville, MD.
<http://www.montgomerycountymd.gov/permitting/services/>.
- Matlock, Marty D., and Robert A. Morgan. 2010. *Ecological Engineering Design : Restoring and Conserving Ecosystem Services*. Wiley.
- Mayer, Audrey L., William D. Shuster, Jake J. Beaulieu, Matthew E. Hopton, Lee K. Rhea, Allison H. Roy, and Hale W. Thurston. 2012. "Environmental Reviews and Case Studies: Building Green Infrastructure via Citizen Participation: A Six-Year Study in the Shepherd Creek (Ohio)." *Environmental Practice* 14 (1): 57–67. <https://doi.org/10.1017/S1466046611000494>.
- Mays, Larry W. 2011. *Water Resources Engineering*. John Wiley.
- McConnell, Virginia, and Margaret Walls. 2005. "THE VALUE OF OPEN SPACE: EVIDENCE FROM STUDIES OF NONMARKET BENEFITS." Washington, DC.
http://www.ce.cmu.edu/~gdrgr/readings/2006/04/04/McConnell_RFF_TheValueOfOpenSpace.pdf.
- Mcperson, E Gregory, David J Nowak, and Rowan A Rowntree. 1994. "Chicago's Urban Forest Ecosystem: Results of the Chicago Urban Forest Climate Project." Radnor, PA.
- Mell, Ian C. 2008. "Green Infrastructure : Concepts and Planning." *FORUM Ejournal* 8 (June): 69–80.
<https://doi.org/10.1177/0956247806063947>.
- Merz, B, and E. J. Plate. 1997. "An Analysis of the Effects of Spatial Variability of Soil and Soil Moisture on Runoff." *WATER RESOUR RES* 33 (12): 2909–22.
<https://doi.org/10.1029/97WR02204>.
- Migon, Christophe, and Valérie Sandroni. 1999. "Phosphorus in Rainwater: Partitioning Inputs and Impact on the Surface Coastal Ocean." *LIMNOL OCEANOGR* 44 (4): 1160–65.
<https://doi.org/10.4319/lo.1999.44.4.1160>.
- Miles, Brian, and Lawrence E. Band. 2015a. "Green Infrastructure Stormwater Management at the

- Watershed Scale: Urban Variable Source Area and Watershed Capacitance.” *HYDROL PROCESS* 29 (9): 2268–74. <https://doi.org/10.1002/hyp.10448>.
- . 2015b. “Green Infrastructure Stormwater Management at the Watershed Scale: Urban Variable Source Area and Watershed Capacitance.” *Hydrological Processes* 29 (9): 2268–74. <https://doi.org/10.1002/hyp.10448>.
- Miles, Brian Christopher. 2014. “SMALL-SCALE RESIDENTIAL STORMWATER MANAGEMENT IN URBANIZED WATERSHEDS: A GEOINFORMATICS-DRIVEN ECOHYDROLOGY MODELING APPROACH.” University of North Carolina at Chapel Hill . <https://cdr.lib.unc.edu/indexablecontent/uuid:84f67003-6421-4b27-9a3a-39f367a1bc8c>.
- Minnesota Pollution Control Agency. 2017. “Design Criteria for Permeable Pavement - Minnesota Stormwater Manual.” 2017. https://stormwater.pca.state.mn.us/index.php?title=Design_criteria_for_permeable_pavement.
- Minsker, Barbara S. 2005. “Genetic Algorithms.” In *Hydroinformatics: Data Integrative Approaches in Computation, Analysis, and Modeling*, edited by Praveen Kumar, 66–73. CRC Press.
- Minsker, Barbara S, Band. Lawrence E, Bardia Heidari, Neely L Law, Lorne N Leonard, and Ankit Rai. 2017. “Crowd Sourcing to Improve Urban Stormwater Management.” In *Abstract (PA31C-07) Presented at 2017 AGU Fall Meeting*,. New Orleans, LA, 11-15 Dec. <https://agu.confex.com/agu/fm17/meetingapp.cgi/Paper/227343>.
- Mortgage Calculator. n.d. “Current Mortgage Rates: Average US Daily Interest Rate Trends for FHA Home Loans, Prime & Other Mortgages.” Accessed April 15, 2017. <https://www.mortgagecalculator.org/mortgage-rates/current.php>.
- “National Atmospheric Deposition Program.” n.d. Accessed May 15, 2017. <http://nadp.sws.uiuc.edu/data/ntn/plots/ntntrends.html?siteID=MD09>.
- Neilson, I. B., and D. Turney. 2010. “Green Infrastructure Optimization Analyses for Combined Sewer Overflow (CSO) Control.” In *Low Impact Development 2010*, 1533–41. Reston, VA: American Society of Civil Engineers. [https://doi.org/10.1061/41099\(367\)132](https://doi.org/10.1061/41099(367)132).
- Nicklow, John, Patrick Reed, Dragan Savic, Tibebe Dessalegne, Laura Harrell, Amy Chan-Hilton, Mohammad Karamouz, et al. 2010. “State of the Art for Genetic Algorithms and Beyond in Water Resources Planning and Management.” *Journal of Water Resources Planning and Management* 136 (4): 412–32. [https://doi.org/10.1061/\(ASCE\)WR.1943-5452.0000053](https://doi.org/10.1061/(ASCE)WR.1943-5452.0000053).
- Niu, Hao, Corrie Clark, Jiti Zhou, and Peter Adriaens. 2010. “Scaling of Economic Benefits from Green Roof Implementation in Washington, DC.” *ENVIRON SCI TECHNOL* 44: 4302–8. <https://doi.org/10.1021/es902456x>.
- Northeast Region Certified Crop Adviser. 2010. “Northeast Region Certified Crop Adviser (NRCCA) Study Resources: Competency Area 2: Soil Hydrology AEM.” Cornell University . 2010. <https://nrcca.cals.cornell.edu/soil/CA2/CA0212.1-3.php>.
- Norton, Briony A., Andrew M. Coutts, Stephen J. Livesley, Richard J. Harris, Annie M. Hunter, and Nicholas S.G. Williams. 2015. “Planning for Cooler Cities: A Framework to Prioritise Green Infrastructure to Mitigate High Temperatures in Urban Landscapes.” *Landscape and Urban Planning* 134 (February): 127–38. <https://doi.org/10.1016/J.LANDURBPLAN.2014.10.018>.

- Nowak, David J. 2000. "The Effects of Urban Trees on Air Quality." *USDA Forest Service*, 1–4. http://www.ncufc.org/uploads/nowak_trees.pdf.
- Nowak, David J., Daniel E. Crane, and Jack C. Stevens. 2006. "Air Pollution Removal by Urban Trees and Shrubs in the United States." *URBAN FOR URBAN GREE* 4 (3–4): 115–23. <https://doi.org/10.1016/j.ufug.2006.01.007>.
- Nylen, Nell Green, and Michael Kiparsky. 2015. "Accelerating Cost-Effective Green Stormwater Infrastructure: Learning from Local Implementation." Berkeley, CA. <http://scholarship.law.berkeley.edu/cleepubs>.
- Otoni Filho, Theophilo Benedicto, Marta Vasconcelos Otoni, Muriel Batista de Oliveira, José Ronaldo de Macedo, and Klaus Reichardt. 2014. "Revisiting Field Capacity (FC): Variation of Definition of FC and Its Estimation from Pedotransfer Functions." *Revista Brasileira de Ciência Do Solo* 38 (6): 1750–64. <https://doi.org/10.1590/S0100-06832014000600010>.
- Pathirana, Assela. 2018. "SWMM5 5.1.0.102 : Python Package Index." <https://pypi.python.org/pypi/SWMM5/>.
- Pearson, Karl. 1895. "Notes on Regression and Inheritance in the Case of Two Parents." In *Proceedings of the Royal Society of London*, 240–42. <https://books.google.com/books?id=60aL0zIT-90C&pg=PA240#v=onepage&q&f=false>.
- Perales-Momparler, Sara, Ignacio Andrés-Doménech, Carmen Hernández-Crespo, Francisco Vallés-Morán, Miguel Martín, Ignacio Escuder-Bueno, and Joaquín Andreu. 2017. "The Role of Monitoring Sustainable Drainage Systems for Promoting Transition towards Regenerative Urban Built Environments: A Case Study in the Valencian Region, Spain." *Journal of Cleaner Production* 163 (October): S113–24. <https://doi.org/10.1016/J.JCLEPRO.2016.05.153>.
- Pickett, S. T. A., and M. L. Cadenasso. 2006. "Advancing Urban Ecological Studies: Frameworks, Concepts, and Results from the Baltimore Ecosystem Study." *AUSTRAL ECOL* 31 (2): 114–25. <https://doi.org/10.1111/j.1442-9993.2006.01586.x>.
- Rawls, W.J., D. L. Brakensiek, and K.E. Saxton. 1982. "Estimation of Soil Properties." *TRANSACTIONS of the ASCE* 25 (5): 1316–20.
- Razavi, Saman, Bryan A. Tolson, and Donald H. Burn. 2012. "Review of Surrogate Modeling in Water Resources." *WATER RESOUR RES* 48 (7). <https://doi.org/10.1029/2011WR011527>.
- Read, Jennifer, Tricia Wevill, Tim Fletcher, and Ana Deletic. 2008. "Variation among Plant Species in Pollutant Removal from Stormwater in Biofiltration Systems." *WATER RES* 42 (4–5): 893–902. <https://doi.org/10.1016/J.WATRES.2007.08.036>.
- Reed, P.M., D. Hadka, J.D. Herman, J.R. Kasprzyk, and J.B. Kollat. 2013. "Evolutionary Multiobjective Optimization in Water Resources: The Past, Present, and Future." *Advances in Water Resources* 51 (January): 438–56. <https://doi.org/10.1016/J.ADVWATRES.2012.01.005>.
- Reed, Patrick M., and Barbara S. Minsker. 2004. "Striking the Balance: Long-Term Groundwater Monitoring Design for Conflicting Objectives." *Journal of Water Resources Planning and Management* 130 (2): 140–49. [https://doi.org/10.1061/\(ASCE\)0733-9496\(2004\)130:2\(140\)](https://doi.org/10.1061/(ASCE)0733-9496(2004)130:2(140)).
- Remodelingexpenses. 2017. "Cost of Permeable Paver - Calculate 2017 Prices Now." 2017.

<http://www.remodelingexpense.com/costs/cost-of-permeable-paver/>.

- Rivera, Samuel J. 2018. "Guiding Green Stormwater Infrastructure Planning through Socio-Ecological Vulnerability: An Integrated and Spatially Scalable Prioritization Framework." University of Illinois at Urbana Champaign.
- Riverside County Flood Control and Water Conservation District. 2011. "Low Impact Development Best Management Practice Design Handbook." Riverside, CA.
http://rcflood.org/downloads/NPDES/Documents/LIDManual/3.3_Permeable_Pavement.pdf.
- Rossmann, Lewis A. 2004. "STORM WATER MANAGEMENT MODEL: USER'S MANUAL, VERSION 5.0." Cincinnati, OH. ftp://84-255-254-95.static.t-2.net/SWMM/epaswmm5_manual.pdf.
- Rossmann, Lewis A., and Wayne C. Huber. 2015. "Storm Water Management Model Reference Manual Volume I – Hydrology." *U.S. Environmental Protection Agency* 3 (July). <https://doi.org/EPA/600/R-15/162A>.
- . 2016. "Storm Water Management Model Reference Manual Volume III – Water Quality." Vol. I. Cincinnati, OH.
- Rossmann, Lewis, and Will Huber. 2015. "Storm Water Management Model Reference Manual Volume I, Hydrology." Washington, DC. <https://doi.org/EPA/600/R-15/162A>.
- Roy-Poirier, Audrey, Pascale Champagne, and Yves Filion. 2010. "Review of Bioretention System Research and Design: Past, Present, and Future." *J ENVIRON ENG* 136 (9): 878–89.
[https://doi.org/10.1061/\(ASCE\)EE.1943-7870.0000227](https://doi.org/10.1061/(ASCE)EE.1943-7870.0000227).
- Sandström, Ulf G. 2002. "Green Infrastructure Planning in Urban Sweden." *Planning Practice and Research* 17 (4): 373–85. <https://doi.org/10.1080/02697450216356>.
- Santamouris, M. 2014. "Cooling the Cities – A Review of Reflective and Green Roof Mitigation Technologies to Fight Heat Island and Improve Comfort in Urban Environments." *Solar Energy* 103 (May): 682–703. <https://doi.org/10.1016/J.SOLENER.2012.07.003>.
- Sehmel, George A. 1980. "Particle and Gas Dry Deposition: A Review." *ATMOS ENVIRON* 14 (9): 983–1011. [https://doi.org/10.1016/0004-6981\(80\)90031-1](https://doi.org/10.1016/0004-6981(80)90031-1).
- Shin, Ong_hoon, and Kyoo-seok Lee. 2005. "Use of Remote Sensing and Geographical Information Systems to Estimate Green Space Surface-Temperature Change as a Result of Urban Expansion." *LANDSC ECOL ENG* 1 (2): 169–76. <https://doi.org/10.1007/s11355-005-0021-1>.
- Shreve, Ronald L. 1966. "Statistical Law of Stream Numbers." *The Journal of Geology* 74 (1): 17–37. <https://doi.org/10.1086/627137>.
- Singh, Abhishek, and Barbara S. Minsker. 2008. "Uncertainty-Based Multiobjective Optimization of Groundwater Remediation Design." *WATER RESOUR RES* 44 (2).
<https://doi.org/10.1029/2005WR004436>.
- Soares, A. L., F. C. Rego, E. G. McPherson, J. R. Simpson, P. J. Peper, and Q. Xiao. 2011. "Benefits and Costs of Street Trees in Lisbon, Portugal." *URBAN FOR URBAN GREE* 10 (2): 69–78.
<https://doi.org/10.1016/j.ufug.2010.12.001>.
- Tague, C. L., and L. E. Band. 2004a. "RHESSys: Regional Hydro-Ecologic Simulation System—An

- Object-Oriented Approach to Spatially Distributed Modeling of Carbon, Water, and Nutrient Cycling.” *Earth Interactions* 8 (19): 1–42. [https://doi.org/10.1175/1087-3562\(2004\)8<1:RRHSSO>2.0.CO;2](https://doi.org/10.1175/1087-3562(2004)8<1:RRHSSO>2.0.CO;2).
- Tague, C L, and L E Band. 2004b. “RHESSys: Regional Hydro-Ecologic Simulation System—An Object- Oriented Approach to Spatially Distributed Modeling of Carbon, Water, and Nutrient Cycling.” *EARTH INTERACT* 8 (1). <https://journals.ametsoc.org/doi/pdf/10.1175/1087-3562%282004%29%3C1%3ARRHSSO%3E2.0.CO%3B2>.
- Tarboton, David G, Ray Idaszak, Jeffery S Horsburgh, Jeff Heard, Dan Ames, Jonathan L. Goodall, Larry Band, et al. 2014. “HydroShare : Advancing Collaboration through Hydrologic Data and Model Sharing HydroShare : Advancing Collaboration through Hydrologic Data and Model Sharing.” In *International Congress on Environmental Modelling and Software. 7*, edited by Daniel P. Ames, Nigel W.T. Quinn, and Rizzoli Andrea E. Vol. 7. San Diego, CA, US. <https://doi.org/10.13140/2.1.4431.6801>.
- Taylor, Richard. 1990. “Interpretation of the Correlation Coefficient: A Basic Review.” *Journal of Diagnostic Medical Sonography* 6 (1): 35–39. <https://doi.org/10.1177/875647939000600106>.
- Teemusk, Alar, and Ulo Mander. 2007. “Rainwater Runoff Quantity and Quality Performance from a Greenroof: The Effects of Short-Term Events.” *ECOL ENG* 30: 271–77. <https://doi.org/10.1016/j.ecoleng.2007.01.009>.
- Tota-Maharaj, Kiran, and Miklas Scholz. 2010. “Efficiency of Permeable Pavement Systems for the Removal of Urban Runoff Pollutants under Varying Environmental Conditions.” *ENVIRON PROG SUSTAIN* 29 (3): 358–69. <https://doi.org/10.1002/ep.10418>.
- Tzoulas, Konstantinos, Kalevi Korpela, Stephen Venn, Vesa Yli-Pelkonen, Aleksandra Kaźmierczak, Jari Niemela, and Philip James. 2007. “Promoting Ecosystem and Human Health in Urban Areas Using Green Infrastructure: A Literature Review.” *LANDSCAPE URBAN PLAN* 81 (3): 167–78. <https://doi.org/10.1016/j.landurbplan.2007.02.001>.
- United States Department of Agriculture. 2018. “Saturated Hydraulic Conductivity | NRCS Soils.” 2018. https://www.nrcs.usda.gov/wps/portal/nrcs/detail/soils/survey/office/ssr10/tr/?cid=nrcs144p2_074846.
- US EPA. 2018. “Outdoor Air Quality Data.” 2018. <https://www.epa.gov/outdoor-air-quality-data/download-daily-data>.
- USGS. 2013. “USGS Current Conditions for USGS 01401000 Stony Brook at Princeton NJ.” 2013. <http://waterdata.usgs.gov/usa/nwis/uv?01401000>.
- . 2015. “USGS Current Conditions for USGS 01589464 STONY RUN AT RIDGEMEDE ROAD AT BALTIMORE, MD.” 2015. https://waterdata.usgs.gov/nwis/uv/?site_no=01589464.
- Vandermeulen, Valerie, Ann Verspecht, Bert Vermeire, Guido Van Huylenbroeck, and Xavier Gellynck. 2011. “The Use of Economic Valuation to Create Public Support for Green Infrastructure Investments in Urban Areas.” *LANDSCAPE URBAN PLAN* 103 (2): 198–206. <https://doi.org/10.1016/j.landurbplan.2011.07.010>.
- Virginia Water Research Center. 2011. “VIRGINIA DEQ STORMWATER DESIGN SPECIFICATION No. 7: PERMEABLE PAVEMENT.” 2011.

<http://vwrrc.vt.edu/swc/NonPBMPSpecsMarch11/VASWMBMPSpec7PERMEABLEPAVEMENT.html>.

- Vittorio, Damien Di, and Laurent Ahiablame. 2015. "Spatial Translation and Scaling Up of Low Impact Development Designs in an Urban Watershed." *Journal of Water Management Modeling*, April. <https://doi.org/10.14796/JWMM.C388>.
- Wagner, Brian J, and Steven M Gorelick. 1989. "Reliable Aquifer Remediation in the Presence of Spatially Variable Hydraulic Conductivity' From Data to Design." *WATER RESOURCES RESEARCH*. Vol. 25. <https://agupubs.onlinelibrary.wiley.com/doi/pdf/10.1029/WR025i010p02211>.
- Wang, Ranran, Matthew J Eckelman, and Julie B Zimmerman. 2013. "Consequential Environmental and Economic Life Cycle Assessment of Green and Gray Stormwater Infrastructures for Combined Sewer Systems." *ENVIRON SCI TECHNOL* 47(19): 11189–98. <https://doi.org/10.1021/es4026547>.
- Wang, Zhiyuan, and Gade Pandu Rangaiah. 2017. "Application and Analysis of Methods for Selecting an Optimal Solution from the Pareto-Optimal Front Obtained by Multiobjective Optimization." *Industrial & Engineering Chemistry Research* 56 (2): 560–74. <https://doi.org/10.1021/acs.iecr.6b03453>.
- Water Environment Reuse Foundation (WERF). 2012. "WERF SELECT Model." 2012. <http://www.werf.org/i/c/Tools/SELECT.aspx>.
- Weiss, P T, J S Gulliver, and a J Erickson. 2007. "Cost and Pollutant Removal of Storm-Water Treatment Practices." *J WATER RES PL* 133 (3): 218–29. [https://doi.org/http://dx.doi.org/10.1061/\(ASCE\)0733-9496\(2007\)133:3\(218\)](https://doi.org/http://dx.doi.org/10.1061/(ASCE)0733-9496(2007)133:3(218)).
- Wong, Tony H. F., Tim D. Fletcher, Hugh P. Duncan, John R. Coleman, and Graham A. Jenkins. 2002a. "A Model for Urban Stormwater Improvement: Conceptualization." In *Global Solutions for Urban Drainage*, 1–14. Reston, VA: American Society of Civil Engineers. [https://doi.org/10.1061/40644\(2002\)115](https://doi.org/10.1061/40644(2002)115).
- Wong, Tony H F, Tim D Fletcher, Hugh P Duncan, John R Coleman, and Graham A Jenkins. 2002b. "A Model for Urban Stormwater Improvement Conceptualisationq "A Model for Urban Stormwater Improvement A Model for Urban Stormwater Improvement Conceptualisation." In *9th International Congress on Environmental Modelling and Software*. Vol. 122. <https://scholarsarchive.byu.edu/iemssconference/2002/all/122>.
- Yan, Shengquan, and Barbara Minsker. 2006. "Optimal Groundwater Remediation Design Using an Adaptive Neural Network Genetic Algorithm." *WATER RESOUR RES* 42 (5): 1–14. <https://doi.org/10.1029/2005WR004303>.
- . 2011. "Applying Dynamic Surrogate Models in Noisy Genetic Algorithms to Optimize Groundwater Remediation Designs." *J WATER RES PL* 137 (3): 284–92. [https://doi.org/10.1061/\(ASCE\)WR.1943-5452.0000106](https://doi.org/10.1061/(ASCE)WR.1943-5452.0000106).
- Yang, Jun, Joe McBride, Jinxing Zhou, and Zhenyuan Sun. 2004. "The Urban Forest in Beijing and Its Role in Air Pollution Reduction." *URBAN FOR URBAN GREE* 3 (2): 65–78. <https://doi.org/10.1016/j.ufug.2004.09.001>.
- Yong, C.F., A. Deletic, T.D. Fletcher, and M.R. Grace. 2008. "The Clogging Behaviour and Treatment Efficiency of a Range of Porous Pavements." In *11th International Conference on Urban Drainage*,

10. Edinburgh, Scotland, UK.
https://www.researchgate.net/profile/Mike_Grace/publication/237204622_The_clogging_behaviour_and_treatment_efficiency_of_a_range_of_porous_pavements/links/0c960531fa2ae7f0f000000.pdf
- Young, Robert F. 2011. "Planting the Living City." *J AM PLANN ASSOC* 77 (4): 368–81.
<https://doi.org/10.1080/01944363.2011.616996>.
- Zhang, Kun, and Ting Fong May Chui. 2018. "A Comprehensive Review of Spatial Allocation of LID-BMP-GI Practices: Strategies and Optimization Tools." *Science of The Total Environment* 621 (April): 915–29. <https://doi.org/10.1016/J.SCITOTENV.2017.11.281>.
- Zhang, Yujia, Alan T. Murray, and B.L. Turner. 2017. "Optimizing Green Space Locations to Reduce Daytime and Nighttime Urban Heat Island Effects in Phoenix, Arizona." *LANDSCAPE URBAN PLAN* 165 (September): 162–71. <https://doi.org/10.1016/J.LANDURBPLAN.2017.04.009>.
- Zhao, Tingting. 2017. "A SERVICE-DRIVEN APPROACH TO ASSIST WATER MANAGEMENT DURING EXTREME EVENTS." University of Illinois at Urbana -Champaign.
<https://www.ideals.illinois.edu/bitstream/handle/2142/98122/ZHAO-DISSERTATION-2017.pdf?sequence=1&isAllowed=y>.
- Zhen, Jenny X., Shaw L. Yu, and Yanyun Zhai. 2004. "A Planning Tool for Watershed LID-BMP Implementation." In *Critical Transitions in Water and Environmental Resources Management*, 1–10. Reston, VA: American Society of Civil Engineers. [https://doi.org/10.1061/40737\(2004\)80](https://doi.org/10.1061/40737(2004)80).
- Zoppou, Christopher. 2001. "Review of Urban Storm Water Models." *ENVIRON MODELL SOFTW* 16 (3): 195–231. [https://doi.org/10.1016/S1364-8152\(00\)00084-0](https://doi.org/10.1016/S1364-8152(00)00084-0).
- Zou, Rui, Wu-Seng Lung, and Jing Wu. 2007. "An Adaptive Neural Network Embedded Genetic Algorithm Approach for Inverse Water Quality Modeling." *Water Resources Research* 43 (8).
<https://doi.org/10.1029/2006WR005158>.
- Zuniga-Teran, Adriana A., Chad Staddon, Laura de Vito, Andrea K. Gerlak, Sarah Ward, Yolandi Schoeman, Aimee Hart, and Giles Booth. 2019. "Challenges of Mainstreaming Green Infrastructure in Built Environment Professions." *J ENVIRON PLANN MAN*, June, 1–23.
<https://doi.org/10.1080/09640568.2019.1605890>.

Appendix A: Lists of SESYNC venture meeting participants/contributors

Table A.1. List of SESYNC venture meeting participants

Name	Affiliation	Role
Ahalt, Stan	Renaissance Computing Institute at UNC (RENCI)	Working group
Babbar-Sebens, Meghna	Oregon State University	Working group
Bacchieri, Jane	City of Portland, OR	Advisor group
Band, Larry	University of North Carolina at Chapel Hill	Working group
BenDor, Todd	University of North Carolina at Chapel Hill	Working group
Carsberg, Steven	City of Phoenix	Advisor group
Cox, John	City of Durham, NC	Advisor group
Duncan, Jon	University of North Carolina at Chapel Hill	Post-Doc
Ellis, Ginger	Anne Arundel County, MD	Advisor group
Felson, Alex	Yale	Working group
Gore, Simon	Yale	Student
Grimm, Nancy	Arizona State University	Working group
Groffman, Peter	Cary I	Working group
Grove, Kimberly	City of Baltimore, MD	Advisor group
Grove, Morgan	US Forest Service	Gov agency
Gustafson, Karl	Renaissance Computing Institute at UNC (RENCI)	Staff
Hager, Guy	Retired-Parks and People Foundation	Advisor group

Table A.1.(cont.) List of SESYNC venture meeting participants

Name	Affiliation	Role
Heidari, Bardia	University of Illinois at Urbana-Champaign	Student
Idaszak, Ray	Renaissance Computing Institute at UNC (RENCI)	Staff
Jiang, Xiangrong	University of Illinois at Urbana-Champaign	Student
LaPlante, Rosanna	City of Baltimore, MD	Advisor group
Law, Neely	Center for Watershed Protection	NGO
Lee, Jong	University of Illinois at Urbana-Champaign	Staff
Li, Danwei	University of North Carolina at Chapel Hill	Developer
Miles, Brian	University of North Carolina at Chapel Hill	Developer
Minsker, Barbara	University of Illinois at Urbana-Champaign	Working group
Navarro, Chris	University of Illinois at Urbana-Champaign	Developer
Neira, Fabian	University of Illinois at Urbana-Champaign	Student
O'Connor, Catherine	City of Chicago, IL	Advisor group
Rai, Ankit	University of Illinois at Urbana-Champaign	Student
Rivera, Sammy	University of Illinois at Urbana-Champaign	Student
Schmidt, Art	University of Illinois at Urbana-Champaign	Working group
Stack, Bill	Center for Watershed Protection	Advisor group
Stealey, Michael	Renaissance Computing Institute at UNC (RENCI)	Developer
Sullivan, William	University of Illinois at Urbana-Champaign	Working group
Suppakittpaisarn, Pongsakorn	University of Illinois at Urbana-Champaign	Student

Table A.1.(cont.) List of SESYNC venture meeting participants

Name	Affiliation	Role
Tarboton, Dave	Utah State University	Guest
Wang, Kexuan	University of Illinois at Urbana-Champaign	Student
Yeakley, Alan	Portland State	Working group
York, Abigail	Arizona State University	Working group

Appendix B: Instruction manual to prepare IDEAS_GI Jupyter notebook

Once you have setup a HydroShare account, you can use following steps to install all models into your environment, and to execute models.

- Login into HydroShare
- Click on Apps located on top of the page.
- Click on “Jupyter Python Notebook at NCSA” icon, second item from left on the first row.
- You should see a Jupyter notebook with a title "Welcome to the HydroShare Python Notebook Server". If you see this page, you are ready to upload the prototype workflow.

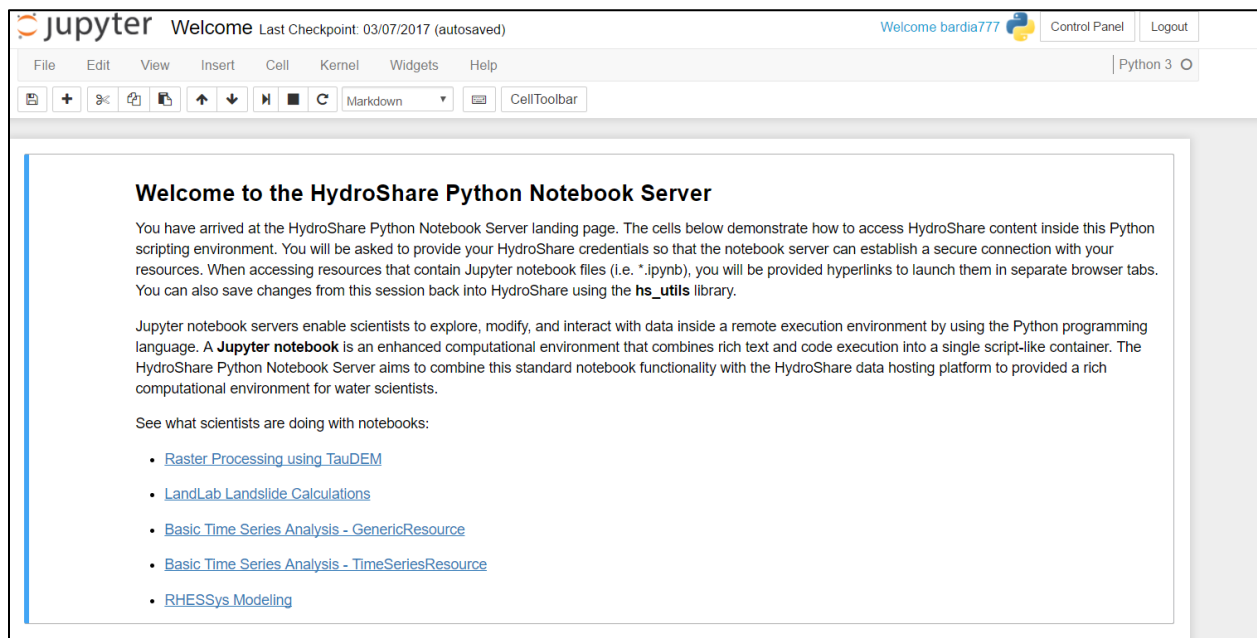


Fig. B.1. Screenshot of the JupyterHub welcome page

- Click on Jupyter sign on top left side of your page. You should see a page that is similar to following picture, but with only one folder “notebooks”. Do not close this page. We will come back to it.

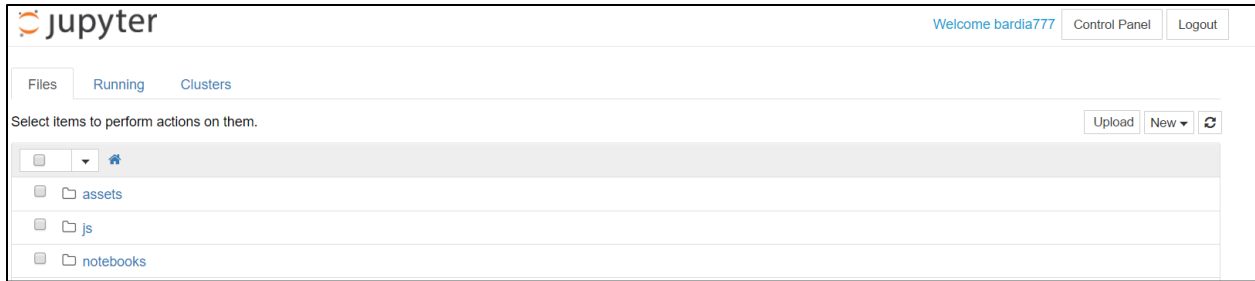


Fig. B.2. Screenshot of the folder in JupyterHub environment

- Open a new tab, and type in <http://www.hydroshare.org/resource/75dfc27015f1467388d712b562657835> to access supporting files for SWMM 5.0 and cost-benefit workflows, or alternatively search for “IDEAS_GI_Deadrun” in Discover tab in your hydroshare profile.
- Scroll down to Contents tab.
- Select IDEAS_GI supporting files and download it, using the third button on top left side of the contents tab.

The screenshot displays the HydroShare web interface for a resource titled "IDEAS for GI_Deadrun". At the top, the HydroShare logo and navigation menu (MY RESOURCES, DISCOVER, COLLABORATE, APPS, HELP) are visible. The resource title is prominently displayed, along with an "Open with..." button and a set of utility icons (share, download, add, refresh, edit, delete). Below the title, the author and owner information is listed: Bardia Heidari Haratmeh. The resource type is "Generic", created on April 24, 2017, and last updated on April 25, 2017. An abstract follows, describing a notebook and supporting files for designing green infrastructure in the Deadrun5 watershed. A subject section contains tags for "interactive design", "Green infrastructure", "SWMM", and "Deadrun watershed". The "How to cite" section provides a citation string and a "Copy" button. The sharing status is set to "Public" and "Shareable". A content viewer at the bottom shows a folder named "IDEAS_for_GI...".

Fig. B.3. Screenshot of the description and contents of IDEAS_GI for GI_Deadrun

- After the download process has finished, folder size is 10MB, go back to Jupyter page.
- Click on notebooks folder.
- Now we want to populate notebooks folder with supporting files as well as our main notebook. Click on upload button on top right side of your page.
- Find the zip file you just downloaded, IDEAS_GI.rar, on your PC and open it.
- Click on blue upload icon to upload the notebook into your environment.
- Now we want to unzip the folder. Click on “New” button on top right side of your page, and then select terminal.

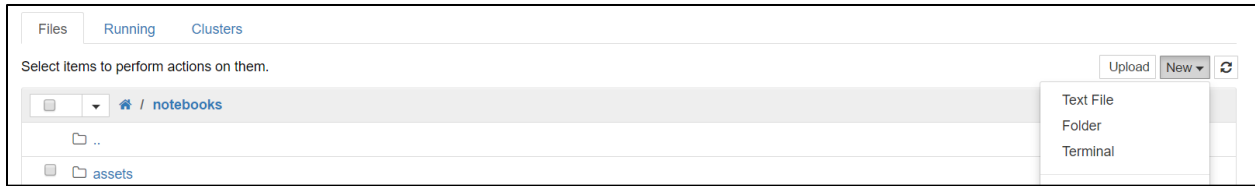


Fig. B.4. Screenshot of the tap needed to upload the zipped files

- A dark page showing terminal interface of your machine at NCSA will pop-up. Type in “cd notebooks” without quotation marks. All the commands you type in this page will be sent to a remote machine, meaning that nothing will be executed on your local machine.
- Type in “unzip IDEAS_GI.rar” without quotation marks.
- A list of documents will appear on your screen now. Type in “cd SWMM5-5.1.0.102” without quotation marks.
- Type in “pip install SWMM5-5.1.0.102”. (If you got red warnings, try “Python setup.py install”.)
 - To check if you have installed Python type in “Python”
 - Please type in “import swmm5”
 - If there are no warnings, the package is installed.
 - Please type “exit()”. As you successfully, import the package, you can skip steps 11 to 19.

```
jovyan@0682d6393c43:~/SWMM5-5.1.0.102$ python
Python 2.7.12 | packaged by conda-forge | (default, Sep  8 2016, 14:22:31)
[GCC 4.8.2 20140120 (Red Hat 4.8.2-15)] on linux2
Type "help", "copyright", "credits" or "license" for more information.
>>> import swmm5
>>> exit()
```

Fig. B.5. Screenshot of the terminal and required commands to verify successful installation of “swmm5” package

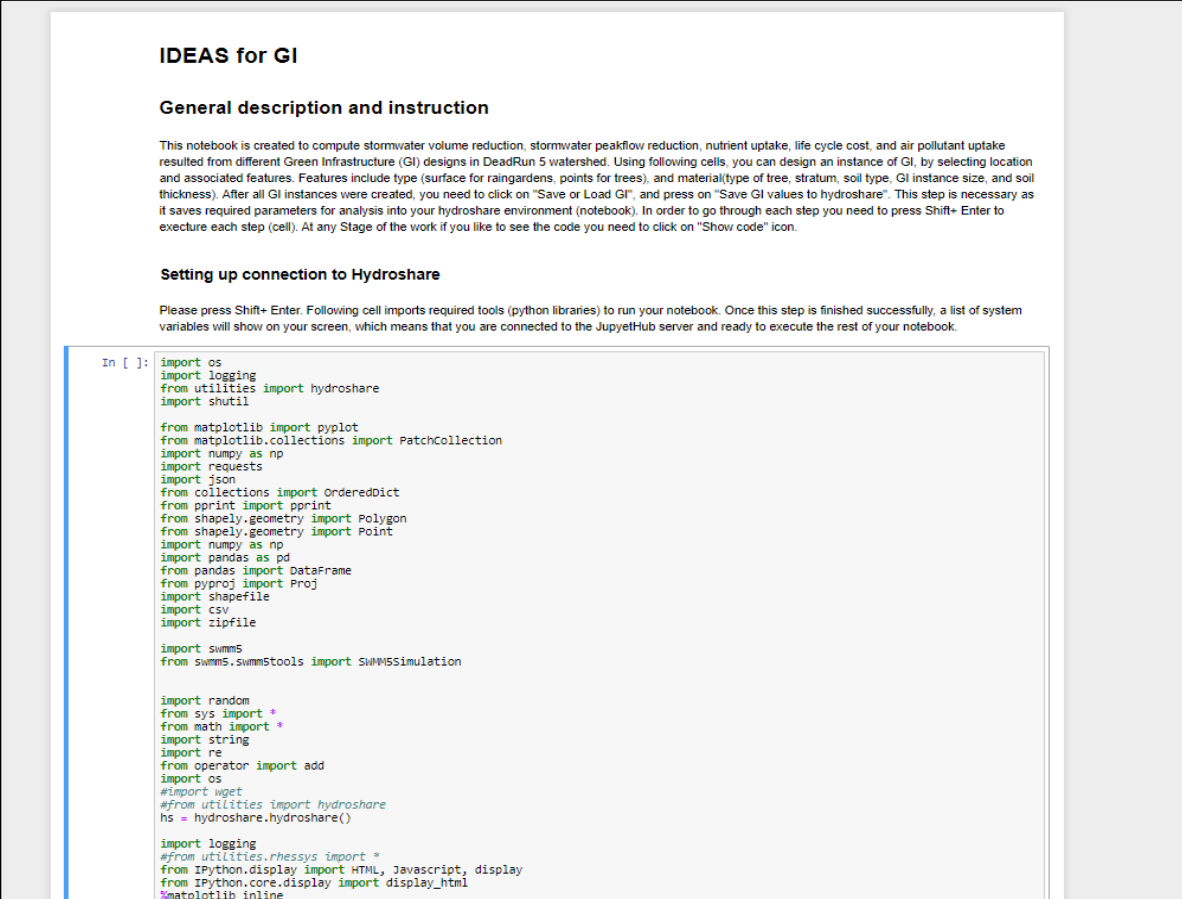
- Close the page you have the terminal open in. Go back to the notebooks folder page. There should be a file named as “IDEAS_GI- DeadRun.ipynb”. You just need this file. The rest are supporting files.
- You should see a new page, notebook, from which you can design Green Infrastructure, run models and get results. This page is all you need. This notebook is the “IDEAS_GI” the version prepared for the Deadr run watershed (case study I). Appendix C describes the steps required to execute this Jupyter notebook file.

Appendix C: Instruction manual to execute IDEAS_GI_Deadrin

This is the IDEAS_GI platform, i.e. Jupyter notebook. This notebook contains two types of cells: (a): Analysis cells, (b): Markup cells. The analysis cells are the cells that require execution from users, while markup cells exist just to provide documentation and guidance for the users. This section describes the steps required to execute the IDEAS_GI successfully, with more focus on analysis cells.

- Before you start, in order to make sure there are no outputs left from previous runs, please click on “kernel” tab and click on “Restart and clear outputs.

Once you restart the notebook, the empty notebook will appear and is ready to be executed by you. Fig. C.1. shows a screenshot of the notebook.



The screenshot shows a Jupyter notebook interface. At the top, the title is "IDEAS for GI". Below the title is a section titled "General description and instruction" with a paragraph of text explaining the notebook's purpose. This is followed by a section titled "Setting up connection to Hydroshare" with a paragraph of text. Below these sections is a code cell with the following Python code:

```
In [ ]: import os
import logging
from utilities import hydroshare
import shutil

from matplotlib import pyplot
from matplotlib.collections import PatchCollection
import numpy as np
import requests
import json
from collections import OrderedDict
from pprint import pprint
from shapely.geometry import Polygon
from shapely.geometry import Point
import numpy as np
import pandas as pd
from pandas import DataFrame
from pyproj import Proj
import shapefile
import csv
import zipfile

import swmm5
from swmm5.swmmstools import SWM5Simulation

import random
from sys import *
from math import *
import string
import re
from operator import add
import os
#import wget
#from utilities import hydroshare
hs = hydroshare.hydroshare()

import logging
#from utilities.rhessys import *
from IPython.display import HTML, Javascript, display
from IPython.core.display import display_html
%matplotlib inline
```

Fig. C.1. Screenshot of the empty notebook ready to be executed by the users

- The first few cells are markup cells explaining the notebook and its functionality.

- Sixth cell is the first analysis cell that you need to press “shift+ enter” to execute. The cell imports the necessary python libraries required for the successful execution of IDEAS. The cell might ask for your HydroShare password as well. Once is the cell is executed, its content, Python scripts, will disappear to the background. At any stage in the execution of the IDEAS, you can click on “show code” button to see the python scripts contents. Fig. C.2 shows a screenshot of the cell once its executed successfully.

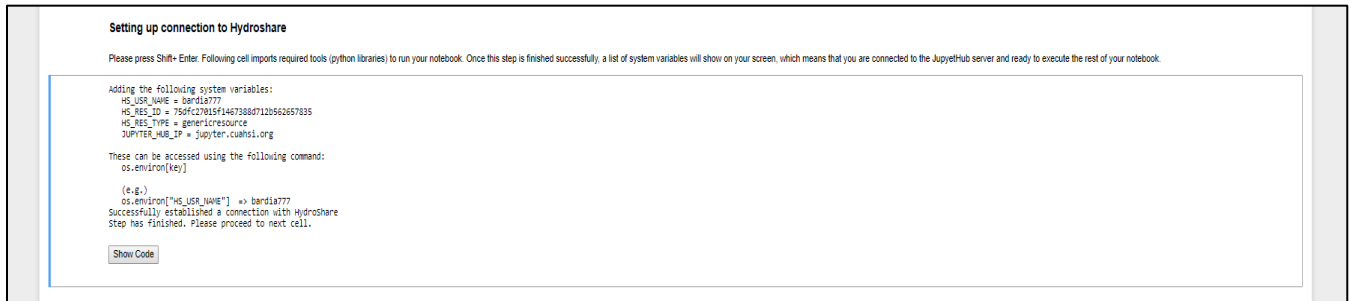


Fig. C.2. Screen shot of the messages that should appear after successful execution of the first analysis cell

- The next step is to execute the ninth cell, i.e. second analysis cell. This cell activates the connection to GI designer server and enables the GI designer interface. Section 2.2 have explained how GI practices can be designed and how the features of designs can be inserted into the Jupyter notebook environment. Fig. C.3 shows a screenshot of the GI designer interface.

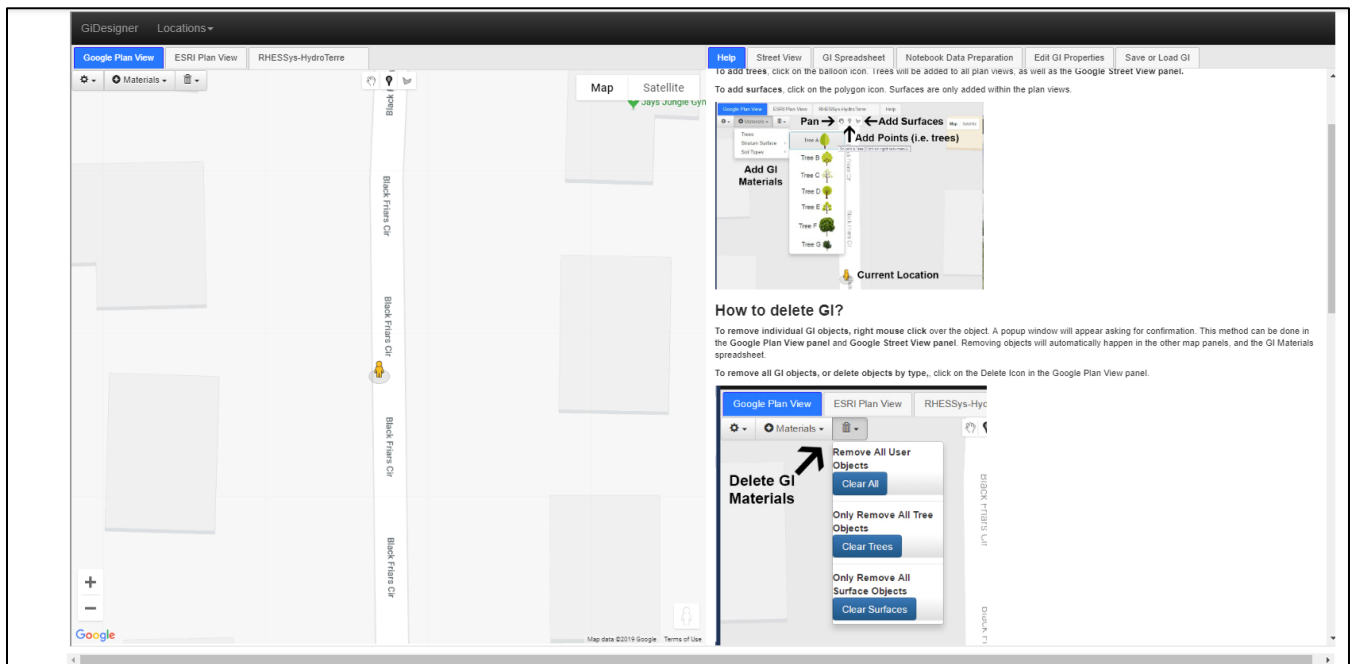


Fig. C.3. Screen shot of the GI designer page

- Once the GI designs are completed “using Save GI values to Hydroshare” button under “Save or Load GP” tab, you need to execute the third analysis cell, 12th cell total, to import the GI features into the Jupyter notebook environment. Upon successful execution of the cell, a message similar to the one in Fig. C.4 will appear.

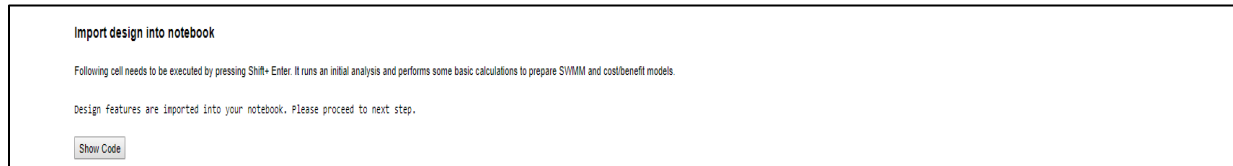


Fig. C.4. Screenshot of the message showing successful import of the GI features into IDEAS_GI environment

- The next analysis cells need to be executed to (1) initialize the models, (2) run the SWMM 5.0 models, (3) run the cost benefit models, and (4) prepare the outputs. Fig. C.5 show the messages appearing after successful execution of the mentioned analysis cells.

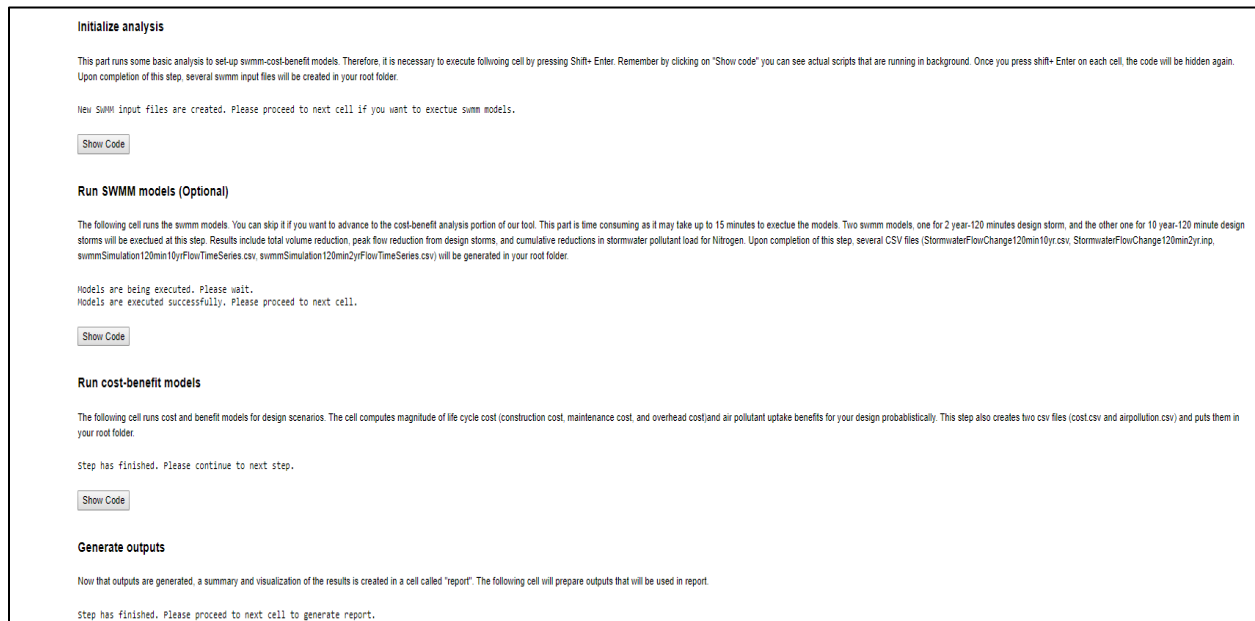


Fig. C.5. Screenshot of the messages showing successful execution of the next analysis cell in IDEAS

- The last analysis cell generates the report detailed in Section 2.2.

Appendix D: Input parameters for the required supporting files to successfully execute IDEAS_GI for any given watershed

This version of IDEAS_GI is capable of being adjusted to any given watershed. The steps are similar to those mentioned in Appendix C. However, there are additional parameters that require to be executed and specified for the successful execution of the tool. Here is a list of the parameters and their description:

D.1. Total_Number_sub: Total number of subwatersheds in the case study area.

D.2. Life_span: The life span of GI practices used of estimation of life cycle cost for rain gardens and trees.

D.3. Max_iteration: Maximum number of iterations that users that you want to run the Monte Carlos simulation for all the models used on this study.

D.4. Vertex_coordinates_file_name: A csv file containing coordinates (in latitude and longitude in WGS 1984 world Mercator projection system) for the vertex coordinates of the subwatersheds. You should follow the format used for the equivalent file in the supporting files for Dead run watershed.

D.5. First_design_Storm_SWMM_file: The name of inp file containing the SWMM 5.0 model for the first design storm.

D.6. Second_design_Storm_SWMM_file: The name of inp file containing the SWMM 5.0 model for the Second design storm.

D.7. Pollutant: The name of the pollutant of interest that will be analyzed at the watershed and subwatershed outlets.

All the parameters will be asked from the cell prior to the execution of GI designer and after execution of the first analysis cell.

By uploading and specifying the name of SWMM 5.0 files, the baseline models, the ones without any GI practices inserted will be executed to generate hydrographs at watershed and subwatersheds outlets. Also, the probabilistic distribution of the pollutant of interest will be created at the subwatershed and watershed outlets by the number of Monte Carlo simulations specified at D.3.

Appendix E: Uncertain continuous parameters

Table E.1. Uncertain continuous parameters

Parameter	Parameter range	Assumed distribution	References
Thickness for rain garden soil	Low depth: 7- 13 cm, average depth: 15- 18 cm, High: 20 cm	Uniform within each category of soil	(Water Environment Reuse Foundation (WERF) 2012)
Hydraulic conductivity for rain garden soil	Clay: 1×10^{-9} - 4.7×10^{-7} (cm/s) Sand: 2×10^{-5} - 6×10^{-1} (cm/s) loam: 4.23×10^{-4} - 1.41×10^{-3} (cm/s)	Triangular within each category of soil	(Domenico and Schwartz 1990; United States Department of Agriculture 2018)
Porosity ratios for rain garden soil	Clay: 0.38, std: 0.12, sand: 0.42-std:0.08, loam: 0.43- std:0.1	Normal within each category of soil	(Rawls et al. 1982)
Field capacity for rain garden soil	Clay: 0.3, std: 0.08, sand: 0.106, std: 0.025, loam: 0.325, std: 0.064	Normal within each category of soil	(Ottoni Filho et al. 2014)
Wilting point for rain garden soil	Clay: 0.05- 0.20, sand: 0.05-0.10, loam: 0.10- 0.15	Triangular within each category of soil	(Northeast Region Certified Crop Adviser 2010; Ottoni Filho et al. 2014)
Suction head for rain garden soil	Clay: 6.39-156.5 (cm), sand: 0.97- 25.36 (cm), loam: 1.33-59.38 (cm)	Normal within each category of soil	(Mays 2011)
Rain garden removal efficiencies for phosphorous (P) removal	70-85 (%)	Triangular	(Roy-Poirier et al. 2010)
Rain garden removal efficiencies for nitrogen (N) removal	5-85 (%)	Triangular	(Roy-Poirier et al. 2010)
Manning values of pervious pavement	0.015-0.03	Triangular	(Chow 1959)
Surface slope for pervious pavement	0-0.01	Triangular	(Virginia Water Research Center 2011)
Pavement layer thickness	7-20 (cm)	Triangular	(Virginia Water Research Center 2011)
Void ratio of pavement layer within pervious pavement	0.015-0.5	Triangular	(Virginia Water Research Center 2011)
Permeability of pavement layer within pervious pavement	63-2260 (cm hr ⁻¹)	Triangular	(Li et al. 2013)
Storage layer thickness within pervious pavement	15-30 (cm)	Triangular	(California Department of Transportation 2014; Riverside County Flood Control and Water Conservation District 2011)
Void ratio of storage layer within pervious pavement	0.3-0.75	Triangular	(California Department of Transportation 2014; Minnesota Pollution Control Agency 2017)
Seepage rate of storage layer within pervious pavement	0.06-0.12 (cm hr ⁻¹)	Triangular	(California Department of Transportation 2014)
Pervious pavement removal efficiencies for phosphorous (P) removal	28-82(%)	Triangular	(Drake et al. 2014; Totamaharaj and Scholz 2010; Yong et al. 2008)

Table E.1. (cont.) Uncertain continuous parameters

Parameter	Parameter range	Assumed distribution	References
Pervious pavement removal efficiencies for nitrogen (N) removal	16-43(%)	Triangular	(Drake et al. 2014; Tota-Maharaj and Scholz 2010; Yong et al. 2008)
Nitrogen (N) concentrations in rainfall	0.5-1.0 (mg L ⁻¹)	Triangular	(“National Atmospheric Deposition Program” n.d.)
Phosphorous (P) concentrations in rainfall	2.4- 419.0 (µg L ⁻¹)	Triangular	(Migon and Sandroni 1999)
Event mean concentration for nitrogen	0.82- 14.7 (mg L ⁻¹)	Triangular	(Brezonik and Stadelmann 2002)
Event mean concentration for phosphorous	0.11- 9.40 (µg L ⁻¹)	Triangular	(Brezonik and Stadelmann 2002)
Initial leaf area ratio	0- 0.2	Triangular	(Center for Neighborhood Technology 2006)
Dry deposition velocity in the ambient environment for ozone	0.001-0.01(m s ⁻¹)	Triangular	(Hirabayashi et al. 2012; Mcpherson et al. 1994; Sehmel 1980)
Dry deposition velocity in the ambient environment for nitrogen dioxide	0.01- 0.004 (m s ⁻¹)	Triangular	(Hirabayashi et al. 2012; Mcpherson et al. 1994; Sehmel 1980)
Dry deposition velocity in the ambient environment for sulfur dioxide	0.008- 0.01 (m s ⁻¹)	Triangular	(Hirabayashi et al. 2012; Mcpherson et al. 1994; Sehmel 1980)
Dry deposition velocity in the ambient environment for carbon monoxide	0.01- 0.000002 (m s ⁻¹)	Triangular	(Hirabayashi et al. 2012; Mcpherson et al. 1994; Sehmel 1980)
Dry deposition velocity in the ambient environment for ozone particulate matter	0.00003- 0.1 (m s ⁻¹)	Triangular	(Hirabayashi et al. 2012; Mcpherson et al. 1994; Sehmel 1980)
Discount factor for GI practices constructed	0-0.39 (%)	Triangular	Conversions with practitioners
Interest rate	0.02-0.06 (%)	Triangular	(Mortgage Calculator n.d.)
Constants for water quality treatment	B ₀ :1540± 480, B ₁ : 0.625± 0.046	Triangular	(Weiss, Gulliver, and Erickson 2007)
Maintenance frequency for rain garden	1-36 months	Triangular	(Water Environment Reuse Foundation (WERF) 2012)
Hours per maintenance for rain garden	0-3	Triangular	(Water Environment Reuse Foundation (WERF) 2012)
Labor cost for rain garden construction	0-45 (\$ hr ⁻¹)	Triangular	(Water Environment Reuse Foundation (WERF) 2012)
Machinery cost for construction of rain garden	0-60 (\$)	Triangular	(Water Environment Reuse Foundation (WERF) 2012)
Material cost per maintenance of rain garden	0-20 (\$)	Triangular	(Water Environment Reuse Foundation (WERF) 2012)
Construction for square feet unit of rain garden practices	55-172 (\$ m ⁻²)	Triangular	(Center for Neighborhood Technology 2006; Water Environment Reuse Foundation (WERF) 2015)

Table E.1.(cont.) Uncertain continuous parameters

Parameter	Parameter range	Assumed distribution	References
Construction for square feet unit of pervious pavement	102-123(\$ ft ⁻²)	Triangular	(Remodelingexpenses 2017)
Ratio of overhead cost for unit area of rain garden	Design: 0-3%, Overhead: 0-5%	Triangular	(Water Environment Reuse Foundation (WERF) 2012)

Appendix F: Uncertain categorical parameters

Table F.1. Uncertain categorical parameters

Parameter	Parameter values	References
Soil type for rain garden soil	Clay- sand- Loam	(Maryland Department of Environment 2009)
Rain garden installation options	Self- installation, professional- installation	(Water Environment Reuse Foundation (WERF) 2012)
Rain garden maintenance options	Self- installation, professional- installation	(Water Environment Reuse Foundation (WERF) 2012)
Rain garden maintenance frequency	High (1 month), Medium (12 months), low (36 months)	(Water Environment Reuse Foundation (WERF) 2012)
Hours spent during each frequency event for rain gardens	High (2 hours), Medium (2 hours), low (1 hour)	(Water Environment Reuse Foundation (WERF) 2012)
Average labor size for rain garden installation	High (2 persons), Medium (1 persons), low (0 person)	(Water Environment Reuse Foundation (WERF) 2012)
Average labor rates for rain garden installation	High (45\$), Medium (30\$), low (0 \$) [Dollar values as of 2008]	(Water Environment Reuse Foundation (WERF) 2012)
Machinery cost for rain garden installation	High (60 \$), Medium (0 \$), low (0 \$) [Dollar values as of 2008]	(Water Environment Reuse Foundation (WERF) 2012)
Materials costs per event of rain garden installation	High (20 \$), Medium (10 \$), low (0\$) [Dollar values as of 2008]	(Water Environment Reuse Foundation (WERF) 2012)

Appendix G: Supplementary results on co-benefits/ costs associated with design scenarios at the two case study watersheds

Table G.1. Estimation of life cycle cost and air pollutant deposition for different GI scenarios in the two case study watersheds

DR5					
Percentage GI coverage from potential pervious candidate area (percentage from the entire watershed area)	Total present value of GI life cycle	Cumulative SO ₂ deposition (kg)	Cumulative NO ₂ deposition (kg)	Cumulative O ₃ deposition (kg)	Cumulative PM ₁₀ deposition (kg)
100 (9.6)	9060	0.1146	0.1001	1.0075	176.1
75 (7.2)	9960	0.1149	0.0957	1.0849	175.5
64 (6.2)	9380	0.1145	0.0961	1.0911	174.4
50 (4.8)	11470	0.1138	0.0976	0.9262	149.2
32 (3.1)	9250	0.1137	0.0968	1.0395	165.3
25 (2.4)	10430	0.1125	0.0981	1.0111	166.8
16 (1.6)	10330	0.1116	0.1053	0.9519	183.6
SR5					
100 (4.8)	3720	0.0159	0.0125	0.1429	24.2
75 (3.6)	3150	0.0154	0.0138	0.1241	24.5
64 (3.1)	2160	0.0155	0.0133	0.1533	22.7

Table G.1. (cont.) Estimation of life cycle cost and air pollutant deposition for different GI scenarios in the two case study watersheds

Percentage GI coverage from potential pervious candidate area (percentage from the entire watershed area)	Total present value of GI life cycle	Cumulative SO₂ deposition (kg)	Cumulative NO₂ deposition (kg)	Cumulative O₃ deposition (kg)	Cumulative PM₁₀ deposition (kg)
50 (2.4)	5690	0.0159	0.0125	0.118	23.4
32 (1.5)	5020	0.0156	0.0149	0.1606	27.1
25 (1.2)	4710	0.0155	0.0128	0.1457	27.5
16 (0.8)	3680	0.0155	0.0142	0.154	24.2

Table G.2. Effect of soil type and soil depth on estimation of life cycle cost

	Feature	Mean of total present value of GI life cycle
Soil type	Clay	4000
	Silt-Clay	4000
	Silty-Clay-Loam	4000
	Sand	4000
	Loamy-Sand	4000
	Sandy-Loam	4000
	Sandy-Clay	4000
	Sandy-Clay-Loam	4000
	Clay-Loam	4000
	Loam	4000
	Silt	4000
	Silt-Loam	4000
Soil depth	1	7000
	0.5	4000
	0.25	3000

Appendix H: Geographic specification of case study I in Section 3.5.2.



Fig. H.1. Tree locations in the design scenario with rain garden implementation scenario



Fig. H.2. Tree locations in the design scenario with tree implementation scenario

Appendix I: Computation of stormwater reduction as a function of GI coverage area

To model the stormwater reduction there needs to be two types of simulation: runoff generation, and conveyance.

The runoff generation simulation portion simulates runoff from the land by assuming the surface of each subwatershed to be a nonlinear reservoir. Inflow consists of precipitation and flow from upstream subwatersheds, while the outflows consists of infiltration, evaporation, and surface runoff to down- stream areas. The depth of water is computed using the following overland flow kinematic wave equation for the subwatershed:

$$\frac{dd}{dt} = i - e - f - q$$

where d = depth of storage, i = rate of rainfall, e = surface evaporation rate, f = infiltration rate (following Green-Ampt equation), and q = runoff rate.

To compute run off, flow is assumed to happen uniformly in a rectangular channel using following equation:

$$q = \frac{1.49W}{A_x \cdot n} S^{0.5} (d - d_p)^{1.67}$$

where n = Manning's roughness coefficient, d_p = depth of depression storage, W = subwatershed width, A_x =surface area of subwatershed, and S = subwatershed slope.

(Rossman and Huber 2015) have provided more details on the hydrological methodology used in SWMM 5.0.

The GI/ LID module provides a process-based simulation of flow. Inflow volume is estimated using upstream watershed simulation results for the BMP. Outflow consists of overflow/outflow, evapotranspiration, and infiltration. The module also simulates infiltrating using the Green-Ampt equation. The contributing area and the area of the GI play a role here to determine the level of storage needed that happens at each GI installment.